

Organic/Inorganic Composite Latexes: The Marriage of Emulsion Polymerization and Inorganic Chemistry

Elodie Bourgeat-Lami and Muriel Lansalot

Abstract This review article describes recent advances in the synthesis and properties of waterborne organic/inorganic colloids elaborated through conventional emulsion polymerization, a well-established technology. These materials can be defined as aqueous suspensions of composite latex particles made up of organic and inorganic domains organized into well-defined core–shell, multinuclear, raspberry-like, multipod-like, or armored morphologies. Particular emphasis is placed on the synthetic strategies for fabrication of these colloidal materials. Two main approaches are described: the polymerization of organic monomers in the presence of preformed inorganic particles, and the reverse approach by which inorganic materials are synthesized in the presence of preformed polymer latexes. The list of examples provided in this review is by no means exhaustive but rather intends to give an overview of synthetic methods for selected inorganic compounds (e.g., silica, iron oxide, pigments, clays, quantum dots, and metals), and briefly reports on potential applications of the resulting materials.

Keywords Clays · Emulsion polymerization · Iron oxide · Metals · Organic/inorganic composite colloids · Particle morphology · Pigments · Quantum dots · Silica · Surface modification

Contents

1	Introduction and Scope	56
2	Polymer–Silica Nanocomposite Particles	58
2.1	Emulsion Polymerization in the Presence of Silica Particles	59
2.2	Coating of Polymer Latexes with a Silica Shell	70

E. Bourgeat-Lami (✉) and M. Lansalot (✉)
Université de Lyon, Univ. Lyon 1, CPE Lyon, CNRS UMR5265, Laboratoire de Chimie,
Catalyse, Polymères et Procédés (C2P2), LCPP team, 43 Bd du 11 Novembre 1918, 69616,
Villeurbanne, France
e-mail: bourgeat@lcpp.cpe.fr; lansalot@lcpp.cpe.fr

3	Synthesis of Magnetic Latex Particles	72
3.1	Encapsulation of Iron Oxide Nanoparticles by Emulsion Polymerization	74
3.2	Synthesis of Iron Oxide Nanoparticles in the Presence of Preformed Polymer Particles	87
4	Pigmented Latexes	89
4.1	Polymer Encapsulation of TiO ₂ Pigments	90
4.2	Titania-Coated Polymer Spheres and Hollow Titania Shells	92
4.3	Other Pigments	93
5	Polymer–Clay Nanocomposite Latexes	95
5.1	PCNs Elaborated by Conventional Emulsion Polymerization	96
5.2	Soap-Free Latexes Stabilized by Clay Platelets	100
6	Synthesis of Quantum Dot Tagged Latex Particles	102
6.1	Encapsulation of QDs Through Emulsion Polymerization	103
6.2	Synthesis of Quantum Dots in the Presence of Polymer Particles	106
7	Synthesis of Metallic Latex Particles	109
7.1	Polymer Encapsulation of Metallic Particles Through Emulsion Polymerization ..	109
7.2	Polymer Particles as Template for the Synthesis of Metallic Shells and Metallic Nanoparticles	110
8	Summary and Outlook	114
	References	115

Abbreviations

1VID	1-Vinylimidazole
2VPy	2-Vinylpyridine
4VPy	4-Vinylpyridine
AA	Acrylic acid
AAEM	Acetoacetoxyethyl methacrylate
AAm	Acrylamide
ACPA	4,4'-Azobis(4-cyanopentanoic acid)
AEMH	2-Aminoethylmethacrylamide hydrochloride
AFM	Atomic force microscopy
AIBA	2,2'-Azobis(2-amidinopropane) dihydrochloride
AIBN	2,2'-Azobis(isobutyronitrile)
AOA	12-Acryloxy-9-octadecenoic acid
BA	<i>n</i> -Butyl acrylate
BMA	<i>n</i> -Butyl methacrylate
CMC	Critical micelle concentration
CS	Chitosan
CTAB	Cetyltrimethyl ammonium bromide
DMAEMA	2-(Dimethylamino)ethyl methacrylate
DSC	Differential scanning calorimetry
DVB	Divinyl benzene
EGDMA	Ethylene glycol dimethacrylate
GA	Gluteraldehyde

GMA	Glycidyl methacrylate
HEMA	2-Hydroxyethyl methacrylate
KPS	Potassium persulfate
MA	Maleic anhydride
MAA	Methacrylic acid
MADQUAT	2-Methacryloyloxy ethyl trimethyl ammonium chloride
MBA	<i>N,N'</i> -Methylene bisacrylamide
MMA	Methyl methacrylate
MMT	Montmorillonite
MPDES	Methacryloxy propyl dimethyl ethoxysilane
MPDMS	Methacryloxy propyl dimethoxysilane
MPTMS	Methacryloxy propyl trimethoxysilane
MTC	2-(Methacryloyl) ethyl trimethyl ammonium chloride
Ms	Saturation magnetization
NaSS	Sodium styrene sulfonate
NIPAM	<i>N</i> -Isopropylacrylamide
NVCL	<i>N</i> -Vinylcaprolactam
OA	Oleic acid
O/I	Organic/inorganic
P4VPy	Poly(4-vinylpyridine)
P2VPy	Poly(2-vinylpyridine)
PCN	Polymer–clay nanocomposites
PDMAEMA	Poly[2-(dimethylamino)ethyl methacrylate]
PDVB	Poly(divinyl benzene)
PEG	Poly(ethylene glycol)
PEGMA	Poly(ethylene glycol) monomethyl ether methacrylate
PMMA	Poly(methyl methacrylate)
PS	Polystyrene
PSD	Particle size distribution
PVA	Polyvinyl alcohol
PVC	Polyvinyl chloride
PVP	Poly(<i>N</i> -vinylpyrrolidone)
QDs	Quantum dots
SDBS	Sodium dodecylbenzene sulfonate
SDS	Sodium dodecyl sulfate
SEM	Scanning electron microscopy
TALH	Titanium(IV) bis(ammonium lactate) di-hydroxyde
TEM	Transmission electron microscopy
TEOS	Tetraethyl orthosilicate
T_g	Glass transition temperature
TGA	Thermogravimetric analysis
TOPO	Tri- <i>n</i> -octylphosphine oxide
VDAC	Vinylbenzyl dimethyl dodecyl ammonium chloride

1 Introduction and Scope

The incorporation of inorganic materials into polymers is of significant theoretical and experimental interest, with a rich history in the polymer and engineering communities. Mineral fillers and extenders such as calcium carbonate, fumed silica, kaolin, and ceramic fibers have been used as additives in polymers for more than a century. Not only can these inorganic solids provide enhanced physical properties such as stiffness, mechanical strength, chemical inertness, thermal resistance, and optical properties (transparency, opacity), but they can also significantly contribute to cost reduction. Although the addition of minerals to enhance polymer performance and impart physical and rheological properties is common in the production of modern plastics and in many industrial formulations (foods, inks, paints, adhesives, paper coatings, textiles, photographic films, pharmaceutical and cosmetic preparations), the remarkable scientific progress in the ability to fabricate, manipulate, and assemble organic and inorganic compounds at the nanometer scale has revolutionized the way such composite materials are envisaged and elaborated.

Organic/inorganic (O/I) composite latexes are typical examples of nanocomposite materials that combine the best attributes of inorganic solids with the processing and handling advantages of organic polymers. The huge breakthroughs that have been achieved in inorganic chemistry now allow the synthesis of nanoparticles of noble metals, metal oxides, and semiconductors with outstanding electronic, optical, magnetic, or catalytic properties in large quantities using thermal decomposition, hydrolysis, reduction and other soft-chemistry processes in solution [1, 2]. On the other hand, synthetic latexes have raised increasing interest in the last century, and large quantities of commodity polymers [polystyrene (PS), polyvinyl chloride (PVC), styrene–butadiene or polychloroprene rubbers] are manufactured as aqueous dispersions. Combining both materials into a unique nanostructured composite particle is of obvious benefit for both the academic and industrial communities. Given the extensive variety of inorganic materials now commercially accessible [clays, quantum dots (QDs), metals, silica, titania, alumina, zirconia, iron oxides and so on], the potential combinations of organic polymers and inorganic nanoparticles, and thus the tailorability of their properties and performances, is essentially endless. Furthermore, the properties of these two-phase colloidal materials not only depend on the chemical nature of the constitutive organic and inorganic components, but may also greatly benefit from the ability to design particle nanostructures. For example, if the organic polymer is located at the outer particle surface (in the so-called core–shell morphology), it can protect the core from environmental aggressions, or provide functional groups to improve interactions with the surrounding medium, or impart specific sensing and colloidal properties. By contrast, when the polymer is surrounded by the mineral, and thus plays the role of a template, hollow particles can be produced by subsequent removal of the core. The structures obtained are of particular interest for encapsulation technologies, drug delivery, or as pigments for the paint industry. Therefore, by controlling the composite particle morphology through appropriate routes and reaction conditions, synergetic behaviors and completely new properties can potentially emerge. Many strategies have been reported

for the elaboration of such colloidal nanocomposites including heterocoagulation, layer-by-layer assembly techniques, and in situ polymerization. The reader is referred to recent reviews and text books for a comprehensive description of these methods [3–15].

In order to avoid overlapping with these previous reviews, we will mainly focus in this article on the synthesis and properties of O/I composite latexes elaborated by emulsion polymerization, a process that is extensively employed industrially to manufacture a variety of products such as paints, adhesives, impact modifiers and so on. Composite particles elaborated through miniemulsion polymerization or controlled radical polymerization, are reviewed elsewhere in this special issue and will not be considered here. As both the synthetic strategies and properties of the resulting materials depend on the type of inorganic particles, this review is organized around the nature of the inorganic phase, namely metal oxides, metals, non-oxide semi-conductors (QDs), and aluminosilicates (clays). A list of inorganic particles of interest is given in Table 1.

For the sake of clarity, the different types of inorganic materials will be discussed separately. For each of them (except for clays), we will distinguish between two synthetic approaches (Fig. 1). In the first approach, the composite colloid is elaborated by in situ emulsion polymerization in the presence of preformed inorganic particles, usually used as seeds but which can also play the role of stabilizers. In the second approach, polymer latexes elaborated through conventional emulsion polymerization are used as templates to grow inorganic domains either within or at the surface of the particles. Given the rapidly expanding body of literature in the field, the intent in the following sections is not to provide an exhaustive list of examples but rather to

Table 1 Some inorganic particles of interest and examples of their potential end-use application

Inorganic material	Chemical formula	Potential application
<i>Oxides</i>		
Silica	SiO ₂	Paints, plastics
Titanium dioxide	TiO ₂	Paints
Iron oxide	Fe ₃ O ₄ /Fe ₂ O ₃	Biomedical, catalysis
Zinc oxide	ZnO	Paints, electronics
Alumina	Al ₂ O ₃	Coatings
<i>Metals</i>		
Gold	Au	Optics, biomedical
Silver	Ag	Optics, biomedical
Palladium	Pd	Catalysis
Copper	Cu	Catalysis
<i>Non-oxide semiconductors</i>		
Cadmium selenide	CdSe	Optics, biomedical
Cadmium sulfide	CdS	Optics, biomedical
<i>Aluminosilicates</i>		
Montmorillonite	–	Plastics, paints
Laponite	–	Plastics, paints

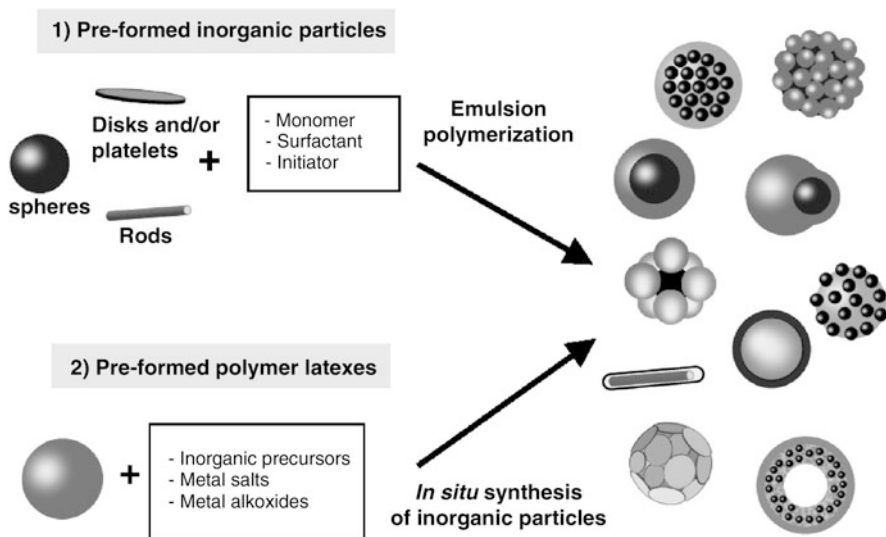


Fig. 1 Two main different approaches to fabrication of O/I particles: (1) organic polymerization in the presence of preformed inorganic particles and (2) inorganic formation at the surface or inside the internal volume of preformed polymer latex particles

give an overview of the various synthetic methods, with emphasis on the techniques that have been developed to control the surface chemistry of the inorganic or organic materials and the morphology of the resulting composite particles.

2 Polymer–Silica Nanocomposite Particles

To date, silica has been the focus of the majority of studies on oxide-based nanostructured materials. One of the major reasons for this is its easy processability, high chemical inertness and exceptional colloidal stability. Moreover, silica can be processed as a thin film with controllable porosity and optical transparency. All these properties make silica ideal for use in model systems, and it is widely used in many industrial areas ranging from paints and drug delivery to composite materials. Zou et al. have recently published a detailed review on the preparation, characterization, properties, and applications of polymer/silica nanocomposites and the reader is referred to this review for in-depth description of the various synthetic routes [16].

Silica particles used in emulsion polymerization are of different origin and, consequently, their sizes and surface properties significantly vary. Although the large majority of works involve the use of anionic silica sols, cationic silica has also been used on some occasions. Silica particles are most often amorphous colloidal silicas of commercial origin with diameters in the range of 10–80 nm. Silica particles of larger diameters are prepared by controlled hydrolysis and precipitation

of tetraethyl orthosilicate (TEOS) from alcohol/water mixtures according to the well-established Stöber process [17]. In this technique, TEOS is introduced into a mixture of alcohol, ammonia, and water to form dense (compact) monodisperse silica spheres through base-catalyzed hydrolysis and condensation reactions. The technique affords a relatively good control over the particle size and size distribution for low solid contents. However, the breadth of the distribution broadens, and the particles become less spherical, for solid contents higher than typically 5 wt%. Numerous methods inspired from the original Stöber process have been therefore developed to increase both particle size and solid content while maintaining narrow particle size distributions (PSDs) [18].

Regardless of the nature of the silica particles, synthetic strategies need to be established in order to increase the chemical affinity with hydrophobic polymers and to control the morphology of the resulting composite colloid. All these methods share a common feature in the sense that they all aim at creating significant interactions at the silica-polymer interface by using suitable primers (adsorbed or grafted on the silica surface) capable of participating in the polymerization reaction or to impart the required compatibility. An overview of these methods is given in the following section.

2.1 Emulsion Polymerization in the Presence of Silica Particles

2.1.1 Silica Particles Functionalized by Methacryloxy Propyl Trimethoxysilane

Silane coupling agents have been used for decades in order to provide enhanced adhesion between a variety of inorganic substrates and organic resins. They are organometallic derivatives of the type R_nSiX_{4-n} , where X is an alkoxy group and R is a functional organic group. Organosilane compounds are known to react with hydroxylated surfaces to form mono- or multilayer coverages, depending on the number of alkoxy groups and the amount of water.

The use of organosilane molecules to generate silica-based composite particles was first demonstrated by Guyot and coworkers in the mid-1990s. The authors reported successful encapsulation of silica particles functionalized by methacryloxy propyl trimethoxysilane (MPTMS) with poly(ethyl acrylate), through emulsion polymerization. The films cast from the composite suspensions were shown to exhibit remarkable mechanical properties, similar to those of vulcanized elastomers reinforced by solid particles [19–21]. It was argued at that time that polymer chains grafted on the silica surface via the silane coupling agent formed a succession of tight loops into which the free polymer chains were entangled, thereby leading to a physical network of silica beads responsible for the unusually high mechanical properties. The strategy was next extended with success to non-aqueous dispersion polymerization [22–24] and later applied by several groups to the synthesis of polymer/silica composite particles of various morphologies (Fig. 2) [25–32].

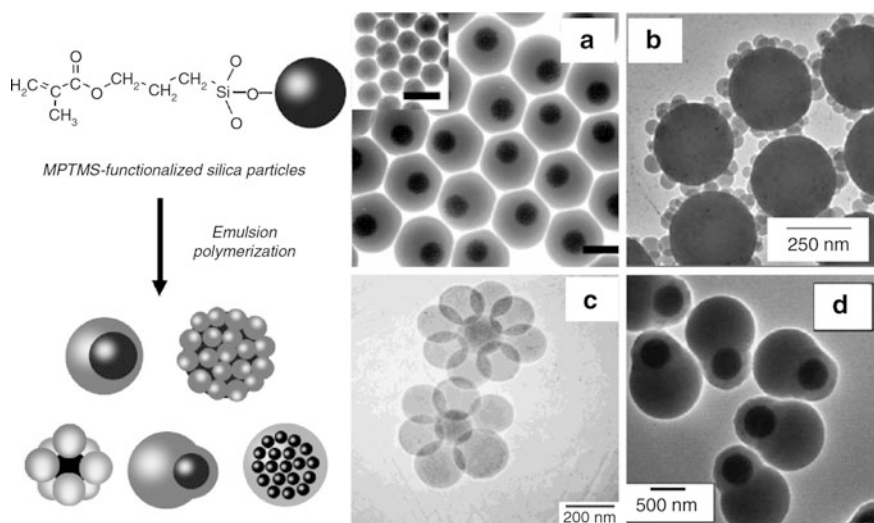


Fig. 2 *Left*: Silica/polystyrene composite particles elaborated through emulsion polymerization using MPTMS as silane coupling agent. *Right*: TEM images reproduced (a) from [25] (scale bars: 200 nm) with permission of Wiley-VCH, (b) from [26] with permission of Springer, (c) from [27] with permission of American Chemical Society, and (d) from [28] with permission of Wiley-VCH

Many factors can influence particle morphology. Among them, the size and concentration of the silica particles and the grafting density of MPTMS appeared to be predominant parameters. As described in [33] and illustrated in Fig. 3, the mechanism of particle formation can be summarized as follows. The initiator starts to decompose in the water phase, giving rise to the formation of radicals. These radicals propagate with aqueous phase monomers until they undergo one of the following fates: (1) aqueous phase termination or (2) entry into a micelle or precipitation (depending on the surfactant concentration), creating somehow a new particle. Aqueous-phase oligomers of all degrees of polymerization can also undergo frequent collision with the surface of the silica seed particles, and therefore have a high probability of copolymerizing with the double bonds of silica, thus generating chemisorbed polymer chains in the early stages of polymerization. These discrete polymer loci are preferred for adsorption of further oligomers or radicals compared with the bare seed surface. As a result, they become discrete loci of polymerization. Provided that the seed develops a sufficient surface area and contains enough double bonds to enable efficient capture of the growing radicals, polymerization exclusively takes place at the silica surface. High MPTMS grafting density thus allows core-shell formation through the efficient capture of a large number of oligoradicals or primary particles in the earlier stage of the reaction. The shell may result from the collapsing of the growing polymer chains on the functionalized silica surface or from the coalescence of freshly nucleated primary particles, the latter situation being promoted by the close proximity of the precursor particles and the low surface energy. For low MPTMS grafting densities, the polymer chains form

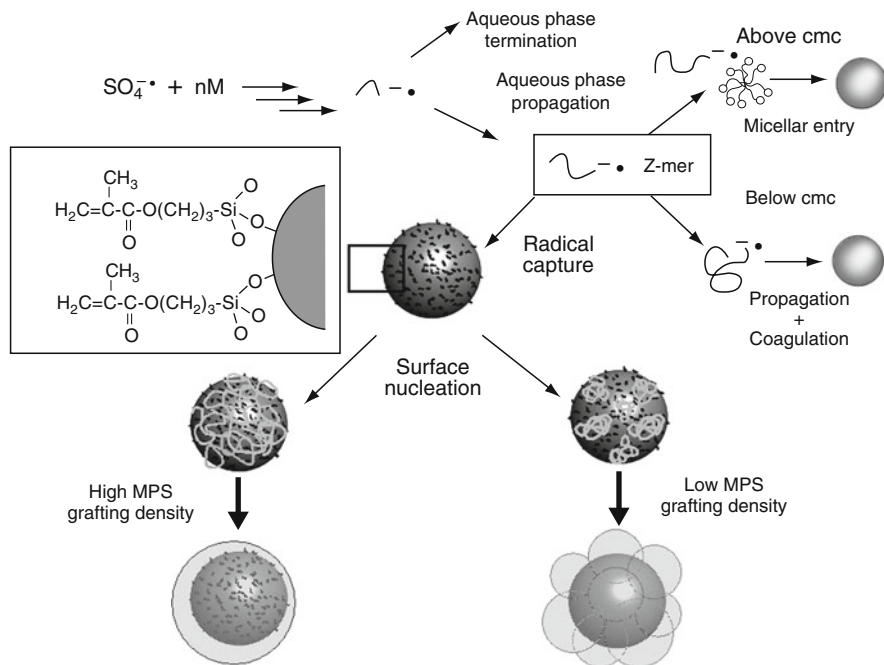


Fig. 3 Main features of the formation of silica/polymer nanocomposite particles through emulsion polymerization using MPS as silane coupling agent. Reproduced from [33] with permission of American Scientific Publishers

segregated domains around the silica particles because the high interfacial energy (due to the presence of unreacted silanol groups) promotes neither spreading of the polymer chains on the surface nor interparticle coalescence.

In agreement with the mechanism of composite particle formation depicted above, multipod-like morphologies with five, six, or eight PS nodules per silica particle were obtained with success using silica seeds treated with small amounts of MPS (in the range $0.1\text{--}1$ molecule nm^{-2}) [27, 33]. It was subsequently reported that the geometry of such binary polymer/silica colloidal clusters could be finely tuned by varying the diameter of the silica seed (Fig. 4) [34]. The resulting complex colloidal assemblies displayed polyhedral arrangements that shared some common aspects with the space-filling models of simple binuclear molecules. To this respect, they could be regarded as “colloidal molecules”, a concept first introduced by van Blaaderen [35], which consists in considering that spherical colloids can be treated as if there were atoms and that molecules can form more complex materials that atoms can. Besides their potential interest as model systems for the physicist community, these colloidal clusters can be used as building blocks for the elaboration of ordered arrays of non-spherical colloids with potential applications in photonic crystals. It is foreseen, for example, that the controlled assembly of tetrapod-like colloids should result in colloidal crystals with a full photonic bandgap.

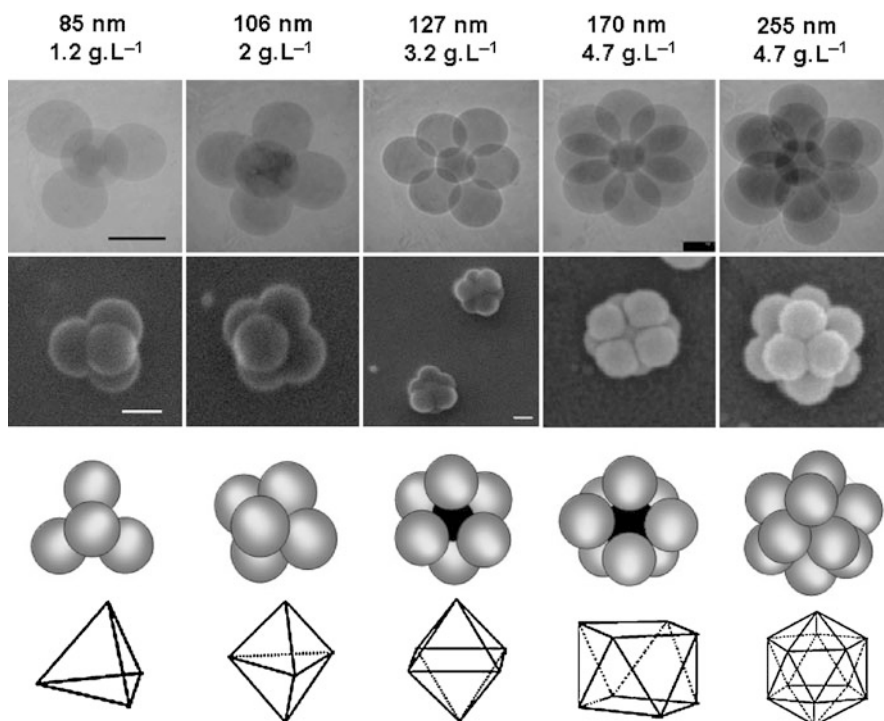


Fig. 4 *Top*: TEM and SEM micrographs of silica/polystyrene binary clusters obtained by emulsion polymerization of styrene (100 g.L^{-1}) using NP_{30} as surfactant (3 g.L^{-1}) and MPTMS-functionalized silica seeds of different diameters. *Scale bars*: 200 nm. The silica particle size and concentration are given above the images. *Bottom*: Sphere configurations, and polyhedra formed by drawing lines from the center of each PS nodule to its neighbors. Adapted from [34] with permission of Wiley-VCH

When the ratio of the number of silica seed particles to the number of PS nodules was equal to one, original silica/PS dumbbell-like or snowman-like morphologies were obtained [36, 37]. Anisotropic colloids have recently gained increasing interest due to their unique properties and performances. Moreover, these dissymmetrical colloids could be further processed into Janus particles (e.g., particles whose surfaces of both hemispheres are different from a chemical point of view). In a typical procedure, the mineral part of the snowman-like particles was selectively functionalized to anchor desirable groups. Then, the protecting PS mask was removed in a subsequent step by ultracentrifugation to allow further selective modification of the freshly generated new hemisphere (Fig. 5) [38]. Although several methods have been developed in the recent literature to synthesize Janus colloids, as reviewed by Perro and coworkers [39], none of them allows the production of large amounts of particles. In this context, the process depicted in Fig. 5, which is potentially amenable to industrial scale-up, offers a versatile methodology for fabrication of large quantities of nanometric Janus structures.

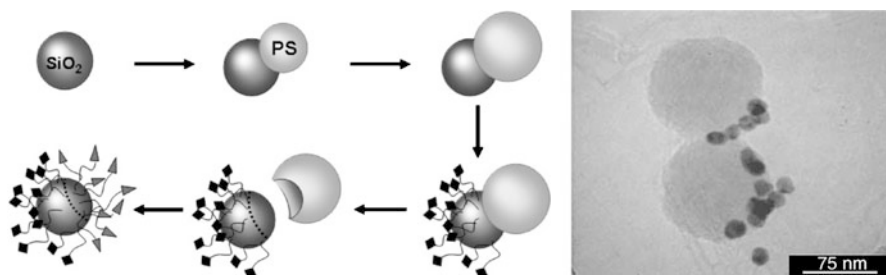


Fig. 5 *Left:* Consecutive stages involved in the formation of Janus nanoparticles through a protection–deprotection route. *Right:* TEM image of Janus nanoparticles. Reproduced from [38] with permission of the Royal Society of Chemistry

Following a slightly different approach, but still based on emulsion polymerization, Nagao et al. also recently reported the synthesis of anisotropic polymer particles composed of silica, poly(methyl methacrylate) (PMMA) and PS in two steps [28]. First, core–shell particles with a silica core and a crosslinked PMMA–PMPTMS copolymer shell were synthesized by emulsion copolymerization of methyl methacrylate (MMA) and MPTMS in the presence of MPTMS-grafted silica particles. The crosslinked polymer-coated silica particles were then used as seeds to grow protruding PS nodules on their surface, resulting in snowman-shaped composite particles (Fig. 2d).

It would be too simplistic to consider that the amount of grafted MPTMS is the only parameter that allows the control of particle morphology. Because interfacial tensions are heavily involved, the nature of the emulsion stabilizer, its concentration, the suspension pH, or the type of monomer could also significantly influence the final morphology [25, 29]. For example, by simply changing the type of surfactant used in the polymerization recipe, the particle morphology can change from multipod to excentered core–shell [33]. In addition, when the number of silica particles is significantly higher than the number of latex particles, composite colloids with internal occluded domains of several silica particles and “inverted” raspberry-like morphologies (the silica particles being located at the surface of the latex spheres) can also be obtained. The latter morphology is observed for low MPTMS grafting densities and is mainly a consequence of the surfactant-like behavior of the inorganic particles in this specific situation.

2.1.2 Macromonomer-Mediated Synthesis of Polymer–Silica Colloidal Clusters

Apart from the use of organosilanes that form covalent bonds with silica surfaces, chemical modification can also be performed through physicochemical adsorption of appropriate molecules (or macromolecules) active in the polymerization process. For instance, Reculosa et al. reported the synthesis of silica/PS raspberry-like

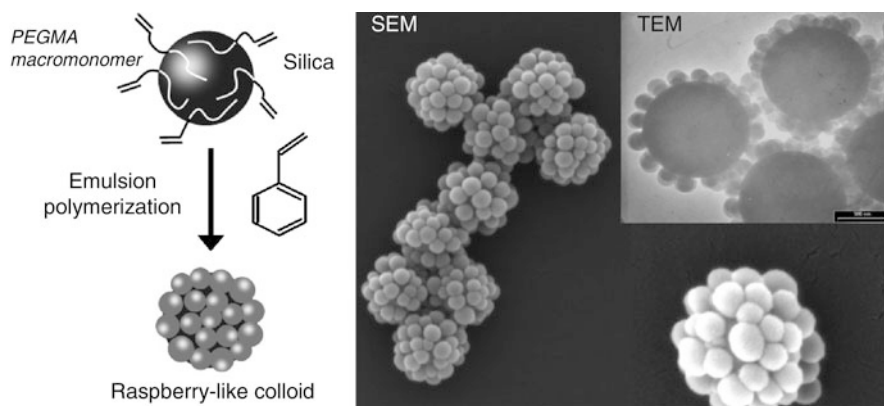


Fig. 6 *Left:* Elaboration of silica/polystyrene raspberry-like colloids through emulsion polymerization using a MMA-terminated poly(ethylene oxide) macromonomer (PEGMA) as coupling agent. *Right:* SEM and TEM pictures of the raspberry-like particles. Adapted from [40] with permission of American Chemical Society

colloids through emulsion polymerization using a MMA-terminated poly(ethylene oxide) macromonomer (PEGMA) [40]. Here, strong cooperative hydrogen bonding interaction between ethylene oxide units and surface silanols replaces covalent bonding, while copolymerization with the methacrylate group enables anchoring of the PS nodules on the silica seed (Fig. 6).

As previously, the morphology strongly depends on the ratio between the number of silica seeds and the number of growing nodules. Dissymmetrical, snowman-like and multipod-like colloids were obtained by varying these respective numbers [36, 41]. But, in contrast to MPTMS, which forms strong covalent bonds with the silica surface, PEO-based macromonomers display only weak, reversible interactions. Taking advantage of this feature, Perro et al. recently demonstrated the possibility of generating planar daisy-shaped, super-triangle and super-square colloidal clusters upon drying of composite suspensions containing silica particles surrounded by six and eight PS nodules, respectively (Fig. 7) [42]. It was shown that the binary clusters had a polyhedral shape in suspension and that the planar arrangement resulted from the falling-in of the PS nodules on the TEM grid. Electronic tomography experiments strongly supported the hypothesis and provided good evidence for the suspected underlying mechanism.

Alternative approaches involving molecules that combine the properties of a monomer with those of a surfactant (so-called polymerizable surfactants) have also been reported. For example, quaternary alkyl salts of dimethyl aminoethyl methacrylate (CnBr) surfactants were used to promote polymer encapsulation of silica gels in aqueous suspension [43, 44]. The polymerizable surfactant formed a bilayer on the silica surface, the configuration of which enabled the formation of core-shell particles. The CnBr amphiphilic molecule was either homopolymerized or copolymerized with styrene adsolubilized in the reactive surfactant bilayer. This concept of admicellar polymerization is detailed in Sect. 3.1. In the recent

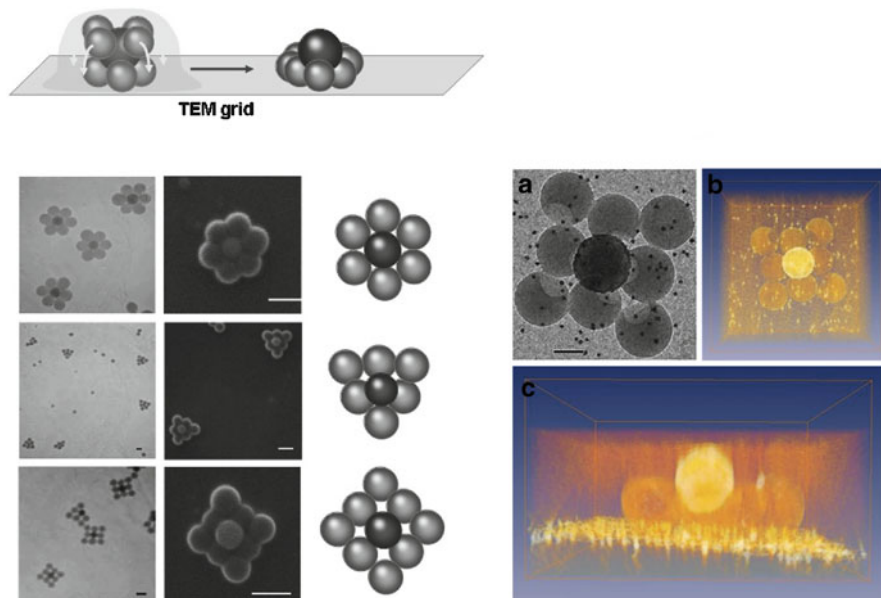


Fig. 7 *Left:* Daisy-shape, super-triangle and super-square colloidal binary clusters obtained by drying a suspension of hexapod- and octopod-like PS/silica particles elaborated through emulsion polymerization using PEGMA as compatibilizer. TEM images are shown next to the corresponding structures. *Scale bars:* 200 nm. *Right:* Super-square colloidal cluster as obtained after an octopod-like PS–silica cluster has fallen in on a copper grid coated with a carbon membrane. **(a)** TEM micrograph as observed in the direction perpendicular to the grid plane. *Scale bar:* 100 nm. **(b)** The same view in the form of a 3D reconstruction calculated from 60 TEM images acquired at different tilt angles (the brighter sphere is the silica seed). **(c)** The same 3D reconstruction observed in a direction parallel to the grid plane. Adapted from [42] with permission of The Royal Society of Chemistry

work of Qu et al., an anionic reactive surfactant was used in combination with a non-ionic surfactant to encapsulate silica particles through emulsion polymerization [32]. For low silica concentrations, and therefore low amounts of adsorbed surfactant, a “rough” shell was observed that was composed of homogeneously distributed polymer protrusions, which presumably originated from the coalescence of polymer nodules formed in the earlier stages of the polymerization. This result is fairly consistent with previous literature involving MPTMS as coupling agent and suggests that both processes follow similar reaction mechanisms.

Another relevant system involves oleic acid (OA) adsorption at the silica–water interface. This method was first demonstrated by Ding et al. [45] and was next used by Mahdavian and coworkers to encapsulate very small silica nanoparticles [46]. In the latter case, a core–shell structure with a core composed of aggregated silica particles and a shell made of MMA, styrene and acrylic acid (AA), was formed. The authors suggest that the polymerization proceeds through oligoradical entry into the OA admicelles.

2.1.3 Utilization of Auxiliary Comonomers

The strategy of using auxiliary (co)monomers exhibiting strong interaction with the surface of silica was first reported by Armes and coworkers, who described the homopolymerization of 4-vinylpyridine (4VPy) in the presence of an ultrafine aqueous silica sol [47]. Here, acid–base interactions between the silanol groups and the pyridine group of the poly(4VPy) chains promoted nanocomposite formation. The polymerization was performed at 60°C under soap-free conditions using ammonium persulfate as initiator, and led to the formation of nanocomposite particles with a “current-bun” morphology. The strategy was further extended to copolymers of 4VPy with MMA, styrene, *n*-butyl acrylate (BA) or *n*-butyl methacrylate (BMA) [48, 49]. In the case of BA, the resulting films showed a high gloss and a good transparency (even for high silica contents), as well as unusually low water uptake. These water-borne colloidal nanocomposites are of potential interest for the elaboration of fire-retardant or abrasion-resistant coatings. More recently, lightly crosslinked silica/P4VPy composite particles were successfully used to stabilize oil-in-water emulsion droplets at pH 8. The emulsion was destabilized upon decreasing the pH, thereby highlighting the pH-responsive properties of this new type of Pickering emulsifier [50, 51].

In addition to 4VPy, 1-vinyl imidazole (1VID) and 2-(methacryloyl) ethyl trimethyl ammonium chloride (MTC) were also shown to be efficient auxiliary comonomers by Chen and coworkers [52, 53]. Both strategies allowed the preparation of silica/PMMA raspberry-like composite particles, provided that enough comonomer was used. Although for 1VID, the composite particle size decreased with increasing silica content as expected, surprisingly the final particle size was independent of the silica concentration in the case of MTC. The overall synthetic scheme is illustrated in Fig. 8 for 1VID. These composite colloids are of potential interest for electrocoating applications, as recently reported by Kammona et al. [54].

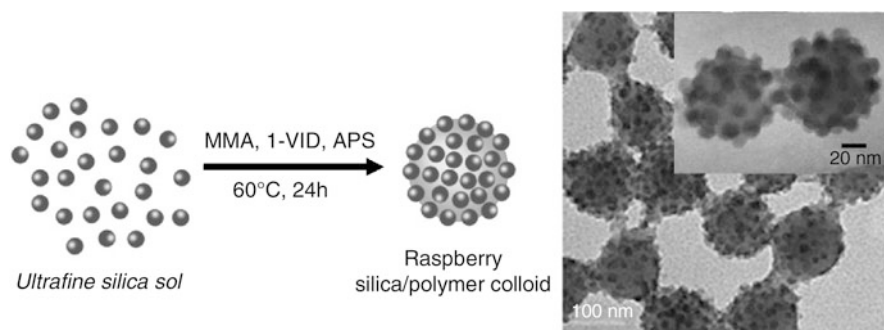


Fig. 8 *Left*: Reaction scheme for the formation of silica/PMMA raspberry-like colloids prepared using 1VID as auxiliary comonomer. *Right*: TEM images of obtained nanocomposite particles. Reproduced from [52, 54] with permission of American Chemical Society and Elsevier, respectively

All the above-mentioned nanocomposite colloid syntheses involving an auxiliary comonomer were performed in the absence of surfactant, the composite particles being stabilized by the nanosized silica particles (below 20 nm in diameter) adhering on their surface. The auxiliary comonomer method can also be extended to larger silica particles provided that some surfactant is used to stabilize the composite latex. Following this strategy, Cheng et al. reported the elaboration of silica/PMMA composite particles through conventional emulsion polymerization using silica particles with diameters of 60, 250, and 500 nm as seeds and 4VPy as auxiliary comonomer [55]. Raspberry-like or core-shell morphologies were obtained depending on the surfactant concentration, the monomer to silica ratio, and the type of monomer addition (either at once or semi-continuously).

2.1.4 Cationic Initiators

Another efficient synthetic route to the formation of polymer/silica nanocomposite colloids is through electrostatic adsorption of the cationic 2,2'-azobis (2-amidinopropane) dihydrochloride (AIBA) initiator. Pioneering works in this field were reported in 2001 by Luna-Xavier et al., who described the synthesis of silica/PMMA nanocomposite latexes by emulsion polymerization using AIBA in combination with a non-ionic surfactant [56–58]. The role of the suspension pH and the influence of the monomer, silica, and initiator concentrations on nanocomposite formation was investigated in depth and analyzed in a quantitative way [57]. Although electrostatic attraction between the cationic polymer end groups and the negatively charged silica surface was shown to be the driving force of composite particle formation at high pH, polymerization in adsorbed surfactant bilayers appeared to be the predominant mechanism at lower pH. Depending on the diameter of the silica beads, either strawberry-like (the silica being inside the particles) or core-shell morphologies (the latex forming the shell) were produced by this method. The approach was extended later by Qi and coworkers to nanometric silica and soft polymers [59]. Under such conditions, the silica particles were mainly located at the polymer surface. The raspberry-like colloids produced in this way were further encapsulated by a PMMA shell.

As shown in the recent work of Dupin et al., AIBA can also be advantageously combined with 2VPy to synthesize polymer/silica composite particles by soap-free emulsion polymerization [60]. Here, strong electrostatic interaction of the cationic initiator with the anionic silica ensured the formation of raspberry-like silica/polymer colloids with high silica aggregation efficiency as compared to the anionic persulfate initiator originally used by the same group (Sect. 2.1.3). Getting almost complete silica incorporation in such syntheses is essential because the excess silica sol may compromise the performance of the nanocomposite material in certain applications. The approach was next extended to a commercially available glycerol-modified silica sol in the absence of any added auxiliary comonomer [61–63]. The authors pointed out the importance of using the cationic AIBA initiator in combination with the glycerol-functionalized silica to achieve the desirable

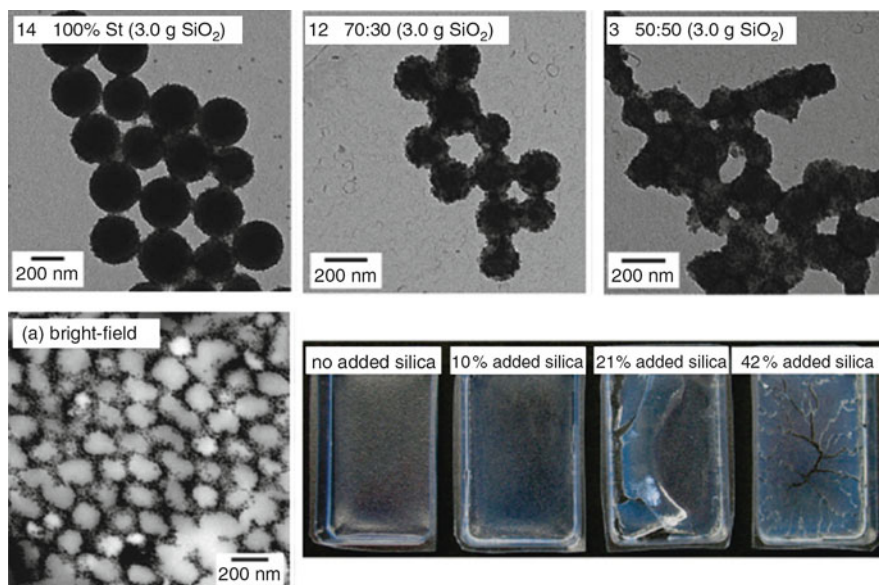


Fig. 9 Top row: TEM images of a series of nanocomposite particles synthesized by emulsion copolymerization of styrene and BA of varying mass ratios in the presence of a cationic azo initiator and a commercial ultrafine glycerol-modified silica sol. Bottom row: TEM of an ultramicrotomed section of nanocomposite particles obtained for a 50:50 styrene:BA mass ratio (bottom left). Digital photographs of nanocomposite films deliberately contaminated by increasing amounts of silica, showing significant embrittlement and illustrating the detrimental effect of excess silica on film properties (bottom right). Reproduced from [63] with permission of American Chemical Society

morphology in very high yields. This optimized protocol was further extrapolated to film-forming poly(styrene-*co*-BA) copolymers [63]. Figure 9 illustrates the morphological variations observed with increasing BA content and the resulting film nanostructure. As highlighted by the authors, these nanocomposites offer great advantages in coating applications compared to composite films prepared by simply mixing the silica sol with a film-forming latex suspension.

2.1.5 Soap-Free Latexes

As mentioned above, almost all polymerizations performed in the presence of an auxiliary comonomer were conducted without surfactant [47–55, 60]. Since these early works, several groups have demonstrated that silica particles can stabilize polymer latexes provided that wetting of the nanoparticles with the polymer chains is favorable [64–68]. The overall process, often referred to as Pickering stabilization by reference to the stabilization of two immiscible liquids by solid particles [69], has

recently found a resurgence of interest as illustrated by the numerous examples provided throughout this review. More details on Pickering emulsions can be found in the review article by Bon [70].

Although the aforementioned articles are relevant to this section, the intent of the following is to complement – rather than repeat – a discussion on these papers. For instance, Zhang et al. have reported the synthesis of latexes with 40% solid content through emulsifier-free emulsion polymerization of BA, hydroxyethyl methacrylate (HEMA), and AA in the presence of a nanometric colloidal silica suspension [65]. Although the mechanism of composite particle formation was not discussed, this is to our knowledge the first example of the synthesis of high-solid-content, film-forming polymer/silica composite particles in the absence of surfactant. Another particular example of interest is the recent work of Colver et al. on the synthesis of PMMA latexes armored with 25-nm diameter Ludox silica nanoparticles [66]. Here, the suspension pH was the key to the process and was maintained around 5.5 to ensure the formation of raspberry-like particles that were uniformly distributed in size without any coagulation. Although the authors did not discuss this point in detail, they stressed that the solid content could be increased up to 45%. Unfortunately, for unclear reasons, the strategy was unsuccessful for both styrene and butyl acrylate, which illustrates that there is still a lot of work to do before getting a clear picture of particle nucleation and stabilization in such systems. Multilayered composite colloids with a hairy outer layer of polyacrylonitrile or a soft shell of poly(*n*-butyl acrylate) were obtained by feeding the armored colloids with the corresponding monomers in the presence of an anionic surfactant. Interestingly, the silica nanoparticles were found to migrate and expand through the soft shell (Fig. 10).

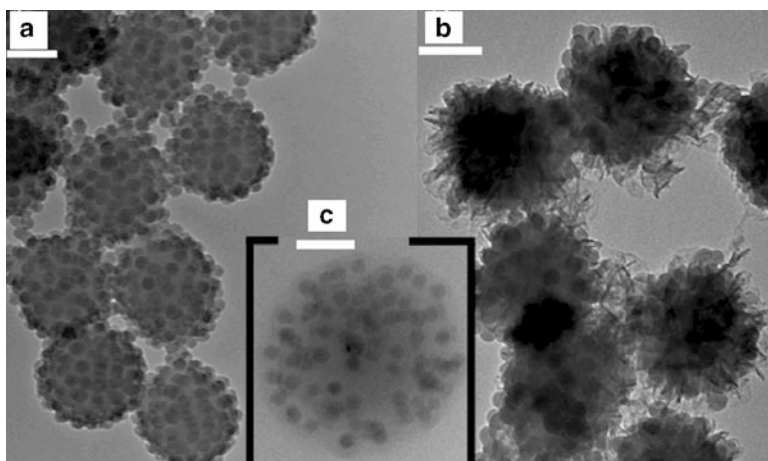


Fig. 10 TEM images (scale bars: 100 nm) of (a) PMMA latex armored with Ludox silica nanoparticles. Multilayered nanocomposite polymer colloids with (b) a “hairy” outer layer of polyacrylonitrile, and (c) a soft shell of poly(*n*-butyl acrylate). Reproduced from [66] with permission of American Chemical Society

Also relevant to this section is the very recent work of Sheibat-Othmann and Bourgeat-Lami on the synthesis of PS latex particles stabilized by Klebosol and Ludox silica particles in the presence of a PEGMA macromonomer [68]. In contrast to the previous work of Colver et al., polymerizations performed under basic conditions provided colloidally stable latexes using Ludox silica and styrene monomer. The PEGMA macromonomer probably plays a determinant role that makes both systems quite different from the physico-chemical point of view, although similar ingredients were used. Even if it can be argued that polymerization into monomer droplets is unlikely in such “Pickering” polymerizations due to the large size of the emulsion droplets compared to the size of the composite particles, the authors showed that the monomer droplets could efficiently compete for silica adsorption, leading to some temporary instability during polymerization. Besides these physico-chemical aspects, the study highlighted the importance of stirring on the reaction rate and particle stability and also showed that, under certain conditions, the silica particles formed a barrier to radical absorption and decreased the polymerization rate.

Finally, it is also worth mentioning the BASF patent on the synthesis of high-solid-content polyacrylate/silica latexes incorporating a high amount of silica [71]. The silica particles appear to be glued together by the polymer, thereby forming some kind of heterocoagulated polymer/silica beads with a rough surface [71]. These latexes have found a commercial application as transparent, flame retardant, scratch-resistant coatings [72]. To our knowledge, this is one of the first and rare examples of commercial polymer/silica nanocomposites.

2.2 Coating of Polymer Latexes with a Silica Shell

Core-shell particles have attracted much research attention in recent years because of their great potential in the protection, modification, and functionalization of the core with suitable shell materials to achieve specific physical or chemical performances. For instance, the optical, electrical, thermal, mechanical, magnetic, and catalytic properties of core particles can be finely tuned by coating them with a thin mineral shell [73, 74]. Silica shells are produced by a variety of methods that can be divided into two groups: (1) the layer-by-layer self-assembly of preformed silica nanoparticles on oppositely charged templates, and (2) seeded polycondensation techniques involving sol-gel precursors. The former method is outside the scope of this article and only the second method will be discussed.

Although many inorganic surfaces can be directly coated with silica because of the significant affinity between both materials, latex particles must be functionalized by grafting or adsorption of appropriate compounds that can enhance the coupling (and thus deposition) of the silica precursor on their surface. These molecules are either groups capable of undergoing a chemical reaction with the sol-gel precursor or ionic molecules capable of promoting electrostatic attraction between the latex core and the inorganic shell.

For instance, Tissot et al. reported the successful incorporation of silanol groups on the surface of PS latex particles using MPTMS as a functional (co)monomer [75–77]. These surface silanols enabled the subsequent growth of a silica shell onto the PS seed by addition of TEOS and ammonia to the colloidal suspension, either in water or in a mixture of ethanol and water. No secondary-nucleated silica particles were formed, indicating strong affinity of the sol–gel precursor for the polymer surface. Burning of the latex core resulted in the formation of hollow silica spheres. One main advantage of this method is that the nature and the size of the polymeric core can be tuned by conventional polymer colloid chemistry, while the shell thickness can be accurately controlled by the silica-to-polymer weight ratio and the diameter of the latex core. The technique was also successfully applied to the synthesis of core–shell latexes made of a soft poly(BA) core coated by a rigid silica shell. Such soft/hard core–shell particles can find applications as nanofillers for impact resistance improvement.

Following a related approach, Castelvetro et al. reported the formation and properties of hybrid latex films resulting from the coalescence of low T_g poly(BA-*co*-MMA-*co*-MPTMS) terpolymer latex particles coated by a silica shell [78]. The latex was synthesized at neutral pH by semi-continuous emulsion polymerization under starved-feed conditions in order to protect the MPTMS monomer from premature hydrolysis and condensation reactions. A substantial amount of free silanols were therefore available for further reaction with the silica precursor. In order to avoid the formation of a densely crosslinked silica network around the latex core, which may significantly alter film formation, the pH was kept at around 2 (at this pH, hydrolysis is promoted and condensation is significantly retarded). TEM and AFM studies of the nanocomposite film indicated that the silica shell formed a continuous percolating network throughout the polymer matrix. A porous film of interconnected hollow silica spheres was next elaborated by thermo-oxidative decomposition of the organic phase.

It is also possible to grow silica shells without functionalizing the latex core. In this case, the opposite charges developed on the core and shell materials promote shell formation through electrostatic attraction. For example, Hotta and coworkers reported the deposition of a thin silica film onto PS spheres by the addition of an acidic hydro-alcoholic solution of pre-hydrolyzed TEOS [79]. The final silica film thickness was optimum at pH below the isoelectric point of silicic acid, at which the electrostatic attraction between the silica precursors and the negatively charged PS spheres was maximized. Ordered macroporous materials were subsequently formed by centrifuging the silica-coated PS particles and removing the latex core by calcination. In a related approach, Cornelissen [80] and Lu [81] used amino-functionalized PS spheres to promote charge attraction between the PS beads and the silica shell. Above pH 10, the amine-functionalized template is slightly positively charged and, consequently, the silica sols could easily nucleate on the surface of each PS bead and eventually merge and grow into a thin uniform silica shell. A similar approach was recently followed by Yang et al., who adsorbed poly-L-lysine (a polyamino acid) on amino-functionalized PS spheres [82]. It was found that poly-L-lysine promoted the growth of a continuous shell without the concurrent formation of secondary nucleated silica particles (Fig. 11).

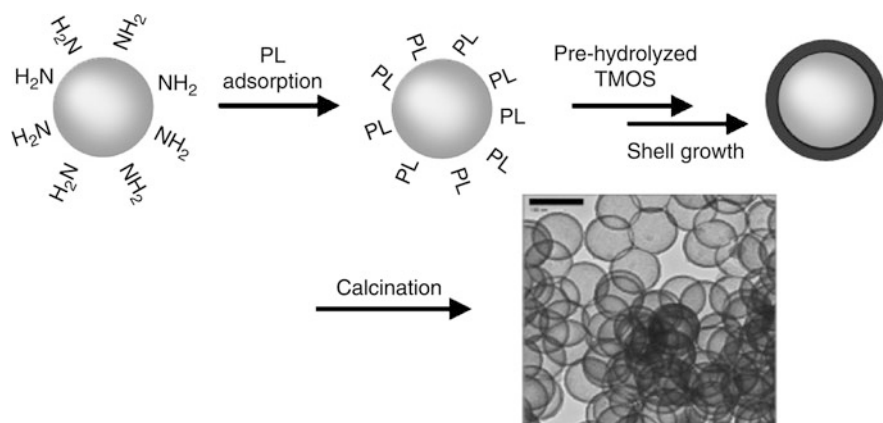


Fig. 11 Representation of the coating of polymer colloids with silica using poly-L-lysine as compatibilizer, with TEM image of the resulting hollow silica spheres. Scale bar: 100 nm Adapted from [82] with permission of American Chemical Society

Graf and coworkers reported a general strategy to coat polymer particles with silica that provided uniform and smooth coatings without the use of silane coupling agents or electrostatic attraction [83]. Here, the deposition was assisted by the addition of poly(*N*-vinyl pyrrolidone) (PVP). Depending on whether PVP was adsorbed flat on the surface or in the form of trains (which in turn depends on PVP molecular weight), either rough or smooth silica coatings were obtained. PVP was also used by Kobayashi et al. with the aim of suppressing the formation of free-standing silica particles and improving shell uniformity [84]. However, the strategy was less successful in this case, as judged from the TEM images. This last example and many other nonconclusive works show that controlling the homogeneity and the thickness of the silica shell without forming rough surfaces and/or plain colloids requires a set of experimental conditions to be fulfilled and is particularly challenging. Although some approaches were undoubtedly successful, there is no universal method to date that allows the formation of high-solid-content suspensions of silica-coated particles with thick, smooth, and uniform shells. There is still much work to be done in this field before one can envisage commercial applications of such products.

3 Synthesis of Magnetic Latex Particles

During the last few years, different synthetic procedures have been reported for the synthesis of magnetic nanoparticles. These methods include co-precipitation, thermal decomposition and/or reduction, microemulsion synthesis, and hydrothermal synthesis. Despite poor shape control and quite polydisperse particles, co-precipitation is probably the simplest synthetic route. By contrast, thermal decomposition is experimentally more demanding but affords the best results in

terms of size and shape control of the nanoparticles. To date, these two routes are the most explored, and they provide magnetic nanoparticles on a large scale. This probably explains why iron oxides used in emulsion polymerization are, in most cases, obtained by co-precipitation. This consists of aqueous solutions of iron salts ($\text{Fe}^{2+}/\text{Fe}^{3+}$) precipitated by the addition of a base, usually under inert atmosphere, at room or elevated temperatures. Various parameters can influence the size, morphology, and composition of the magnetic nanoparticles: Fe^{2+} to Fe^{3+} initial ratio, temperature, pH, and ionic strength. Stable aqueous or organic dispersions of the magnetic nanoparticles (3–30 nm in size) are obtained by the use of surface-active species capable of generating repulsive interactions between the particles. These species could be: (1) charged molecules (e.g., citrate or tetramethyl ammonium ions), (2) surfactant (e.g., OA), or (3) polymer [e.g., poly(acrylic acid) (PAA) or polyvinyl alcohol (PVA)]. The obtained stable dispersions are often called “ferrofluids”. Indeed, the strong interactions between the solvent molecules and the iron oxide nanoparticles ensure a uniform magnetic behavior of the whole fluid, which behaves like a single-phase system when a magnetic field is applied [85]. Regarding their magnetic properties, these nanoparticles are superparamagnetic, which means that they respond to a magnetic field but lose their magnetization when the field is removed. Readers who are interested in a detailed review on the synthesis, properties, and applications of magnetic nanoparticles are referred to the recent paper from Lu et al. [86].

Bare magnetic nanoparticles are sensitive to oxidation in air therefore it is necessary to develop efficient strategies to avoid any stability issues. This can be achieved by the production of a polymer shell, which will not only protect the inorganic component, but will also provide the nanoparticles with selective functionalities needed for further applications. The nanoparticles can also be gathered into one larger polymer particle. Indeed, polymer particles incorporating magnetic iron oxide nanoparticles such as magnetite (Fe_3O_4) or maghemite ($\gamma\text{-Fe}_2\text{O}_3$) find a wide range of applications, notably in catalysis, environment and food analysis, water treatment, and biotechnology, for which the magnetic properties of the particles are sought for effective separation steps [86–88]. To date, the major field of interest remains the biomedical field, in which the magnetic nanoparticles have been successfully used as solid support for the purification, extraction, and concentration of biomolecules in biomedical diagnostics, as contrast agents in magnetic resonance imaging, as mediators in hyperthermia, and as carriers for guided drug delivery [86, 89–92].

Whatever the targeted applications, the PSD has to be narrow to ensure a uniform response to an external magnetic field, and the magnetic material has to be homogeneously distributed and properly encapsulated in order to avoid any leakage of iron oxide. Moreover, appropriate surface functionalities should allow further selective binding with (bio)molecules. Finally, the size of the magnetic particles must be finely tuned according to the targeted application. Those in the submicrometer range are particularly interesting because of their low sedimentation rate, large specific surface area for immobilization of (bio)molecules, and potential integration in microfluidic-based technologies.

Instead of presenting an exhaustive survey of all the literature, which would by far exceed the scope of this review, we will present typical and representative

examples of the synthesis of magnetic latex particles using emulsion polymerization as one of the key step of their synthesis. In addition, this article will focus on iron oxide nanoparticles such as magnetite Fe_3O_4 and maghemite $\gamma\text{-Fe}_2\text{O}_3$, which are the most-described magnetic nanoparticles for the synthesis of magnetic latex particles. Besides, they are currently the only accepted non-toxic magnetic materials for medical applications [93]. The literature also offers a few examples using cobalt [94], cobalt ferrite (CoFe_2O_4) [95], nickel or cobalt metal [96–98], $\text{Ni}_{0.5}\text{Zn}_{0.5}\text{Fe}_2\text{O}_4$ [99], and NiS [100].

3.1 Encapsulation of Iron Oxide Nanoparticles by Emulsion Polymerization

The preparation of magnetic latex particles using emulsion polymerization in the presence of a freshly prepared ferrofluid was first reported in the late 1970s and at the beginning of the 1980s but was not investigated in detail [101–103]. Since then, a great number of studies have been published in the literature, and magnetic nanoparticles are one of the most documented types of inorganic particle being used to form composite colloids. Most of the reported works rely on the synthesis of polymer particles through conventional emulsion polymerization methods carried out in the presence of colloidal iron oxides (most often used as magnetic seeds). An overview of the various methods reported in the literature is given in the following sections.

3.1.1 Surfactant Bilayer (Admicellar Polymerization)

One of the basic requirements for efficient encapsulation of inorganic nanoparticles is to enhance the interfacial affinity between the nanoparticles and the monomer. One frequently encountered strategy for achieving this is to create hydrophobic loci inside a bilayer of surfactant(s). Indeed, the primary surfactant is the one coating the nanoparticles after their synthesis and allowing dispersion of the nanoparticles in nonpolar solvents. Once the excess of the primary surfactant is removed, the nanoparticles are coated with a secondary surfactant to form a self-organized bilayer of the two surfactants on the surface of the nanoparticles, thus allowing their dispersion in water [104–106]. The hydrophobic interlayer thus formed between the two surfactants can solubilize the monomer and finally promote the polymerization close to/at the vicinity of the surface of the nanoparticles, according to the so-called admicellar polymerization mechanism (Fig. 12).

Meguro et al. were among the first to explore this method for the encapsulation of non-magnetic iron oxide ($\alpha\text{-Fe}_2\text{O}_3$) and titanium dioxide through emulsion polymerization of styrene adsolubilized into adsorbed bilayers of sodium dodecyl sulfate (SDS) [107]. Using the same concept, magnetic PS and PMMA particles were obtained by Yanase et al. [108, 109] using a commercial ferrofluid with magnetite particles covered by sodium oleate and sodium dodecylbenzenesulfonate

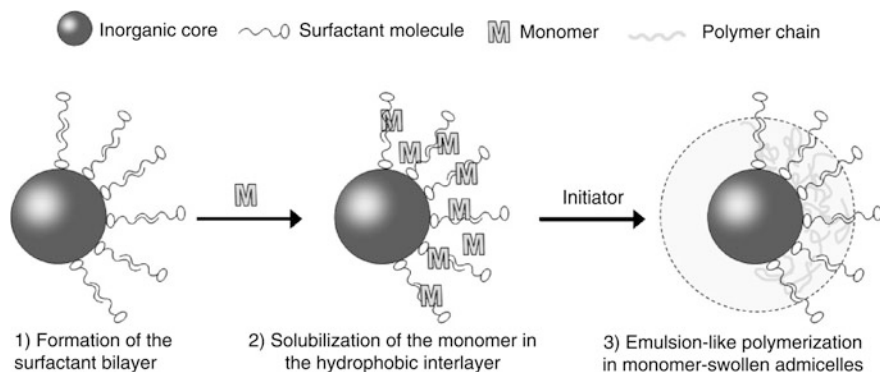


Fig. 12 Pigment encapsulation through an emulsion-like polymerization reaction. The process involves (1) formation of surfactant bilayers, (2) solubilization of monomer, and (3) free radical polymerization

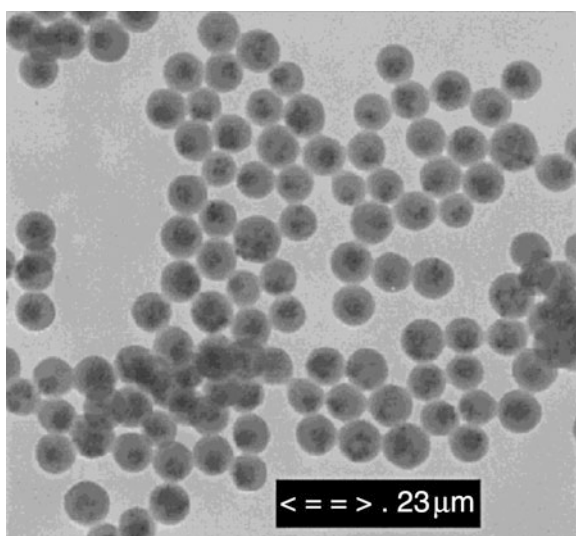


Fig. 13 TEM image of PS-iron oxide composite particles. Reprinted from [110] with permission of the American Chemical Society

(SDBS). The process yielded PS particles with up to 20 wt% of encapsulated Fe_3O_4 . However, the latex yield was generally low and the PSD quite broad, leading to an inhomogeneous distribution of magnetite from one particle to another. Still using the bilayer procedure with OA and SDBS-coated $\gamma\text{-Fe}_2\text{O}_3$, highly charged and monodisperse superparamagnetic latex particles of poly[styrene-*co*-MMA-*co*-sodium styrene sulfonate (NaSS)] were prepared (Fig. 13). These were then assembled into colloidal crystals, which were found particularly suitable for the creation of unique magnetically induced photonic bandgap materials [110, 111].

Magnetic latex particles of PMMA (in the range of 100 ± 50 nm) were obtained by soapless seeded emulsion polymerization performed in the presence of 10-nm Fe_3O_4 nanoparticles coated with a bilayer of lauric acid [112]. This work shed light on the importance of keeping a good balance between the amount of iron oxide nanoparticles (and hence the surfactant bilayer) and the initial amount of MMA: too high an amount of monomer (higher than the bilayer could accommodate, thus leading to destruction of the bilayer) led to the expected seeded emulsion polymerization but also to a crop of particles generated by self-nucleation (including either homogeneous or micellar nucleation) (Fig. 14). The particle size was consequently larger in this case. Kinetic modeling of this system was also established [113]. In an approach very similar to Wang's work, $\gamma\text{-Fe}_2\text{O}_3$ modified by myristic acid and soluble in octane was dispersed in SDS solution [114]. Subsequent polymerization of styrene, divinylbenzene (DVB) and NaSS provided composite particles, but iron oxide nanoparticles were confined to the surface of the polymer particles. These particles nevertheless easily aligned in the presence of a magnetic field and could find potential applications in proton-exchange membranes. Another related work reports the soapless emulsion polymerization of styrene/BA/methacrylic acid (MAA) in the presence of sodium dodecylsulfonate– Fe_3O_4 [115]. The influence of various parameters on particle size and PSD was discussed, in particular the effect of the polarity medium (through the addition of a polar solvent).

The admicellar polymerization concept was also applied to the synthesis of thermosensitive magnetic latex particles based on *N*-isopropylacrylamide (NIPAM). In this case, however, the polymerization could be better defined as seeded precipitation polymerization owing to the water solubility of this monomer. Kondo et al. [116] were among the first to synthesize PNIPAM particles using Fe_3O_4 nanoparticles covered with two layers of OA and SDBS. *N,N'*-Methylene bisacrylamide

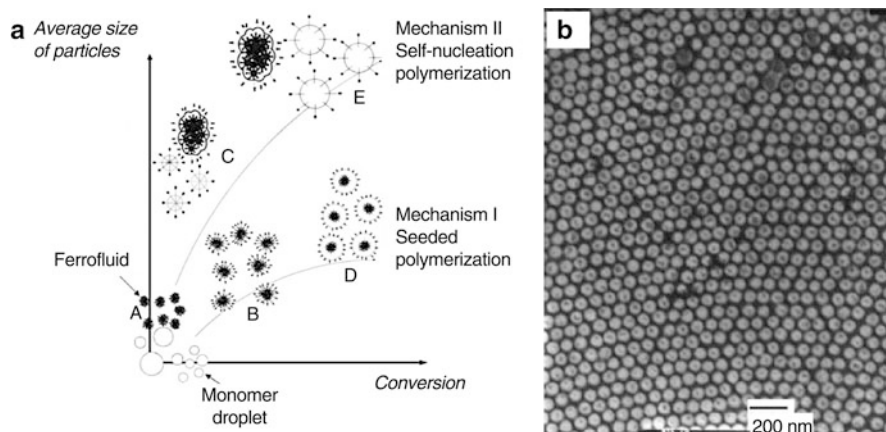


Fig. 14 (a) Mechanisms proposed in [112] for particle nucleation and growth in the case of MMA soapless emulsion polymerization in the presence of Fe_3O_4 coated with a bilayer of lauric acid. (b) TEM image of an example of composite magnetic particles obtained. Adapted from [112] with permission of Wiley Periodicals

(MBA) was used as a crosslinker, and MAA allowed the introduction of carboxyl groups for the subsequent covalent immobilization of proteins. Monodisperse magnetic and thermosensitive particles loaded with up to 10 wt% of magnetic material were obtained and successfully used for enzyme immobilization. The thermosensitivity of the particles could be varied by introducing styrene [117]. First, magnetite nanoparticles modified by a double layer of OA and SDBS were encapsulated inside PS particles using surfactant-free emulsion polymerization. These particles were then used as seeds for the emulsion copolymerization of NIPAM and MAA. The surface of the obtained submicrometer particles (loaded with up to 10 wt% of magnetic material) were then functionalized via covalent immobilization of bovine serum albumin (BSA) using carbodiimide chemistry, and successfully used in anti-BSA antibody purification. In some cases, NIPAM was polymerized in the presence of a few percent of AA in order to impart pH sensitivity [118].

More recently, Lee et al. [119, 120] described the synthesis of the same kind of particles (without, however, referring to the previous work of Kondo). The difference lies in the coverage of Fe_3O_4 nanoparticles, which were in this case coated with either a bilayer of lauric acid or with PAA oligomers. For each surface treatment, the influence of the initiator (either potassium persulfate (KPS) [119] or AIBA [120]) on the mechanism of particle formation, PSD, and particle morphologies was discussed. PSD was generally quite broad and the iron oxide nanoparticles were either located in the PS core or adsorbed at the surface. Further encapsulation with poly(NIPAM-*co*-MAA) provided core-shell particles.

In many of the works described above, a functional monomer such MAA, AA, or NaSS was introduced to provide the particles with chemical groups that allowed their utilization in specific applications. A variety of functional magnetic particles were prepared for various purposes. For instance, carboxyl-functionalized magnetic PS particles were produced from 10-nm Fe_3O_4 coated with a bilayer of OA and sodium 10-undecenoate as primary and secondary surfactants, respectively [121]. The authors discussed the influence of the initiator on the morphology of the final particles (homogeneous encapsulation with KPS, not with benzoyl peroxide). Up to 42 wt% of magnetic material could be encapsulated (with a corresponding saturation magnetization, M_s , of 30 emu g^{-1}). Successive immobilization of proteins such as BSA was achieved. In the same way, chaperone protein was immobilized on carboxyl-functionalized magnetic particles to assist the *in vitro* refolding of a lipase (i.e., *B. cepacia* lipase) [122].

β -Diketone groups were introduced on the surface of magnetic particles through the emulsion copolymerization of styrene and acetoacetoxyethyl methacrylate (AAEM) in the presence of sodium-oleate-modified 10-nm $\gamma\text{-Fe}_2\text{O}_3$ nanoparticles [123]. Varying the initial iron oxide to monomer ratio or initial AAEM concentration led to composite particles incorporating up to 15 wt% of maghemite (M_s ca. 16 emu g^{-1}) and displaying various morphologies, including raspberry-like particles. The PSD was, however, quite broad, whatever the final particle size (600–200 nm, depending on the initial recipe). In another relevant work, Pd catalysts were immobilized onto superparamagnetic polymer nanoparticles consisting of a $\gamma\text{-Fe}_2\text{O}_3$ core and a poly[styrene-*co*-DVB-*co*-4-vinylbenzene chloride (VBC)]

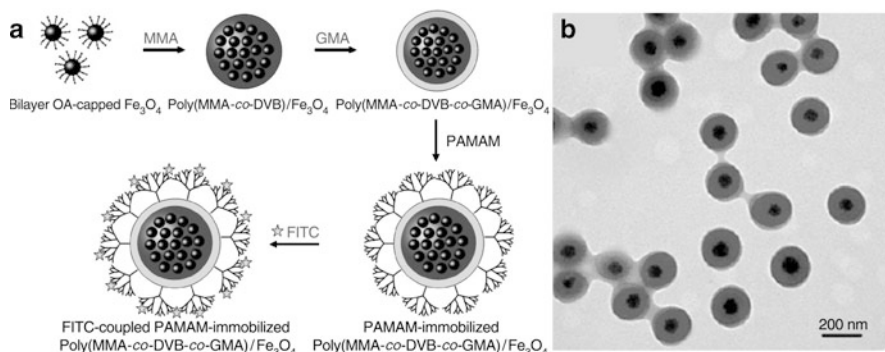


Fig. 15 (a) Preparation of dendritic PAMAM-immobilized magnetic poly(MMA-co-DVB-co-GMA) particles and coupling with FITC. (b) TEM image of the magnetic poly(MMA-co-DVB-co-GMA) microspheres with 10 wt% of DVB. Adapted from [126] with permission of the American Chemical Society

shell [124]. The chloro group was used to introduce N-heterocyclic carbenes that could form strong complexes with Pd catalysts. The obtained Pd-supported nanoparticles successfully promoted Suzuki cross-coupling reactions. Acrylamide (AAm) was recently used as a functional monomer in the emulsion polymerization of styrene carried out in the presence of Fe_3O_4 coated by OA/SDS bilayer [125]. Using microwave irradiation to initiate the polymerization, monodisperse magnetic particles of poly(styrene-co-acrylamide) were formed with up to 46 wt% of magnetite. The aim of the authors was to use amidocyanogen groups for further covalent binding of biomolecules; however, this was not demonstrated. Magnetic particles with an increased degree of functionality were recently produced through the attachment of poly(amidoamine) (PAMAM) dendrimers using the epoxy groups available at the surface of poly[MMA-co-DVB-co-glycidyl methacrylate (GMA)] magnetic particles obtained using bilayer-OA-coated Fe_3O_4 nanoparticles (Fig. 15) [126]. Highly fluorescent particles were then obtained through the covalent coupling of fluorescein isothiocyanate (FITC).

As illustrated by the studies detailed above, admicellar polymerization can lead to various morphologies and very often not to the expected core-shell ones. Nevertheless, despite the variety of obtained morphologies, the aforementioned particles (when properly functionalized) have found applications in various fields such as catalysis, optoelectronics, or biotechnology. Some of the works presented so far show very interesting and promising results, with an effective and homogeneous distribution of iron oxide nanoparticles inside the synthesized polymer particles, together with a high magnetic content. But, most suffer from one or several of the following drawbacks: the PSD can be quite broad, the magnetic content is not systematically high, the distribution of iron oxide may be inhomogeneous from one particle to another and inside the particle (in the core versus at the periphery), or the solid content of the final latex can be quite low. To circumvent some of these limitations (but unfortunately not all of them at the same time), alternative procedures have been developed.

3.1.2 Other Surface Coatings of Iron Oxide Nanoparticles

The surfactant bilayer strategy is obviously not the only method that has been developed to favor polymerization at the surface of iron oxide nanoparticles. Thus, other (macro)molecules have been employed to this aim. Recently, various polymers such as PAA [119, 120], PMAA [127], chitosan [128], or dextran derivatives [129–131] have been used as steric stabilizers to form aqueous dispersions of iron oxide nanoparticles for use in emulsion polymerization. In the case of PMAA [127], the cationic AIBA azo initiator was first adsorbed on PMAA-coated Fe_3O_4 to favor monomer polymerization in the vicinity of the nanoparticles. The magnetic nuclei thus formed aggregated and yielded magnetic PS particles with a raspberry-like morphology. Dextran derivatives were used for the synthesis of PGMA magnetic particles.

Poly(ethylene glycol) (PEG) was also used to modify the surface of iron oxide nanoparticles. For instance, fluorescent and magnetic polysaccharide-based particles were prepared in three steps [132]. First, commercial magnetite powder and europium phthalate complex (fluorescent) were blended and dispersed in a PEG solution to obtain fluorescent magnetite colloid particles (FMCPs). Copolymerization of styrene and maleic anhydride in the presence of FMCPs seeds led to magnetite europium phthalate/poly(styrene-*co*-maleic anhydride) core-shell composite microspheres. Finally, heparin was conjugated with the surface anhydrides to form FMCPs/SMA heparin glycoconjugate core-shell composite particles. In another work, commercial Fe_3O_4 was modified with PEG for the synthesis of azidocarbonyl-functionalized magnetic particles via a two-step procedure [133]. First, magnetic poly(styrene-*co*-AAm-*co*-AA) particles were obtained through emulsion polymerization performed in water/ethanol mixture in the presence of PEG-modified Fe_3O_4 and a small amount of SDS. Azidocarbonyl groups were then converted into amido groups and successfully used for covalent protein immobilization. Margel's group very recently reported the use of gelatin-modified $\gamma\text{-Fe}_2\text{O}_3$ in the emulsion polymerization of two particular monomers: (1) an iodinated methacrylate, allowing the synthesis of radio-opaque magnetic core-shell nanoparticles for X-ray imaging applications [134], and (2) a fluorinated acrylate, leading to the formation of magnetic core-shell nanoparticles used for inhibition of insulin amyloid fibril formation [135]. Using the same polymerization procedure, the formation of poly(divinyl benzene) (PDVB)-coated maghemite nanoparticles was also studied [136]. Air-stable carbon-coated iron ($\alpha\text{-Fe/C}$) crystalline nanoparticles were obtained by annealing the PDVB-coated maghemite nanoparticles to form magnetic particles with higher Ms (83 emu g^{-1} versus 33 emu g^{-1} for $\gamma\text{-Fe}_2\text{O}_3$ based particles).

3.1.3 Emulsion Polymerization-Related Procedures

Some of the works depicted in the literature cannot be rigorously classified as emulsion polymerization methods. These strategies, sometimes quite original and innovative, usually imply multiple steps (one of them being emulsion polymerization).

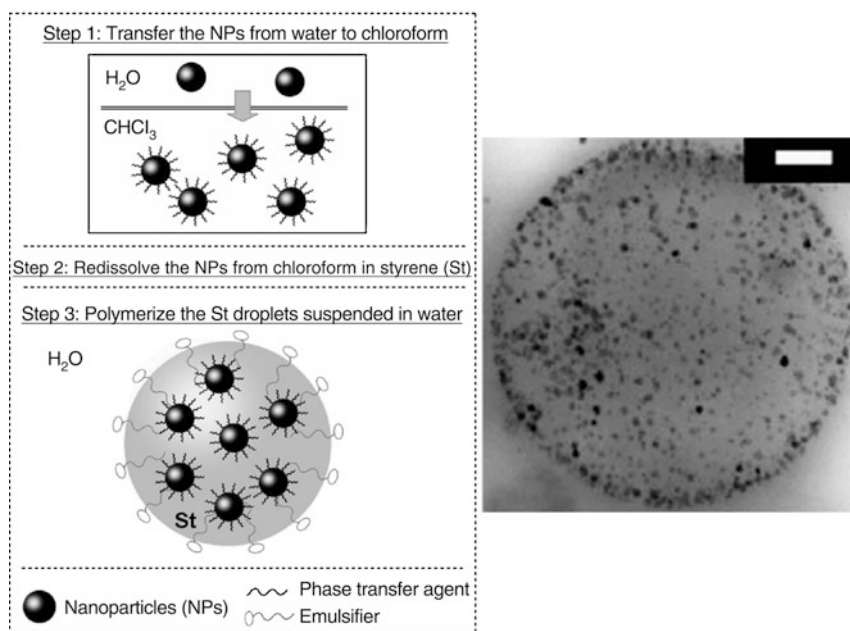


Fig. 16 Synthesis of Fe_3O_4/PS particles. *Left*: Scheme of the process. *Right*: TEM photo of Fe_3O_4/PS particle (scale bar: 100 nm). From [137] with permission of the Royal Society of Chemistry

They rely on vigorous stirring or ultrasonication, either to help the dispersion of iron oxides in water or in the monomer, or to achieve a fine dispersion of the monomer droplets before starting the polymerization. They also imply an intermediate step consisting in the encapsulation of several iron oxides in a silica particle, or the use of a magnetic emulsion as a seed instead of iron oxide nanoparticles. These processes are described below.

Yang et al. [137] described a very nice approach (though inadequately termed “mini-emulsion polymerization”) for efficient encapsulation of aqueous nanoparticles such as Fe_3O_4 , Au, and CdTe (Fig. 16). The nanoparticles were first transferred from water to chloroform using a polymerizable surfactant as phase transfer agent. The solid NPs obtained after chloroform evaporation were then dissolved in styrene containing 2,2'-azobis(isobutyronitrile) (AIBN). An aqueous solution of a polymerizable emulsifier and a co-emulsifier (Triton X-100) was added to the styrene solution and the resulting mixture was submitted to mechanical stirring for 30 min. Polymerization was then carried out at $80^\circ C$ for 6 h. The resulting magnetic polymer particles showed a very homogeneous distribution of Fe_3O_4 inside the polymer particles of a few micrometers (typically $3\ \mu m$, with broad PSD). Bifunctional (magnetic with Fe_3O_4 and fluorescent with CdTe) particles were also reported by the same team [138]. Better results in terms of fluorescence were obtained if the magnetic NPs were first coated with silica and functionalized with MPTMS. In addition, use of ultrasonication instead of mechanical stirring allowed decreasing particle size (from a few micrometers to 136 nm) and narrowing of the PSD.

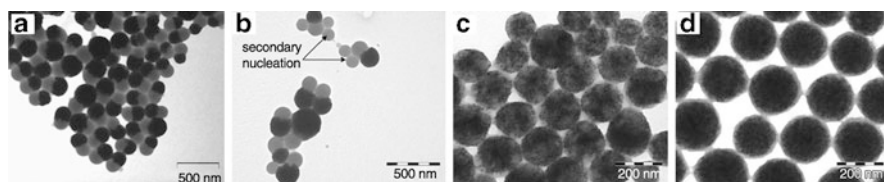


Fig. 17 TEM images of PS magnetic particles obtained with (a) AIBN only, (b) KPS only, (c) AIBN/DVB, and (d) KPS/DVB. Adapted from [139] with permission of Wiley Periodicals

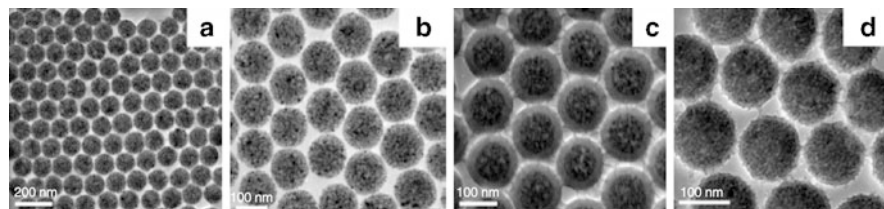


Fig. 18 (a, b) TEM images of as-synthesized magnetic $\text{Fe}_3\text{O}_4/\text{PS}$ nanospheres, and (c, d) silica-coated magnetic $\text{Fe}_3\text{O}_4/\text{PS}$ nanospheres. From [140] with permission of the American Chemical Society

Instead of using stable aqueous dispersions of iron oxides, Montagne et al. [139] successfully synthesized highly magnetic latex particles (60 wt% of magnetic material), starting from a commercial oil-in-water magnetic emulsion. Depending on the initial conditions, various morphologies could be obtained (Fig. 17). The desired core-shell structure was effectively obtained with a given styrene to DVB ratio, KPS as the initiator, and an amphiphilic functional copolymer as the stabilizer of the starting magnetic emulsion. The use of this copolymer not only provided the latex with a high degree of functionalization but also ensured its colloidal stability in media of high ionic strength.

A multistep procedure combining modified miniemulsion/emulsion polymerization and the sol-gel technique was implemented by Xu et al. [140] to obtain monodisperse, nanoscale (100 nm), superparamagnetic $\text{Fe}_3\text{O}_4/\text{PS}$ spheres coated with an adjustable silica shell (2–30 nm thick) (Fig. 18). $\text{Fe}_3\text{O}_4/\text{PS}$ particles incorporated a very high magnetite content (86 wt%). This amount obviously decreased with the presence of the silica shell (the thicker the shell, the lower the Ms). The influence of the following parameters was studied in detail for the synthesis of $\text{Fe}_3\text{O}_4/\text{PS}$ particles: (1) type of initiator on composite morphology, (2) feed ratio of the magnetite-containing miniemulsion and styrene macroemulsion on magnetite content, and (3) hydrophobic agent or amount of surfactant on size and size distribution. The obtained conversions were, however, low [141].

Another strategy (which could be related to seeded emulsion polymerization) was recently developed by Ding et al. [142, 143] to promote the formation of polymer chains close to the surface of iron oxides. The procedure, based on the formation of polymer-monomer pairs, was the following: PVA-coated Fe_3O_4 nanoparticles were mixed with chitosan (CS) and AA polymer-monomer pair to form micelles

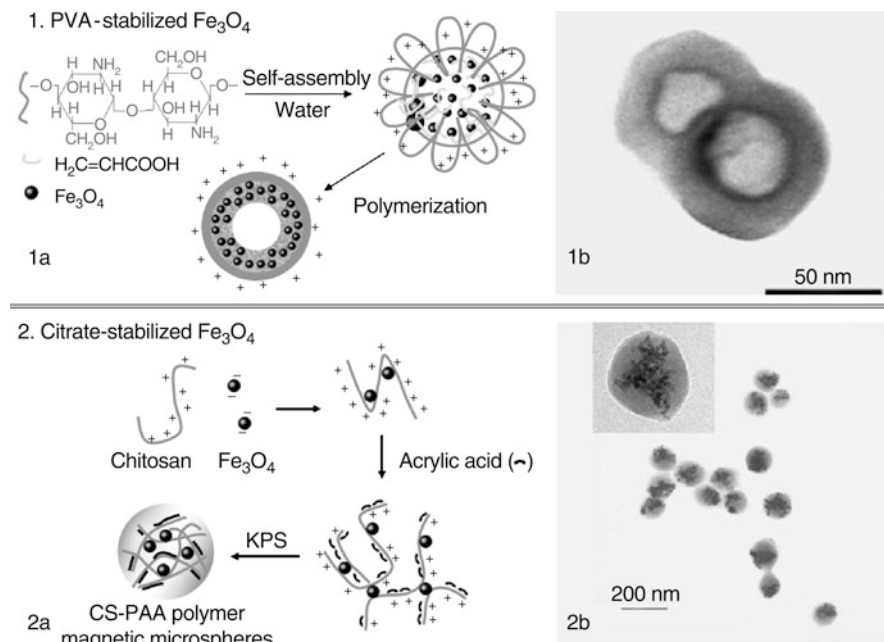


Fig. 19 Strategy based on polymer–monomer pair with (1) PVA-stabilized Fe_3O_4 : preparation of hollow magnetic particles (1a), and example of particle (cut-section TEM photo) (1b). (2) Citrate-stabilized Fe_3O_4 : preparation of plain magnetic particles (2a), and example of particle (TEM photo) (2b). Adapted from [142] with permission of Wiley-VCH and from [144] with permission of Elsevier

loaded with Fe_3O_4 . The cores consisted of the polyionic complexes of CS and AA (i.e., positively charged protonated CS chains and negatively charged dissociated AA), and the shells consisted of protonated CS chains. The polymerization of AA was then initiated by KPS, and followed by crosslinking of the shells with glutaraldehyde (GA) at the end of polymerization to form magnetic hollow Fe_3O_4 /polymer hybrid nanospheres (ca. 80 nm in size) (Fig. 19-1). By adjusting the initial amount of CS, AA, and GA, the size could be increased to 200 nm [143]. In addition, high Ms could be attained ($M_s = 41 \text{ emu g}^{-1}$). The PVA-stabilized Fe_3O_4 nanoparticles interacted with AA (or PAA) via hydrogen bonds. In a second approach, citrate/ Fe_3O_4 nanoparticles were used [144] to form an electrostatic assembly. As a result, plain instead of hollow magnetic particles were obtained with 36 wt% of magnetite (corresponding to $M_s = 23 \text{ emu g}^{-1}$) (Fig. 19-2). Their capacity to act as drug carriers was also shown. Finally, the concept was recently extended to the preparation of CS–PMAA magnetic particles [145]. In this last case, the particles were not only magnetic but also luminescent through the incorporation of negatively charged CdTe QDs.

Another valuable approach, which was detailed in Sect. 2 for silica particles, is based on the use of silane derivatives carrying vinyl groups (such as MPTMS)

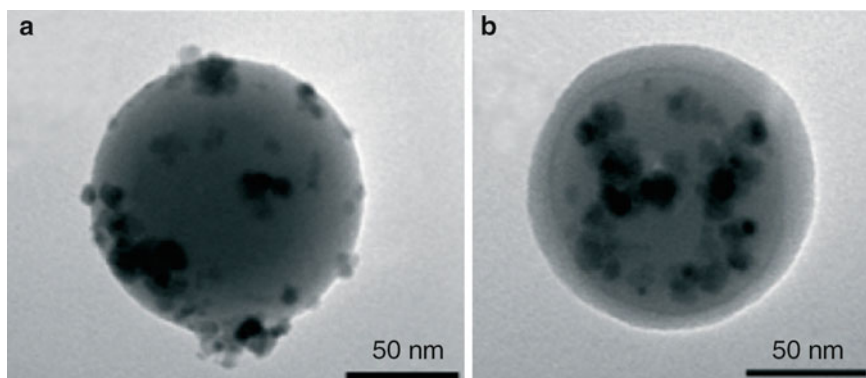


Fig. 20 Examples of composite core-shell colloids without (a) and with (b) PMMA outer shell. The particle core consists of polymerized MPTMS-droplets stabilized by magnetite (a). Adapted from [147] with permission of Wiley-VCH

that are attached to the nanoparticles via the surface hydroxyl groups of iron oxide. Using MPTMS as a coupling agent, Sacanna et al. [146, 147] successfully obtained magnetic PMMA nanoparticles. The key step relied on the condensation of MPTMS on iron oxide nanoparticles in conditions leading to the formation of a nanoparticle-stabilized emulsion (referred to as a Pickering emulsion [148]), which was then further “frozen” by MPTMS polymerization. Because the magnetite was exposed on the surface, the obtained stable composite particles were coated with a PMMA shell through seeded emulsion polymerization (Fig. 20). The controlled magnetic moment of the resulting magnetic polymer particles was exploited for field-induced colloidal crystallization and (dipolar) chain formation.

Very original morphologies were obtained using silica-coated Fe_3O_4 core-shell nanoparticles, subsequently functionalized with MPTMS [149]. Indeed, when used in styrene emulsion polymerization, anisotropic structures could be obtained by adjusting the interfacial tension (excentric spherical particles), crosslinking (concentric spherical particles), crosslinking and a large amount of styrene (anisotropic ellipsoids), or pre-swelling of concentric particles (asymmetric doublets) (Fig. 21). Using the same kind of MPTMS-grafted $\text{Fe}_3\text{O}_4/\text{SiO}_2$ as seeds in styrene emulsion polymerization in the presence of pyrene, composite particles with a magnetic silica core and a fluorescent polymer shell were recently reported [150].

In a closely related work using silica-coated iron oxide nanoparticles, thermoresponsive and magnetic latex particles were produced through colloid-template polymerization, which consists in a three-step procedure [151]. Magnetite nanoparticles of 10 nm were obtained by co-precipitation and stabilized by citrate groups, and subsequently covered by a silica layer via a modified Stöber method. The surface of the resulting 100-nm silica-coated magnetite nanoparticles aggregates was then modified with MPTMS to introduce polymerizable groups onto the surface. These template cores were finally used as seeds in the polymerization of NIPAM in

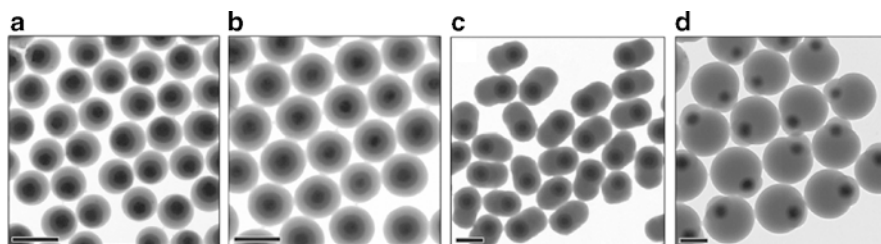


Fig. 21 TEM images of a series of $\text{Fe}_3\text{O}_4/\text{SiO}_2/\text{PS}$ composite colloids with complex structures and shapes produced by emulsion polymerization of styrene using MPTMS grafted $\text{Fe}_3\text{O}_4/\text{SiO}_2$ particles as seeds. **(a, b)** Spherical colloids produced in one-step emulsion polymerization **(a)** without and **(b)** with DVB as crosslinker. **(c)** Ellipsoids formed by swelling and phase separation in one-step emulsion polymerization. **(d)** Doublets produced by separated steps of swelling and phase separation. Scale bars: 400 nm. Reprinted from [149] with permission of the American Chemical Society

the presence of MBA as a crosslinker. The crosslinking density appeared to play an important role in the encapsulation process: for a MBA to NIPAM weight ratio lower than 10%, the silica-coated magnetic particles were not efficiently encapsulated by PNIPAM, and for values over 30% some particles would adhere to each other. The shell thickness could be tailored by varying the initial amount of NIPAM, and the size or concentration of the template cores. The obtained particles effectively showed thermosensitivity (the higher the amount of MBA, the lower the swelling ratio) with a slightly higher volume phase transition temperature (37°C , versus 32°C for pure and lightly crosslinked PNIPAM), and superparamagnetic behavior. This increase in the volume phase transition temperature could be explained by the presence of the magnetic nanoparticles, which acted as additional physical crosslinkers. Cai et al. [152] described a very similar approach consisting in the use of $\text{Fe}_3\text{O}_4/\text{silica}$ particles modified with MPTMS (ca. 100 nm in size), which were subsequently used as seeds for the copolymerization of NIPAM and 2-(dimethylamino)ethyl methacrylate (DMAEMA).

Using a very similar procedure, magnetite/silica nanoassemblies were produced to serve as magnetically recoverable catalyst supports [153]. In detail, 100-nm silica-coated Fe_3O_4 nanoparticles were functionalized with MPTMS and then used as seeds in NIPAM/MBA precipitation polymerization. After swelling these $\text{Fe}_3\text{O}_4/\text{silica}/\text{PNIPAM}$ colloids in an aqueous solution of AgNO_3 , Ag nanoparticles were directly synthesized inside the polymer network through in situ reduction with NaBH_4 . This “ Ag^+ absorption–reduction” process can be repeated to increase the number density of Ag particles embedded in the polymer shells. An additional sol–gel process was performed to form satellite silica by using Ag nanoparticles as templates, producing $\text{Fe}_3\text{O}_4/\text{SiO}_2/\text{PNIPAM}/\text{SiO}_2$ assemblies (Fig. 22). The use of these assemblies as recoverable catalyst supports was further evidenced in the case of Au-catalyzed reduction of 4-nitrophenol in the presence of NaBH_4 .

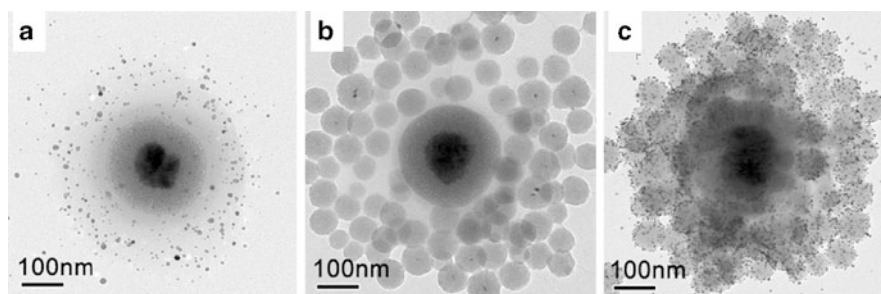


Fig. 22 TEM images showing the evolution of hierarchical assemblies: (a) $\text{Fe}_3\text{O}_4/\text{SiO}_2/\text{PNIPAM}/\text{Ag}$, (b) $\text{Fe}_3\text{O}_4/\text{SiO}_2/\text{PNIPAM}/\text{SiO}_2$, and (c) $\text{Fe}_3\text{O}_4/\text{SiO}_2/\text{PNIPAM}/\text{SiO}_2\text{-Au}$. Adapted from [153] with permission of the American Chemical Society

3.1.4 Heterocoagulation Followed by Emulsion Polymerization

Another strategy involving emulsion polymerization is based on the heterocoagulation of inorganic nanoparticles arranged on a polymer particle as a magnetic surface layer. The heterocoagulation is an electrostatically driven interaction between colloids of opposite charges, so the pH has to be carefully chosen. Then, a compound is added to improve the hydrophobicity of the heterocoagulates (through the formation of a surfactant–bilayer–admicellar polymerization). This ensures the formation of a third layer through emulsion polymerization using the heterocoagulates as seeds, and finally provides a composite particle with a trilayer morphology (Fig. 23).

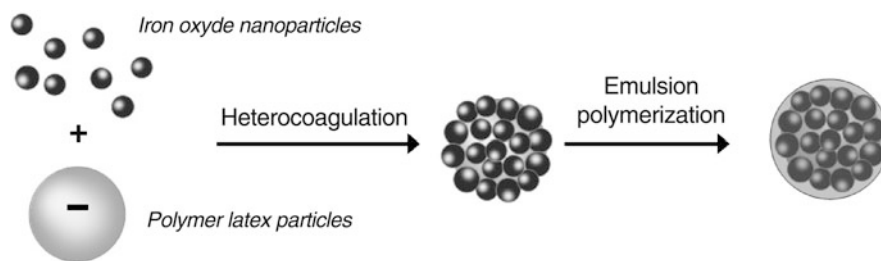
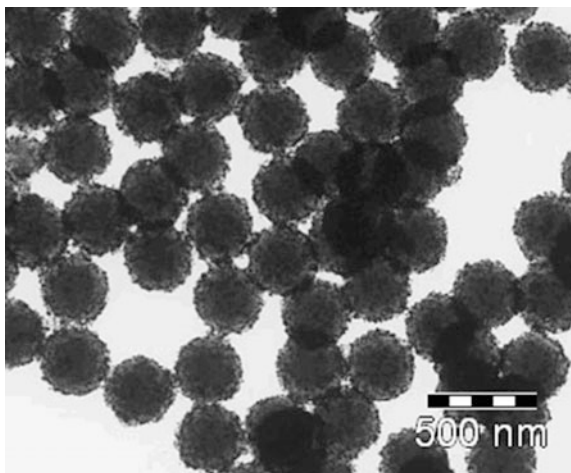


Fig. 23 Encapsulation of iron oxide nanoparticles in a two-step procedure: electrostatic-driven adsorption of iron oxide nanoparticles onto polymer particles, followed by encapsulation of the obtained heterocoagulates by emulsion polymerization

The first work describing this procedure was published by Furusawa et al. [154] using $\text{NiO} \cdot \text{ZnO} \cdot \text{Fe}_2\text{O}_3$ as the magnetic component and PS latexes as the particulate support (with 40 wt% of magnetic material). After the addition of sodium oleate, efficient encapsulation of the heterocoagulates by a PS layer was effectively observed, providing spherical magnetic particles with a smooth surface. The same kind of trilayer composite particles were obtained by first adsorbing $\gamma\text{-Fe}_2\text{O}_3$ on a poly(styrene-*co*-BA-*co*-AA) core. After addition of sodium methacrylate, a third

Fig. 24 TEM image of composite particles with a trilayer morphology using poly[styrene-*co*-(*N*-isopropylacrylamide)] as cationic seed. Adapted from [158] with permission of Springer



layer of poly(styrene-*co*-BA-*co*-AA) was formed [155]. The photovoltaic properties of the composite particles were also evaluated [156].

Still using the same two-step procedure, monodisperse and thermoresponsive magnetic latex particles based on PNIPAM were prepared [157, 158]. Anionic iron oxide nanoparticles were first adsorbed onto preformed cationic particles of various compositions [PS, poly(styrene-*co*-NIPAM) core-shell, or PNIPAM]. The obtained heterocoagulates were then encapsulated with crosslinked PNIPAM through seeded precipitation polymerization (Fig. 24). The magnetic content varied from 6 to 23 wt%. These particles were successfully used for the covalent immobilization of antibodies, and the resulting conjugates were tested as solid phases in immunoassays [159].

A slightly different procedure was depicted by Gu et al. [160]. Negatively charged PS particles were first formed in the presence of a silane coupling agent. After a given reaction time, silane-modified magnetic nanoparticles were continuously supplied into the reactor under acidic conditions, inducing the heterocoagulation of these cationic nanoparticles onto the anionic polymer particles. The morphology of the magnetic particles was strongly dependent on the silane coupling reagents. Trifunctional MPTMS led to disk-like or concave-like shapes, whereas difunctional methacryloxy propyl methyl dimethoxy silane (MPDMS) produced spherical particles. Addition of NaSS improved the colloidal stability of the magnetic polymer particles [161]. However, the amount of incorporated Fe_3O_4 remained quite low (5 wt%), therefore resulting in low M_s ($<0.5 \text{ emu g}^{-1}$).

3.1.5 Miscellaneous

A few systems that do not follow any of the procedures described so far are detailed below. Lee and Senna [162] described the synthesis of magnetic PS microparticles of the core-shell type prepared by emulsion polymerization of styrene in the presence of PS seed microspheres and magnetite coated with a bilayer of sodium oleate.

Small composite nanoparticles were produced in the continuous phase through emulsion polymerization. These nanoparticles were shown to adhere to the seed surface, giving rise to the formation of large PS microspheres covered with a layer of smaller nanocomposite particles. Owing to the complexity of the initial system (micrometric PS seeds, sodium oleate-coated- Fe_3O_4 , SDS micelles), the mechanisms leading to the formation of the particles was unclear, probably combining seeded, micellar, and admicellar emulsion polymerization.

In another work, Fe_3O_4 nanoparticles were covered by poly(MMA-co-MAA) using very high surfactant to monomer ratios [163]. The best results in terms of magnetic properties and colloidal features were obtained using KPS and SDS, with magnetite to monomer ratio of 25 wt% ($M_s = 3.2 \text{ emu g}^{-1}$). However, there were neither TEM photos to illustrate the obtained morphologies nor indication of the weight fraction of magnetic particles to evaluate the success of the synthesis.

A final example implies no surface modification. Using magnetite nanoparticles as seeds, Sun et al. [164] described the synthesis of magnetic core-poly(AAm) shell particles obtained by UV irradiation of an aqueous solution of Fe_3O_4 , AAm, and MBA. The surface of the particles was then modified to introduce amino groups, subsequently linked to L-histidine labeled with ^{188}Re , one of the most efficient radioisotopes for cancer radiotherapy.

Although out of the main focus of this paper, it is worth mentioning the case of inverse emulsion. This involves the polymerization of water-soluble monomers such as AAm or NIPAM [165, 166]. Only a few studies report on the synthesis of magnetic particles using this process [167–172].

3.2 Synthesis of Iron Oxide Nanoparticles in the Presence of Preformed Polymer Particles

All the studies detailed in the previous section rely on the use of preformed iron oxide nanoparticles, in the presence of which emulsion polymerization has been carried out. By contrast, this section focuses on the synthesis of iron oxide nanoparticles inside or onto the surface of preformed polymer particles. The studies using this strategy are by far less numerous and are detailed below.

This approach was pioneered in the work of Ugelstad et al. [173, 174] (Fig. 25). In their method, magnetic iron oxides were formed in situ inside preformed micrometric polymer particles. The pores of monodisperse, porous PS particles contained oxidizing surface groups and were filled with a solution of FeCl_2 . Increasing the pH and the temperature induced the formation of superparamagnetic iron oxides in the pores. The composite particles were finally coated by a polymer shell to avoid any desorption of the magnetic nanoparticles. The diameter of the particles ranged from 1 to $30 \mu\text{m}$, with iron oxide loading up to 30 wt% and various surface-reactive groups (hydroxyl, carboxylic, amine, and aldehyde). These particles are currently marketed under the trade name Dynabeads[®].

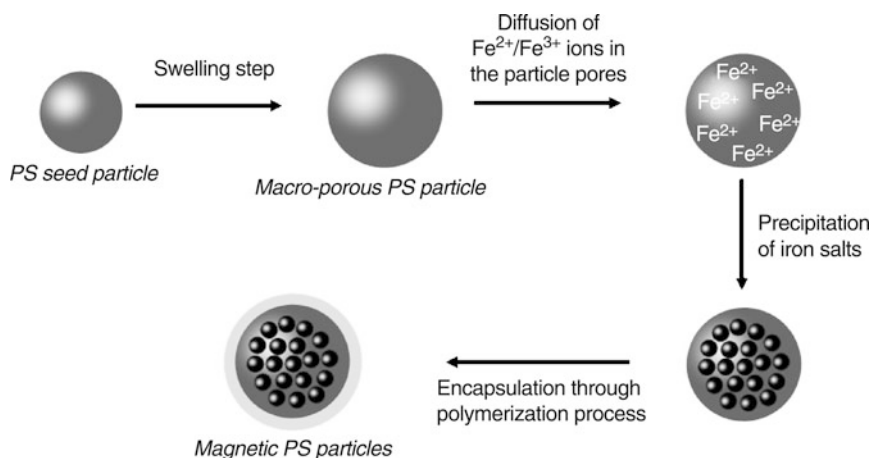


Fig. 25 Synthesis of magnetic polymer particles according to the process developed by Ugelstad et al. [173, 174]

Using a similar procedure, smaller magnetic particles (400–700 nm in diameter) were produced by Lindlar et al. [175]. Polymer particles of poly(MMA-*co*-GMA) were first synthesized by surfactant-free emulsion polymerization. Ethylene diamine was then added to obtain internal anchor groups able to favor the subsequent impregnation and hydrolysis of iron salts inside the particles. The final composite particles were monodisperse in size and the magnetic loading was close to 25 wt%.

Related studies report on the formation of iron oxides onto the surface of polymer particles adequately functionalized to chelate precursor metal ions. Pich et al. [176] prepared β -diketone-functionalized PS latexes through surfactant-free emulsion copolymerization of styrene and AAEM. Solutions of FeCl_2 and FeCl_3 were added to the dispersion, followed by the dropwise addition of NH_4OH . After washing, up to 14 wt% of iron oxides could be deposited on the particles but the Ms remained low ($< 1 \text{ emu g}^{-1}$). Temperature-sensitive and magnetic hybrid hydrogels of *N*-vinylcaprolactam (VCL) and AAEM incorporating up to 15 wt% of Fe_3O_4 were reported by the same group [177]. Emulsion polymerization of GMA was performed in the presence of seeds of PS particles (2.4 μm , obtained by dispersion polymerization) to afford core-shell latexes functionalized with a thin layer of epoxy groups [178]. Fe_3O_4 nanoparticles were then synthesized onto the surface of PS/PGMA core-shell particles by nucleation and controlled growth mechanisms. The obtained magnetic particles contained about 6 wt% of Fe_3O_4 , corresponding to a Ms value of 3 emu g^{-1} .

Another work describes the synthesis of magnetic nanocontainers (i.e., hollow spheres) of magnetite formed using PS particles obtained by emulsion polymerization as sacrificial core [179]. The coating procedure involved the controlled hydrolysis of aqueous solution of FeCl_3 in the presence of the PS latex, urea, and PVP. The particles coated with hematite (non-magnetic) that were obtained after aging at 95°C were then heated to 500°C to provide hollow hematite spheres.

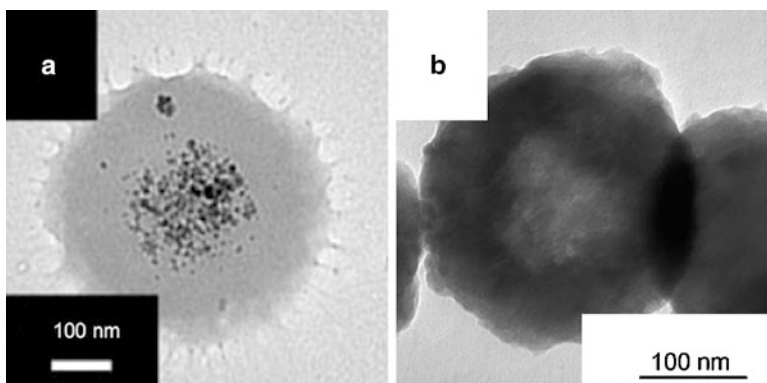


Fig. 26 Examples of iron oxide nanoparticles synthesized inside PNIPAM particles. (a) Sulfonate-functionalized particles based on poly(NIPAM-*co*-GMA). Reprinted from [180] with permission of Springer. (b) Poly(NIPAM-*co*-sodium acrylate) particles. Reprinted from [181] with permission of the American Chemical Society

Further heating at 350°C for 1 h under hydrogen atmosphere finally led to hollow magnetite spheres displaying superparamagnetic behavior, with M_s close to that of bulk material (67 emu g^{-1}).

A substantial amount of work has been dedicated to the in situ synthesis of iron oxide nanoparticles inside microgel particles (i.e., crosslinked latex particles), generally obtained by precipitation polymerization. Although not strictly speaking in the scope of this review article, which focuses on emulsion polymerization, it is worth mentioning the synthesis of these particles, which actually find many applications in various fields. For instance, Fe_3O_4 nanoparticles could be synthesized within preformed PNIPAM-based particles (Fig. 26) [180–183]. Of particular interest is the recent work of Brugger et al. [184], who used PNIPAM-based magnetic microgel particles as stimuli-responsive emulsifiers for oil-in-water emulsions, allowing controlled breaking of such emulsions.

4 Pigmented Latexes

Pigments (and extenders) are the main and most important constituents of water-based coatings and play a crucial role in, for instance, the papermaking and paint industries. A proper pigmentation drives not only the aesthetics of the film (such as gloss, opacity, and color) but also ensures long-term protection against environmental aggression and preserves the mechanical and performance properties of the film. In the paint industry, high quality coatings with a high gloss and color strength are generally required. In gloss and semi-gloss paints, the pigment is predominantly titanium dioxide (TiO_2), whilst in matte paints significant quantities of extenders (such as calcium carbonate, China clay and silica) are included in the paint formulation.

Adequate formulations depend not only upon the selection of raw materials, but also on accurate calculation and optimization of the amounts of its constituents. To achieve the optimum visual and economic benefits of a pigment, it is essential that the surface is uniformly and completely covered by the coating formulation. Opacity is therefore an essential requirement of latex paints. Opacity is most readily achieved by using a pigment of high refractive index, TiO_2 being the most widely used although ZnO or SbO_2 can also be employed. Whatever the paint composition, high quality coatings are obtained for optimal pigment dispersion, which is to say for optimum particle size and stability. To improve and to stabilize paint dispersions, it is common to use polymeric dispersants [185, 186]. However, this is generally not sufficient and a lot of pigments need a surface treatment to maximize their efficiency. Indeed, a problem of paint formulation is not only to promote pigment dispersion in the latex blend but also to maintain a minimum distance between individual pigment particles in the dried film. In practice, this never occurs. This issue can be solved by coating the inorganic pigment with a thin polymer layer. This way, optimal disposition of the inorganic particles within the polymeric film can be achieved, resulting in optimal light scattering and hence better opacity and good film properties [187]. Some of these methods are described in the following section for TiO_2 and a few other selected pigments.

4.1 Polymer Encapsulation of TiO_2 Pigments

Owing to the major technological importance of TiO_2 pigments in the paint industry, it is not surprising that most published works in this field are found in the patent literature [188–196]. Among the various approaches, emulsion polymerization is by far the technique the most frequently reported. In a typical procedure, the pigment particles are dispersed into water under high shear in the presence of surfactant to help dissociate the pigment agglomerates [197–199]. Then, a monomer or a mixture of monomers is introduced into the suspension medium, and a water-soluble free radical initiator is subsequently added to start polymerization. In most examples, the coating takes place through the admicellization/adpolymerization mechanism described in Sect. 3.1.1 for iron oxide encapsulation. This process is highly dependent on the geometry of the bilayer structure and on the surfactant packing density, which in turn are functions of the soap concentration. Emulsifier concentrations that are too low can lead to incomplete pigment coverage, whereas too large a concentration can result in the formation of free polymer particles that do not participate in the coating. The nature of the surfactant also plays an important role in the coating mechanism. For instance, Solc [190, 193] and Hasegawa [200, 201] claimed the use of water-soluble anionic surfactants, while Martin [191, 195] recommended the use of non-ionic oxyethylenic amphiphiles. As shown by Hoy and Smith, it can also be advantageous to use a combination of surfactants. For example, they demonstrated that more uniform coverages and better coating efficiencies could be achieved by using an amphiphathic polymer in combination with a companion surfactant [194, 202].

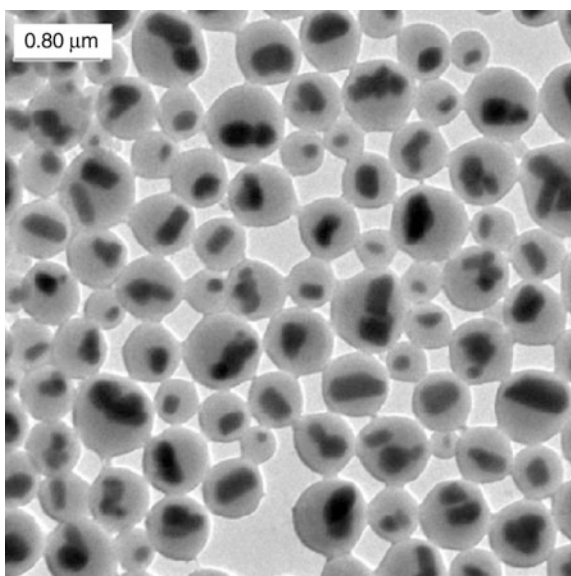
The fundamental aspects of polymer encapsulation of TiO_2 pigments were widely studied in the 1990s by the group of German and van Herk [203–209] with the successive Ph.D. theses of Caris [210] and Janssen [211]. With the intention of achieving high coating efficiencies, Caris used a polymerizable titanate coupling agent (diisopropyl methacryl isostearoyl titanate) to covalently attach polymer chains onto the surface of the TiO_2 pigments according to the coupling strategy previously described for silica. A similar strategy was also recently reported by Yang et al. [212]. Preventing secondary nucleation is essential because newly formed particles may compete for surfactant adsorption and consequently lead to pigment coagulation. Maintaining a good stability of the encapsulated powders is also critical for pigment encapsulation through emulsion polymerization. Soap deficiency can be determined by following the evolution of the surfactant concentration through on-line conductivity measurements. Secondary nucleated particles lead to a decrease of the conductivity signal due to surfactant adsorption from the continuous phase, whereas severe coagulation is identified by an increase of conductivity consequent to surfactant desorption. It is therefore possible to use this technique to optimize the surfactant concentration in order to obtain the best encapsulation efficiency with maximum stability of the encapsulated pigment.

With the objective of promoting polymer formation at the surface of TiO_2 pigments and prevent secondary nucleation, Haga et al. used a diazoic amidinium initiator previously anchored on the mineral surface [213], whereas Janssen used redox initiators [208]. Although real benefit was taken from the nature of the initiator, in particular in the case of hydrophilic monomers like MMA, there was still a competition between the formation of surface polymer and free latex particles in these systems. In both cases, better results were obtained when the monomer was introduced under starved-feed conditions, which enabled a significant decrease in the extent of secondary nucleation.

It is worth mentioning the recent work of Nguyen et al. [214], who succeeded in TiO_2 encapsulation through controlled radical polymerization via the Reversible Addition-Fragmentation chain Transfer (RAFT) process (Fig. 27). Encapsulation of TiO_2 using RAFT polymerization was also recently reported by Daigle et al. [215]. In this case, the method was also applied to metals (Mo, Zn) or other metal oxides (ZrO_2 , CuO, BaTiO_3 , Al_2O_3). In both studies, the use of macro-RAFT copolymers displaying a strong affinity for the pigment surface first enabled the formation of stable dispersion of the inorganic pigments. In a second step, the active chain end of the copolymer could be reactivated for the polymerization of hydrophobic monomers, thus leading to the formation of an encapsulating polymeric shell. More details on the use of controlled radical polymerization techniques for the synthesis of composite colloids can be found in the review article by Charleux et al. [216].

When successful, polymer encapsulation of TiO_2 pigments provides an efficient way to control pigment interparticle spacing and enables better paint performances, such as higher hiding power, tinting strength, gloss, scrub resistance, or stability, compared to conventional paint formulations. As illustrated in recent articles, these materials are also of potential interest for the elaboration of electrophoretic displays [217–219] and lithium ion batteries [220].

Fig. 27 Encapsulation of TiO_2 pigment particles by a poly(BA-*co*-MMA) shell using a poly(BA₅-*co*-AA₁₀) macro-RAFT agent as dispersant. Reprinted from [214] with permission of the American Chemical Society



Apart from encapsulation reactions, a few groups also attempted to use TiO_2 particles to stabilize polymer microspheres. For instance, Liu et al. reported a two-step procedure in which composite latex particles, coated with HEMA-functionalized TiO_2 nanoparticles synthesized in a first step, were used in a second step as Pickering stabilizer to form micron-size beads through a suspension-like process [221]. Chen and coworkers also reported a method (which looks closer to suspension than to emulsion polymerization) for fabrication of hollow spheres through Pickering stabilization of emulsions microdroplets [222]. Another particular example that deserves attention is the synthesis of polyacrylate core- TiO_2 shell nanocomposite particles by in situ emulsion polymerization [223]. The authors argued that the core-shell structure resulted from the judicious combination of a cationic surfactant with an anionic persulfate initiator under controlled pH conditions. The exact mechanism for the formation of these core-shell particles remains nevertheless unclear.

4.2 Titania-Coated Polymer Spheres and Hollow Titania Shells

The high refractive index and photocatalytic properties of TiO_2 make titania particles of great interest for various applications, including coatings, photonic crystals, and photovoltaic devices [224–226]. In particular, hollow titania spheres with a low-index core and a high-index shell are suitable building blocks for colloidal crystals, provided that the spheres are monodisperse in size with a smooth surface. However, since titania precursors are highly reactive, avoiding the formation of free-standing titania particles and rough coatings, is highly challenging. Therefore,

over the past 10 years, a number of groups have explored methods to address this challenge and to generate hollow titania spheres with smooth shells. The success of these methods relies on several parameters and requires precise optimization of the reaction conditions, as briefly described below.

In 2001, Shisho and Kawahashi reported the first successful formation of uniform TiO_2 coatings on the surface of 420-nm diameter PS latexes by hydrolysis of titanium tetrabutoxide in ethanolic solutions in the presence of PVP [227]. The shell thickness was controlled by adjusting the concentration of the precursor solution, and a 30-nm-thick TiO_2 coating was achieved without formation of separate inorganic particles under optimized conditions. A very similar procedure was followed some years later by Li [228], Syoufian [229], and Wang [230] (using albeit slightly different experimental conditions). In 2001, Imhof demonstrated the possibility of generating very thin and homogeneous titania coatings using cationic latexes as the seed, and titanium isopropoxyde as inorganic precursor [231]. The coating was again performed in ethanol media, and PVP was used to help stabilize the particles. The positive groups ensured quick deposition of the titania precursors on the latex seed and enabled the formation of 7- to 50-nm-thick titania shells without formation of secondary particles. Crystalline hollow spheres were further obtained by calcination of the TiO_2 -coated particles at elevated temperatures. Increasing the temperature up to 600°C yielded hollow crystalline anatase titania particles, whereas the rutile form of TiO_2 was obtained by calcining at $900\text{--}1000^\circ\text{C}$ (Fig. 28).

Using the layer-by-layer method, Caruso and coworkers reported in the same period that PS colloidal particles coated with polyelectrolyte multilayers can be used as templates to produce hybrid hollow spheres by infiltration with a water-soluble and stable TiO_2 precursor, namely titanium(IV) bis(ammonium lactate) di-hydroxyde (TALH) [232]. In virtue of the high chemical stability of the TALH precursor, a highly uniform coating was produced without the undesirable formation of titania particles in solution, which often occurs using more conventional precursors. Refluxing the TALH-coated particles at 100°C converted TALH to titania anatase nanoparticles, whereas calcination at 450°C gave hollow titania spheres. Macroporous titania spheres of the rutile phase were produced at a higher temperature (950°C). Eiden and Maret also described the successful formation of hollow spheres of rutile by templating negatively charged PS beads with $\text{Ti}(\text{OEt})_4$ from absolute ethanol, followed by calcination at elevated temperatures under an oxygen atmosphere [233]. Unfortunately, no TEM images for evaluating the quality of the coating were provided in this article.

4.3 Other Pigments

Besides TiO_2 , a few other pigments like aluminum [234–236], zinc oxide [237, 238], and calcium carbonate [207, 239–241] have also been reported. Some of them will be briefly discussed below.

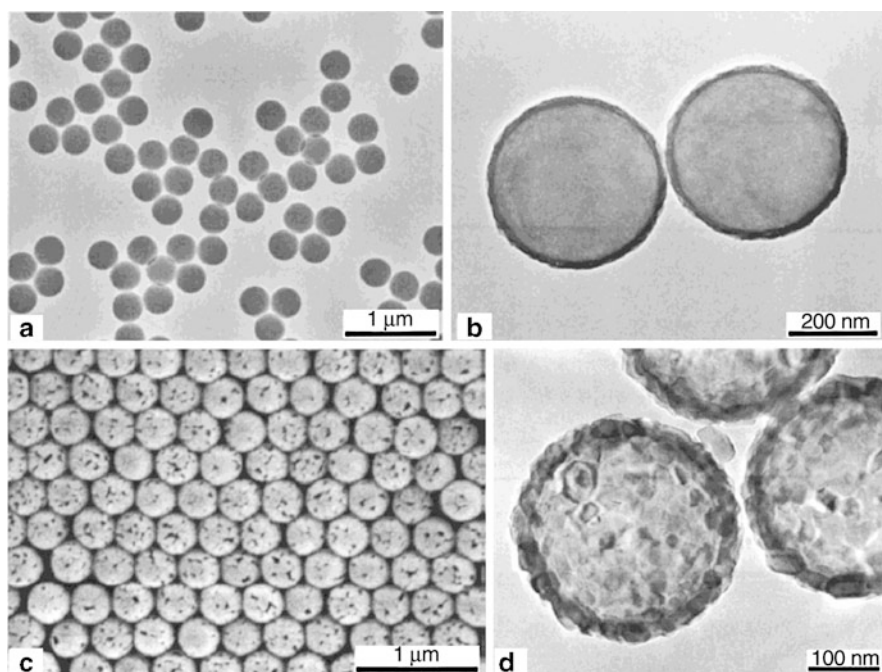


Fig. 28 TEM images of (a) the polystyrene latex spheres used as the core and (b) the same particles coated with a thin 25 nm titania shell. (c) SEM image of hollow titania spheres obtained by calcination of the polystyrene/TiO₂ core-shell particles at 600°C under air. (d) Enlarged TEM view of some hollow titania particles showing the small anatase crystallites that compose the shell. Reproduced from [231] with permission of the American Chemical Society

For example, Batzilla and co-authors described the encapsulation reaction of commercial aluminum pigments through an emulsion-like polymerization process [242]. They reported the use of phosphorous-containing protecting agents to provide a good dispersion of the Al pigment and control its reactivity. They also recommended using monomers with strong adhesion with the metal surface (e.g., carboxylic acid derivatives).

Another class of extender widely used in coating applications is calcium carbonate (CaCO₃). Despite potential interest in polymer encapsulation of CaCO₃ powders, only few studies can be found in the literature. Janssen et al. employed emulsion polymerization to encapsulate titanate-functionalized CaCO₃ pigments with PS [207]. Thermogravimetric analysis (TGA) showed that only 10% of PS was tightly bound to the inorganic surface, the remaining 90% polymer being extractable with toluene. Yang et al. [239] also described CaCO₃ encapsulation by PS using soap-free polymerization, while Yu et al. [240] reported the preparation of CaCO₃/PS composite particles using a polymerizable silane derivative previously attached on the mineral surface. The pretreated CaCO₃ particles were shown to act as comonomers during the emulsion polymerization process in a similar way to that discussed in Sect. 2.1.1 for silica. More recently, Wu and coworkers

observed an increase of polymerization rate with increasing CaCO_3 concentration during the preparation of $\text{CaCO}_3/\text{PMMA}$ composite particles by soap-free emulsion polymerization [241]. TEM studies of the nanocomposite particles indicated successful pigment encapsulation, whereas TGA and X-ray photoelectron spectroscopy suggested PMMA grafting on the nano- CaCO_3 surface.

5 Polymer–Clay Nanocomposite Latexes

In addition to spherical particles, anisotropic fillers such as layered aluminosilicates (commonly called clays) have received much attention in recent literature. Indeed, because of their high aspect ratio, clay platelets of a few nanometers thick and several hundred nanometers long allow a substantial improvement in strength, elastic modulus, and toughness whilst retaining optical transparency. Additional benefits are enhanced resistance to tear, radiation, and fire as well as a lower thermal expansion and a lower permeability to gases. It is generally admitted that end-use properties of polymer–clay nanocomposites (PCNs) heavily depend on their nanostructure. Three main morphologies are usually reported: segregated, intercalated, and exfoliated. The exfoliated morphology consists of individual silicate layers dispersed in the polymer matrix as a result of extensive polymer penetration and delamination of the silicate crystallites, whereas a finite expansion of the clay layers produces intercalated nanocomposites (Fig. 29). In general, the greatest property enhancements are observed for exfoliated nanocomposites, which could be regarded as the “ideal” morphology, although in practice many systems fall short of this idealized nanostructure.

As outlined in a considerable number of texts and reviews covering the synthesis, characterization, and properties of PCNs [243–246], many parameters can

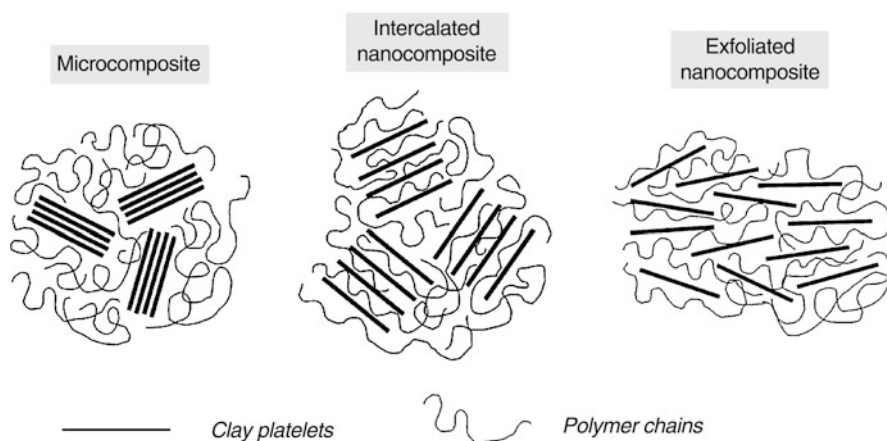


Fig. 29 Different morphologies encountered in polymer-layered silicate nanocomposites: phase segregated (*left*), intercalated (*middle*), and exfoliated nanocomposites (*right*)

influence the nanostructure, such as the type of clay, the nature of the polymer, and the polymerization process (e.g., bulk, solution, suspension, miniemulsion or emulsion polymerization). However, so far there is no clear general consensus as to which process is the best suited to provide the requested exfoliated morphology for a given set of conditions (given type of clay and monomer composition). This is due in part to the high complexity of these systems and the multiple parameters involved. Compared to more traditional solvent-borne or melt-processing approaches, waterborne processes in general and emulsion polymerization in particular nevertheless offer some obvious advantages, as detailed in the following section. The reader is referred to the recent review of Paulis and Leiza for complementary information [247].

5.1 PCNs Elaborated by Conventional Emulsion Polymerization

Although both natural and synthetic aluminosilicates have long been reported to be effective free radical initiators for the aqueous polymerization of vinylic monomers [248–251], their utilization in nanocomposite materials was reported only recently.

The first papers on the synthesis of PCNs through emulsion polymerization were published in the 1990s by Lee et al. [252–255]. Intercalated nanocomposites based on Bentonite [which consists of 70 wt% montmorillonite (MMT)] and PMMA [252], PS [253], or styrene/acrylonitrile copolymers [254, 255] were successfully obtained using pristine clays as seeds, KPS as initiator, and SDS as surfactant. Confinement of the polymer chains in the interlayer gallery space was evidenced by differential scanning calorimetry (DSC) and TGA, and was suspected to originate from ion–dipole interactions between the organic polymer and the MMT surface. Unfortunately, since the latex was coagulated before characterization, no information was given at that time on particle morphology. In every case, it was shown that a non-negligible part of the polymer was adsorbed on the clay surface after extraction of the pulverized product in hot toluene, indicating significant polymer–clay interaction. However, it remains unclear whether such interactions occurred in suspension or were induced by the coagulation process.

Following a very similar procedure involving KPS as initiator and SDS as surfactant, Tong et al. reported *in situ* emulsion polymerization of ethyl acrylate in the presence of pristine Bentonite [256]. Drying of the latex suspension produced films exhibiting enhanced mechanical and thermal properties as well as reduced permeability to water vapor. Generally speaking, and regardless of synthetic procedures, nanoscale dispersion of layered silicates in plastics produces glassy modulus enhancements of one to two times and rubbery modulus increases of five- to 20-fold. Improved thermal properties are also observed in many systems, including intercalated nanocomposites obtained by emulsion polymerization. Such improvements are mainly due to the nanometric dimensions of the platelets. TEM analysis of an ultramicrotomed section of the film indicated, in the case described above, an intercalated (partially exfoliated) morphology as shown in Fig. 30. Recently, Pan et al. also showed enhanced mechanical properties for PVC/MMT nanocomposites elaborated in a similar way [257], and Kim et al. observed a shift

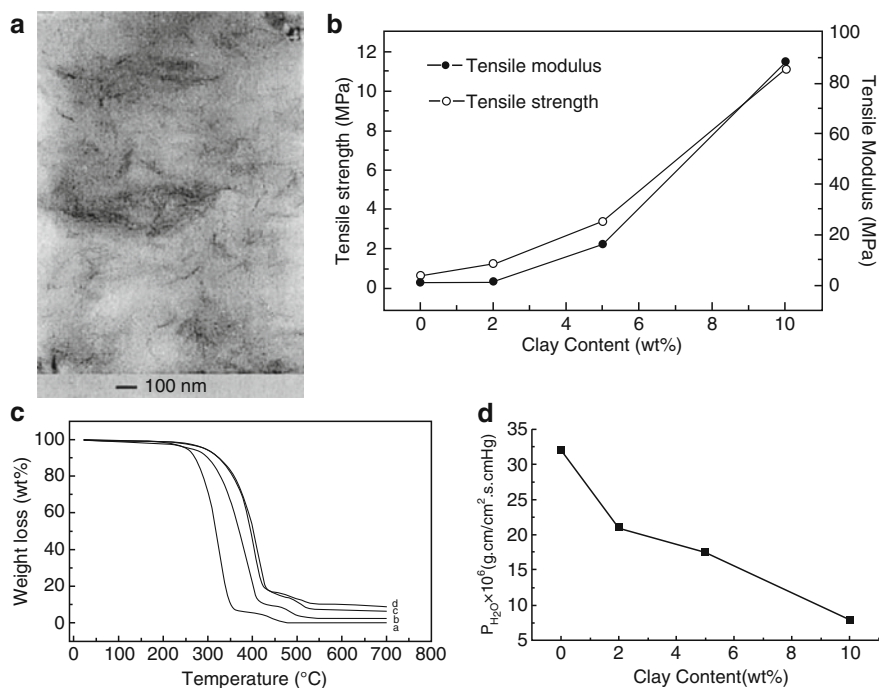


Fig. 30 (a) Representative TEM image of exfoliated-intercalated clay in a poly(ethyl acrylate) matrix containing 5 wt% of clay. Dependence of mechanical (b), thermal (c), and permeation (d) properties with clay loading. Adapted from [256] with permission of Wiley Periodicals

of the onset of the thermal degradation toward higher temperatures as a function of clay content in exfoliated PS/MMT nanocomposites [258]. Bandyopadhyay et al. synthesized PMMA/MMT nanocomposites through emulsion polymerization with SDS as the emulsifier and showed enhanced thermal stability and an increase in T_g of 6°C [259].

Although a straight comparison between these different systems would be appealing, a comprehensive discussion on structure–property relationships will not be attempted in this review. Indeed, the diversity of systems in terms of type of clay, surface modification, and polymerization methods renders this exercise quite risky. Therefore, we will not try to compare the properties of the different systems described, and only discuss those whose properties bring a clear “added-value” to the nanocomposite material.

Besides properties (which are usually enhanced by adding clay), another crucial factor of PCN materials elaborated through emulsion polymerization is their solid content. Although this point is less frequently addressed, most of the polymer/clay composite latexes reported in literature have solid contents below 20%. However, solid contents between 40% and 60% and sometimes higher are required for industrial applications. Using a seeded semi-batch emulsion polymerization process and a procedure otherwise very similar to that described above for Bentonite,

Diaconu et al. recently reported the successful preparation of poly(BA-*co*-MMA)/MMT latexes of 45% solids with moderate viscosities and containing 3 wt% of clay [260, 261]. This is to our knowledge one of the first and rare examples of “high solids” PCN latex in the literature. A further increase of the solid content to meet the requirements of industrial recipes remains a real challenge.

The very simple methods depicted above show that, in virtue of their high swelling capabilities in water, pristine clays are valuable candidates for the elaboration of exfoliated nanocomposites through in situ emulsion polymerization. In spite of that, a number of groups have performed organic modification of clay particles with the objective of increasing interfacial interactions and controlling particle morphology. These works are presented below.

Quite a lot of studies have dealt with the use of organoclays in emulsion polymerization. In most of these studies, the organoclay is dispersed in water and the polymerization proceeds as in conventional emulsion polymerization by monomer diffusion from the droplets to the organophilic clay surface, where propagation of polymer chains takes place. However, in a few examples, the organoclay is dispersed in the monomer phase. This monomer clay suspension is next emulsified (sometimes with the aid of ultrasound to help dispersion and promote clay exfoliation) and the resulting droplets are polymerized [262–267]. The latter processes look closer to suspension or miniemulsion (depending on the nature of the initiator) than emulsion polymerization and will not be discussed further.

Organic modifiers are generally used to render clay surfaces hydrophobic and to promote monomer penetration in the interlayer space. Organic modifiers carrying suitable reactive end groups can also react with the polymer matrix and further strengthen the interfacial polymer–clay interaction, as reported by many groups. For instance, Qutubuddin et al. have incorporated vinylbenzyl dimethyl dodecyl ammonium chloride (VDAC) in MMT using cation exchange [268]. The amount of VDAC was kept well below the cation exchange capacity of the clay in order to preserve clay colloidal stability (an issue that is surprisingly neglected in the literature). A partially exfoliated nanocomposite was obtained upon polymerization of styrene in the presence of the organoclay, but the latex colloidal stability was only moderate because there was no surfactant to stabilize the resulting particles. Very recently, Sedlakova and coworkers followed a similar approach using the cationic 2-(acryloyloxy) ethyl trimethyl ammonium chloride monomer [269]. Choi et al. also reported the preparation of PS/MMT nanocomposites through in situ emulsion polymerization using SDBS as surfactant and 2-acrylamido-2-methyl-1-propanesulfonic acid (AMPS) as functional comonomer to promote adhesion at the polymer–clay interface [270]. Exfoliated nanocomposites with clay contents of up to 20 wt% with respect to polymer were successfully achieved by this method. It was speculated that the hydrogen ions of sulfonic acid protonated the amido group of the AMPS comonomer, which could then undergo exchange reactions with the clay counter-ions. The method was further extended to acrylonitrile [271], styrene/MMA [272], and acrylonitrile–butadiene–styrene [273] (co)polymers. However, no mention was made in these papers of particle size or latex colloidal stability. It should be noted here that AMPS was also used by Li et al. in the synthesis of poly(BA-*co*-AA)/MMT latexes by semi-batch emulsion polymerization for pressure-sensitive

adhesives [274]. It is worth mentioning the recent work of Greesh and coworkers, who systematically investigated the effect of the nature of the organic modifier on the microstructure and thermomechanical properties of poly(styrene-*co*-BA)/MMT composite films containing 10 wt% of clay [275]. The ability of the clay modifier to efficiently interact with the clay surface, its compatibility with the monomer, and its reactivity were all found to be determinant parameters for achieving fully exfoliated morphologies. AMPS was shown to fulfill all these requirements.

Besides reactive organic modifiers, a few groups have also reported the use of “simple” surfactants to promote clay exfoliation [276, 277]. For instance, Meneghetti and Qutubuddin synthesized partially exfoliated PMMA/MMT nanocomposites using SDS as regular surfactant and a zwitterionic octadecyl dimethyl betaine as organic modifier [278]. It was shown that the zwitterionic modifier provided better colloidal stability as compared to a cationic surfactant. This can be interpreted in terms of charge neutralization of the SDS-stabilized latex particles by the cationic surfactant (although this was not discussed in the paper). Li et al. also found that emulsion polymerization of styrene, conducted in the presence of MMT functionalized by a zwitterionic surfactant, produced exfoliated nanocomposites as proved by TEM and by the disappearance of the d_{001} peak in the X-ray diffraction pattern [279].

All the examples of PCN latexes described thus far involved MMT as the clay. Although MMT is by far the most commonly used layered silicate in PCN syntheses, other types of clays have also been reported.

For instance, Herrera et al. recently conducted a series of experiments on Laponite [280–283]. Laponite is a synthetic clay that is similar in structure to MMT, except for the nature of the interlayer cation (Mg^{2+} for Laponite and Al^{3+} for MMT) and the clay dimensions. Each elementary Laponite disk has a thickness of around 1 nm and a diameter of 30–40 nm. In addition, Laponite also has the advantage over natural clays of being chemically pure and free from external contaminations. All these properties make Laponite a valuable candidate for use in PCN synthesis.

Following strategies similar to those mentioned in Sect. 1.1 for silica, film-forming poly(styrene-*co*-BA)/Laponite composite particles were synthesized in batch through conventional emulsion polymerization using organically modified Laponite as seed. The clay particles were functionalized either through ion exchange of a cationic initiator (AIBA) or a cationic monomer [2-methacryloyloxy ethyl trimethyl ammonium chloride (MADQUAT)], or through the reaction of the edge-hydroxyls with suitable polymerizable organosilane molecules (such as methacryloxy propyl dimethyl ethoxysilane). The so-obtained organoclays were further suspended in water, which required the use of ultrasound. For organoclays functionalized by cation exchange, a small amount of tetra-sodium pyrophosphate was introduced in the suspension to reverse the edge positive charges and promote clay–clay repulsions. Then, emulsion polymerization was carried out in batch in the presence of the organoclay (10 wt% based on monomer) using SDS as surfactant and KPS or 4,4'-azobis(4-cyanopentanoic acid) (ACPA) as initiators, except when AIBA was used as organic modifier. The overall process is illustrated in Fig. 31.

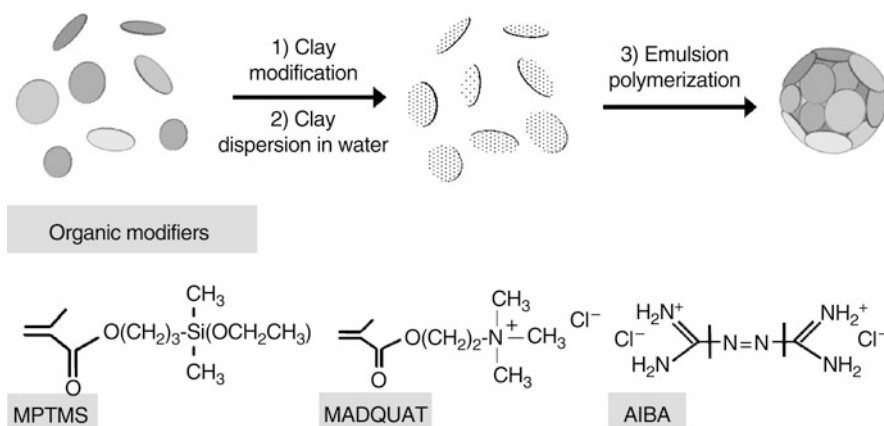


Fig. 31 Procedure used for the synthesis of polymer/Laponite composite particles through emulsion polymerization

Regardless of the nature of the organic modifier, colloiddally stable composite latexes with diameters in the range 50–150 nm were successfully obtained, provided that the original clay suspension was sufficiently stable and un-aggregated. All three methods produced clay-armored composite particles characterized by a polymer core surrounded by an outer shell of clay platelets, as evidenced by cryo-TEM. Transparent films that exhibited remarkable mechanical and thermal properties were produced upon drying of the composite latexes. Cryo-microtomy revealed a honeycomb distribution of Laponite within the film, consistent with the armored morphology (Fig. 32). Quite recently, Ruggerone et al. also reported a similar morphology for PS/Laponite films containing up to 20% of clay and investigated the resulting mechanical properties [284].

A similar strategy involving Laponite or MMT platelets grafted with polymerizable organotitanate and organosilane molecules was recently reported by Voorn et al. [285, 286]. Here, starved-feed soap-free emulsion polymerization of MMA conducted in the presence of the organoclay led to clay encapsulation. However the solid content was quite low (typically around 7%).

5.2 Soap-Free Latexes Stabilized by Clay Platelets

Very recently, a number of groups have explored methods of preparing clay-armored latexes by soap-free emulsion polymerization (referred to as “Pickering polymerization” [69] by analogy with the stabilization of emulsions by inorganic solids). In this process, the monomer is simply emulsified in a water dispersion of clay platelets that ultimately stabilize the hybrid particles by adhering on their surface and forming a protecting armor.

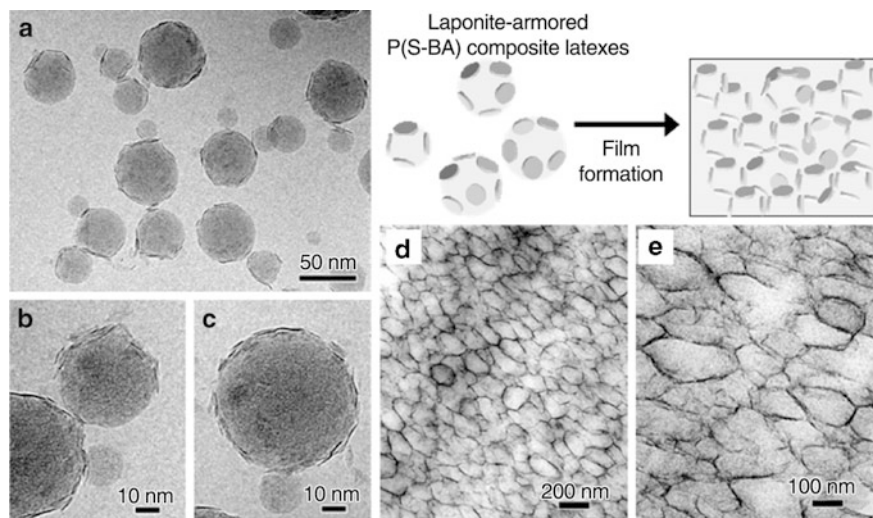


Fig. 32 (a–c) Cryo-TEM images of poly(styrene-*co*-BA)/Laponite nanocomposite particles prepared through emulsion polymerization using MADQUAT as reactive compatibilizer. The nanoparticles are seen embedded in a film of vitreous ice. (d, e) Electron micrographs at intermediate and high magnifications of an ultrathin cryosection of a film prepared from the composite latex suspension. The thin dark layer covering the surface of the polymer particles corresponds to 1-nm thick diffracting clay platelets that are oriented edge-on with respect to the direction of observation. Adapted from [283] with permission of Wiley-VCH

For instance, using the afore-cited AMPS comonomer (un-correctly defined as reactive surfactant in a subsequent paper), Choi et al. reported the preparation of PMMA/MMT nanocomposites through in situ soap-free emulsion polymerization [287]. However, at that time, the authors did not stress the role of the clay as stabilizer. Park et al. synthesized PMMA/MMT nanocomposites for optical applications by soap-free emulsion polymerization, but again the article focused on the properties and there was no mention of colloidal aspects [288]. In the same period, Lin and coworkers reported the formation of 300–600 nm diameter PMMA latex particles initiated by KPS and stabilized by MMT platelets [289]. The authors argued that KPS intercalation inside the clay galleries was the driving force that enabled the polymerization to take place at the clay surface. Although the solid content was quite low and the amount of MMT rather high, this article remains nevertheless very instructive.

Using an original approach, Zhang and coworkers recently reported the synthesis of PMMA latex particles stabilized by MMT platelets tethered with poly[2-(dimethylamino)ethyl methacrylate] (PDMAEMA) brushes (Fig. 33) [290]. The PDMAEMA polyelectrolyte brush was synthesized by atom transfer radical polymerization using a cationic initiator previously introduced in the clay galleries. The PDMAEMA-functionalized clay platelets were further used to stabilize the emulsion polymerization of MMA initiated by the remaining free radical initiator present on the clay surface.

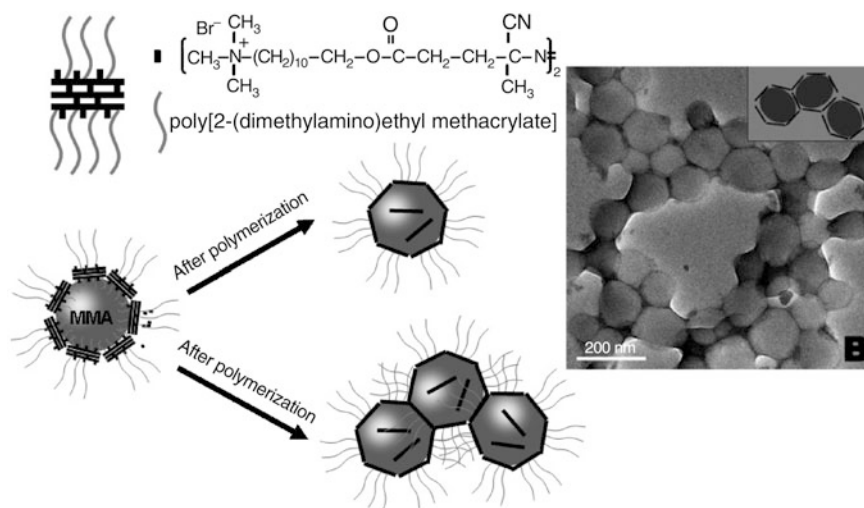


Fig. 33 *Left*: Synthesis of clay-armored PMMA latexes through soap-free emulsion polymerization using PDMAEMA-tethered clay as stabilizer. *Right*: TEM image of the so-obtained PMMA/clay composite colloid. Reproduced from [290] with permission of Wiley Periodicals

Recently, a number of groups have also reported the Pickering stabilization of monomer-containing lipid droplets by clays, and their subsequent free radical polymerization [291]. As these articles fall outside the scope of this review, they will not be discussed further. Although not strictly speaking in the scope of the present review, it is also worth mentioning the recent work of Voorn et al. on the first surfactant-free inverse emulsion polymerization stabilized with hydrophobic MMT platelets [292].

6 Synthesis of Quantum Dot Tagged Latex Particles

QDs are semiconductor nanoparticles typically 1–10 nm in size that show unique luminescence properties due to 3D size-confinement effects [293–295]. Regardless of the excitation wavelength, a narrow emission peak is observed, the wavelength of the emitted light being size-dependent. Furthermore, QDs show excellent photostability, and different-sized QDs can be simultaneously excited by a single wavelength because each type of QD exhibits a specific emission peak. Due to their outstanding optical and electronic properties, QDs have found increasing applications in the fields of biotechnologies (e.g., diagnostic, imaging, optical tracking), optoelectronics (e.g., light emitted diodes) and photonics (e.g., photonic crystals) [295].

The most often encountered inorganic semiconductors in the literature are those from groups II–VI, i.e., ZnO, ZnS, ZnSe, CdTe, CdS and CdSe, the last two being the most studied and documented. QDs are in most cases made as colloidal solutions

[294, 296]. In this approach, precursors of the material are reacted in the presence of a stabilizing agent that will restrict the growth of the particle and keep its dimensions within the limits of the quantum-size effect that gives the QDs their outstanding properties. The most popular route is based on the pyrolysis of organometallic precursors in a hot coordinating solvent that mediates nanoparticle growth and stabilizes the inorganic surface [297–299]. For instance, a typical synthesis of CdSe is the following: dimethyl cadmium $\text{Cd}(\text{CH}_3)_2$ and trioctyl phosphide selenide are initially dissolved in the organic solvent tri-*n*-octylphosphine and injected into a hot coordinating solvent of tri-*n*-octylphosphine oxide (TOPO) at 350°C under argon atmosphere. The temperature is lowered to 300°C by the injection. The rapid introduction of the reagent mixture produces a yellow/orange solution that is characteristic of CdSe nanocrystal formation. The growth of the QDs after the injection is then carried out at a given temperature in the range of 250–300°C. Since the growth of the QDs is dependent on the process of Ostwald ripening, the size of the QDs can be tuned by the temperature. Careful control of the reaction conditions produces CdSe QDs that are relatively homogeneous in size, and tunable in the 2–8 nm range. However, because the organometallic precursors are extremely toxic, expensive, and explosive, alternative procedures using metallic oxides (e.g., CdO) and organic stabilizing agents have been developed [300, 301]. For instance, less experimentally demanding procedures can be carried out using aqueous solutions of Cd(II) salts [for instance $\text{Cd}(\text{ClO}_4)_2$ or $\text{Cd}(\text{NO}_3)_2$] mixed with anionic or Lewis basic polymers such as sodium polyphosphate or polyamines [302, 303], or a polymerizable stabilizer [304]. The subsequent addition of a sulfide source (such as H_2S or Na_2S) produces CdS nanoparticles that are in the 1–10 nm size range. The size of the nanocrystals depends on a large number of experimental conditions, such as the relative concentrations of the precursors and rates of addition.

The stability of the QDs, and hence their luminescence, can be improved by coating the QDs with an additional layer of another semiconductor material with a wider band gap energy (e.g., CdSe coated with ZnS [305, 306]). Other strategies have also been envisioned to improve their stability, their compatibility with various media, and their functionality. Ligand exchange, encapsulation by phospholipids, polymers or silica, or coating by biological molecules (proteins, DNA, antibodies) are a few examples of such modifications. Obviously, incorporating QDs in polymer particles using emulsion polymerization is a very attractive challenge for many scientists targeting applications in the biomedical field (diagnosis, image tracking, bar-coding) or in photonics (photonic crystals).

6.1 Encapsulation of QDs Through Emulsion Polymerization

6.1.1 Conventional Emulsion Polymerization

Only a few papers report on the encapsulation of QDs inside polymer particles through conventional emulsion polymerization. Indeed, at the end of the most popular routes used for QDs synthesis, the obtained nanocrystals are usually

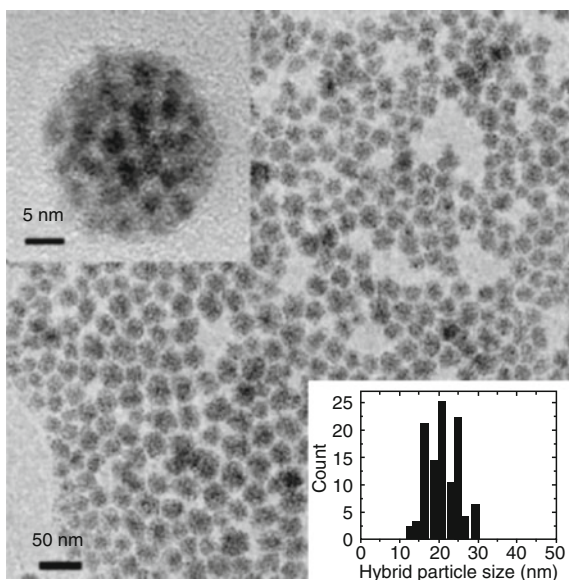
hydrophobic. Thus, the incorporation of hydrophobic QDs into polymer particles via a proper emulsion polymerization may be very challenging owing to the poor aqueous-phase transport of these species. Various synthetic strategies related to emulsion polymerization have been developed to improve the compatibility between the QDs and the reagents.

In one of the reported works, TOPO-coated CdSe QDs were dispersed in a micellar solution of surfactant, which could be subsequently swollen by monomer [307]. In detail, a toluene solution of CdSe was first added dropwise to a micellar solution of cetyltrimethyl ammonium bromide (CTAB). Then, a mixture of styrene, DVB, AA, and AIBN was added dropwise at 0°C. Finally, the system was heated to 70°C for 20 h. Submicrometer particles were prepared with an effective incorporation of hydrophobic TOPO-coated CdSe into carboxylic functionalized and crosslinked PS particles. The QD-tagged PS particles were then coated with a fluorescent silica shell through TEOS addition. Particle sizes ranging from 300 nm to 20 µm were produced, depending on the recipe used for the synthesis. However, the solid content was quite low and there was no information about the amount of QDs incorporated.

Another strategy consists in the use of QDs coated with a cysteine acrylamide, a polymerizable stabilizer [304]. Successful incorporation of hydrophilic cysteine-acrylamide-stabilized QDs into 80–200 nm fluorescent latexes was achieved via emulsion polymerization, as reported by Sherman et al. [308], using two different procedures. In the first, a two-step shot growth surfactant-free emulsion polymerization of styrene and NaSS was performed in the presence of a solution of hydrophilic cysteine-acrylamide-stabilized CdS or CdSe/CdS QDs. In the second approach, CdSe/CdS QDs were first electrostatically modified by vinylbenzyl(trimethyl)ammonium chloride and subsequently copolymerized with styrene in the presence of SDS. A third approach was also described in this paper: coating of cationic PS particles with anionic poly(cysteine acrylamide)-coated QDs through electrostatic-driven interactions.

Using a procedure that probably relies on admicellar polymerization, Lee et al. [309] successfully entrapped CdSe or CdSe/ZnS QDs in various polymer particles. TOPO-coated QDs were first dissolved in chloroform in the presence of a large amount of sodium bis(2-ethylhexyl)sulfosuccinate (AOT). The waxy solid obtained after solvent evaporation was then dissolved in water at 80°C (probably stabilized by a bilayer of TOPO and AOT). After centrifugation and dialysis, and dilution in water, monomer was added to the reaction mixture, stirred for 1 h and heated to 60°C. Polymerization was initiated with KPS, and 20 nm hybrid particles containing a few tens of QDs each were successfully obtained (Fig. 34). This procedure was, however, limited to QDs smaller than 5 nm in size. The versatility of the process was demonstrated by the successful synthesis of hybrid colloids using various monomer(s): pure styrene or a mixture of styrene/DVB (1:1), pure P4VPy or a mixture of P4VPy/DVB, or pure PMAA. The pure PDVB particles showed, however, better robustness to post-synthesis treatments. The main drawback of the process was the quenching of the photoluminescence of the QDs. This problem was circumvented by the use of CdSe coated with a protective ZnS shell.

Fig. 34 TEM images of hybrid colloidal nanoparticles of CdSe and PDVB. The *upper inset* is a high magnification image showing individual CdSe nanocrystals within the PDVB colloidal particle. The *lower inset* shows the PSD. Reprinted from [309] with permission of the Royal Society of Chemistry



6.1.2 Emulsion Polymerization-Related Procedures

Using the procedure described above for the synthesis of magnetic particles and depicted in Fig. 16 (see Sect. 3.1.3), CdTe QDs of different size (and thus different emission wavelength) were embedded in PS particles using emulsion polymerization [137, 310]. The obtained micrometric particles showed good photoluminescence properties and the photostability of the QDs was even enhanced when encapsulated in the PS particles, compared to an aqueous solution of CdTe. In addition, the labeling of PS particles with both green- and red-emitting QDs was demonstrated, showing the possible application of this approach to the synthesis of multiplexed optical coding (Fig. 35). Bifunctional (magnetic with Fe_3O_4 and fluorescent with CdTe) particles were also reported by the same team [138] (see Sect. 3.1.3).

The concept of polymer–monomer pairs depicted above for the synthesis of magnetic particles also proved to be efficient for QDs encapsulation (see Sect. 3.1.3, Fig. 19) [145]. CdTe QDs coated with mercapto propionic acid (MPA) were first embedded in CS/PMAA particles providing raisin-bun or core–shell morphologies, depending on the initial ratio of $[-\text{COOH}]$ to $[-\text{NH}_2]$. The photoluminescence properties of the core–shell morphology were found to be pH-dependent. CdTe QDs were then encapsulated together with magnetic Fe_3O_4 nanoparticles to afford multifunctional particles that were able to act as imaging agents. The magnetic content could be varied from 11 to 32 wt%, but it was found that too high a magnetic content led to a decrease or quenching of the QD fluorescence. Finally, these particles were evaluated for magnetically enhanced cellular uptake.

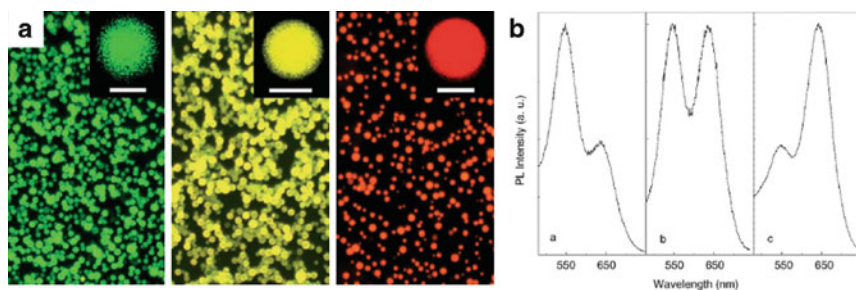


Fig. 35 (a) Fluorescence images of PS particles loaded with green (*left*), yellow (*middle*), and red CdTe dots (*right*). The *insets* are the corresponding confocal fluorescence images. *Scale bars*: 2 μm . (b) Fluorescence spectra of PS beads incorporated with both green and red CdTe dots with their photoluminescence (PL) peak-intensity ratio being 2:1 (a), 1:1 (b), and 1:2 (c). The initial input ratio of green to red dots was 1:0.3 (a), 1:0.6 (b), and 1:1.2 (c). Reprinted from [310] with permission of Wiley-VCH

6.1.3 Miscellaneous

A recent work reported the inverse (mini)emulsion polymerization of NIPAM in paraffin oil using water-soluble CdSe/ZnS QDs coated with a polymerizable amphiphilic copolymer [311]. The QDs were homogeneously distributed inside the obtained particles (ca. 1 μm in size, broadly distributed), which effectively displayed photoluminescence properties. In addition, the presence of QDs did not interfere with the thermosensitive behavior of PNIPAM.

Finally, as in the case of iron oxides, a few studies report the incorporation of QDs inside microgel particles obtained by precipitation polymerization. For instance, hydrosoluble CdTe nanocrystals capped with thioglycolic acid could be reversibly incorporated inside poly(NIPAM-*co*-4VPy) copolymer particles by varying the pH [312]. The entrapment of QDs was dominated by the physical entanglement of the collapsed network and electrostatic interactions between the loaded QDs and the gel network. In another study from the same group, CdTe QDs co-stabilized by both thioglycerol and thioglycolic acid were incorporated inside PNIPAM microspheres through hydrogen bonding [313]. Finally, CTAB-modified CdTe QDs were entrapped into poly(NIPAM-*co*-AA) microgels through electrostatic interactions [314].

6.2 Synthesis of Quantum Dots in the Presence of Polymer Particles

As mentioned above, different synthetic procedures have been developed for the formation of QDs, and each of them has its own advantages and drawbacks. When envisioning the synthesis of QDs inside or at the surface of polymer particles obtained by emulsion polymerization, aqueous-based procedures will be logically favored.

One of the first examples of QDs synthesis onto the surface of latex particles was reported by Zhang et al. [315, 316], who recently described the synthesis of monodisperse nanocomposite particles with inorganic CdS nanocrystals deposited onto poly(MMA-*co*-MAA) latex particles (varying from 150 to 600 nm) obtained by emulsion polymerization (Fig. 36). In a first step, latex particles were ion-exchanged with a Cd(ClO₄)₂ solution. The Cd²⁺ ions thus introduced into the electrical double layer were further reduced into CdS by addition of a Na₂S solution. By adjusting the initial MMA to MAA ratio and consequently the density of surface COO⁻, as well as adjusting the ratio of Cd²⁺ to surface COO⁻, the size of CdS nanoparticles could be varied from 3 to 8 nm and the surface coverage could reach 40%. Colloidal arrays with interesting optical properties were obtained when the nanocomposite particles were sedimented under gravity [316]. The CdS-loaded nanocomposite particles could be subsequently recovered by a film-forming polymer shell by reacting MMA and BA monomers. The resulting colloidal nanocomposites were finally assembled into 3D periodic arrays consisting of rigid poly(MMA-*co*-MAA)/CdS core particles regularly distributed within the soft polymer matrix. In contrast to what was anticipated in Fig. 36, QDs were uniformly mixed with the shell-forming polymer, leading to the doping of the poly(MMA-*co*-BA) matrix [315].

Using a similar procedure, poly[styrene-*co*-(2-methacrylic acid 3-(bis-carboxy methylamino)-2-hydroxypropyl ester)] [poly(styrene-*co*-GMA-IDA)] latex particles (70–130 nm in size) obtained by surfactant-free emulsion polymerization were successfully coated with CdS nanoparticles [317]. The GMA-IDA groups offered coordination sites for chelating metal ions, at which CdS nanoparticles were grown. The density and size of CdS nanoparticles could be varied by adjusting the ionic content and concentration of chelating groups, providing nanocomposite particles

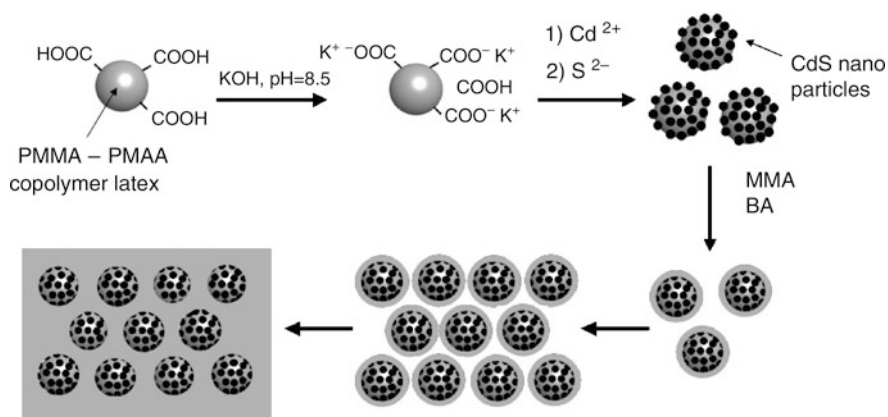


Fig. 36 Synthesis of poly(MMA-*co*-MAA)/CdS/poly(MAA-*co*-BA) multilayered hybrid particles with a periodic structure. Redrawn and adapted from [315] with permission of the American Chemical Society

with luminescent properties. The same study was then carried out with poly(MMA-*co*-MA-*co*-GMA-IDA) particles displaying various T_g to investigate the influence of this parameter on CdS formation [318]. The addition of a protective ZnS shell on CdS nanoparticles provided hybrid particles with enhanced photoluminescence properties [319].

Particles of poly(styrene-*co*-DMAEMA) have also been reported for the effective synthesis of luminescent CdS/polymer composite particles [320]. The difference in this case was that surfactant-free emulsion copolymerization was performed in the presence of Cd^{2+} ions that were coordinated to DMAEMA.

Alternatively, QDs can be synthesized inside preformed microgels particles (200–600 nm) obtained by the copolymerization of NIPAM, AA, and 2-hydroxyethyl acrylate in the presence of MBA [182]. An aqueous solution of $\text{Cd}(\text{ClO}_4)_2$ (the Cd^{2+} source) was first added to the particles to induce ion exchange between the cations of the microgels and Cd^{2+} . After dialysis, slow addition of Na_2S solution induced the formation of CdS nanocrystals. The optical properties of the embedded QDs (versus free QDs) were maintained and only slightly affected (e.g., red-shift or broader emission peak). The microgels could be further coated by a polymeric shell, and the resulting hydrophobic QD-doped particles were used as building blocks for the fabrication of photonic crystals (Fig. 37) [321].

Optical detection of glucose by CdS QDs immobilized inside microgels was very recently reported [322]. This original approach relies on the formation of copolymer microgels constituted of poly(*N*-isopropylacrylamide-*co*-acrylamide-*co*-phenyl boronic acid). These particles were obtained in two steps: synthesis of poly(NIPAM-*co*-AAm-*co*-AA) microgels, and coupling of 3-aminophenylboronic acid to the $-\text{COOH}$ groups of the AA units. Then, Cd^{2+} complexation was achieved by the PAAm segments through the addition of $\text{Cd}(\text{ClO}_4)_2$. After removal of excess Cd^{2+} , a thioacetamide solution was added dropwise and the dispersion heated to 85°C for 1 h to afford CdS-embedded microgels. Phenyl boronic acid is known to

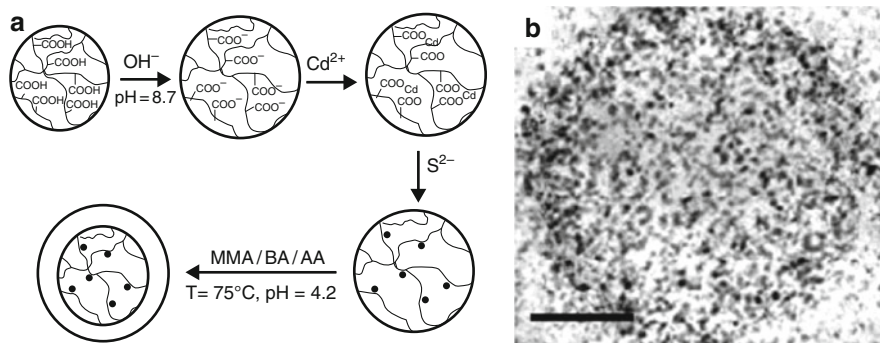


Fig. 37 (a) Synthesis of hybrid core-shell particles doped with CdS quantum dots. Reprinted from [321] with permission of Wiley-VCH. (b) TEM photo of the core microgels. Scale bar: 50 nm. Reprinted from [182] with permission of the American Chemical Society

strongly bond to glucose, allowing the fluorescence of the in situ synthesized QDs to be reversibly quenched and anti-quenched when the microgels undergo swelling and deswelling in response to the changes in glucose concentration.

7 Synthesis of Metallic Latex Particles

The strong interest in the incorporation of metallic nanoparticles into polymer latexes arises from the outstanding optical, magnetic, and catalytic properties of metal nanoclusters with potential uses in electronic and optical devices, magnetic recording media, biological labeling, and catalysis. The formation of metal colloids or clusters by the controlled reduction, nucleation, and growth of metal salts in aqueous solution has been investigated for over a century. Nevertheless, studies dealing with the preparation of metallic polymer particles through emulsion polymerization are scarce.

7.1 *Polymer Encapsulation of Metallic Particles Through Emulsion Polymerization*

In 1999, Quaroni and coworkers reported for the first time the elaboration of polymer-coated silver nanoparticles through emulsion polymerization [323]. The silver colloids (around 100 nm diameter and irregular in shape) were previously modified by adsorption of a double layer of OA. Then, a uniform layer of poly(styrene-co-MAA) copolymers was formed on the hydrophobized inorganic seed particles, providing a protective organic and functional shell to the metal particle. Whereas thin coatings (<10 nm) were shown to follow the shape of the metal core, thicker coatings assumed more globular shapes. As the authors noted, the polymer shell induced only minor changes in spectral properties under conditions where the particles were un-aggregated. The plasmon resonance underwent only a small red shift, which was ascribed to an increase of the dielectric constant in the particle environment. A similar approach was described by Bao et al. who used 100 nm silver nanoparticles onto which was adsorbed an azo initiator (ACPA) [324]. Emulsion copolymerization of styrene and NaSS was performed in the presence of PAA as a steric stabilizer in a water/ethanol mixture. A thin polymeric shell (5–10 nm) was thus formed onto the silver nanoparticles, protecting them from dissolution when nitric acid was added to the medium. Non-spherical metallic particles could also be encapsulated, as reported by Obare et al. CTAB-coated gold nanorods were covered by a PS shell, which induced only slight modifications of the optical properties of the nanorods [325], as previously observed by Quaroni et al. for silver particles [323]. The Au core was then dissolved by KCN to provide hollow PS nanotubes.

In a related approach, Gu et al. reported the synthesis of multilayered gold/silica/PS core-shell particles through seeded emulsion polymerization. In this

study, silica-coated gold colloids were encapsulated by PS using MPTMS as silane coupling agent according to the procedure previously described for silica (see Sect. 2.1.1). These particles were subsequently transformed into hollow spheres by chemical etching of the silica core in acidic medium [326].

Metal/polymer hybrid particles displaying an eccentric structure were very recently reported [327, 328]. The key parameter for the formation of such morphologies was the addition of the metal nanoparticles after the polymerization was started. The reaction was performed in a water/ethanol mixture (40/60 by weight), ethanol playing a key role in the reduction of charge effects. Each hybrid particle contained only one metal nanoparticle anchored on the poly(styrene-*co*-DVB-*co*-NaSS) polymer particle. The strategy proved to be successful for gold, palladium, and platinum.

Finally, even if microgels are out of the scope of the present review, it is worth mentioning that gold nanoparticles have also been encapsulated inside thermo- and pH-responsive poly(NIPAM-*co*-AA) microgel particles using 60 nm OA-coated nanoparticles as seeds [329, 330].

7.2 Polymer Particles as Template for the Synthesis of Metallic Shells and Metallic Nanoparticles

Polymer particles can serve as colloidal templates for the in situ synthesis of either metallic nanoparticles or metallic shells. This is achieved by the reaction of the metal salt precursors previously adsorbed on their surface through ion exchange or complexation chemistry. The colloidal templates must contain surface groups with strong affinity for the metal precursors. Functional groups issued from carboxyl ($-\text{COOH}$), hydroxyl ($-\text{OH}$), thiol ($-\text{SH}$), amino ($-\text{NH}_2$), cyano ($-\text{CN}$), or pyridino derivatives can be easily introduced into polymer latexes by copolymerization of the corresponding monomer. In this method, the surface-complexed metal salts are then directly transformed into metal colloids by the addition of reducing agents. For instance, polymer particles with a PS core and a P4VPy shell were used as template for the synthesis of noble metal (including palladium, gold and silver) nanoparticles in the shell layer (Fig. 38) [331]. The Pd-functionalized composite particles were successfully used as catalysts in Suzuki cross-coupling reactions.

Similarly, using the same particles as those used for the synthesis of CdS QDs (see Sect. 6.2, Fig. 36), silver nanoparticles could be deposited onto carboxylated poly(MMA-*co*-MAA) particles using silver salts as precursors [315, 316]. As for the case of CdS, periodic structures of polymer/silver hybrid colloids were elaborated. The method obviously opens a new avenue for production of optically responsive materials with a controlled periodicity. In another work using commercial 110 nm carboxylate-functionalized PS particles as templates, Hao et al. reported the synthesis of silver nanodisks formed through chemical reduction of silver salts in DMF [332]. The composite particles obtained (Fig. 39) exhibited an intense electronic spectrum differing markedly from those of spheres. Still using

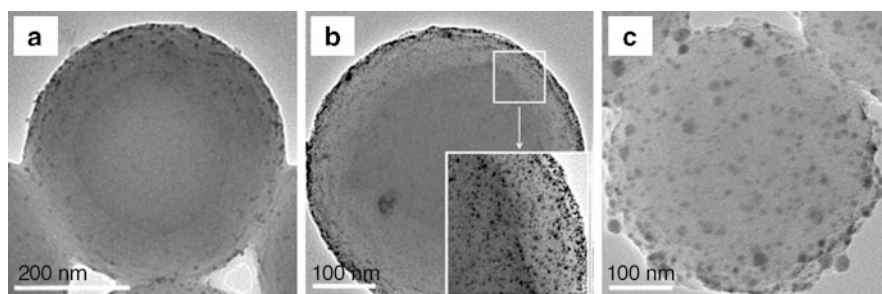


Fig. 38 TEM images of (a) poly(styrene-*co*-4VPy)/Pd, (b) poly(styrene-*co*-4VPy)/Au, and (c) poly(styrene-*co*-4VPy)/Ag composite particles produced via chemical reduction of the corresponding metal salts previously adsorbed on the surface of poly(styrene-*co*-4VPy) core-shell particles. Adapted from [331] with permission of the American Chemical Society

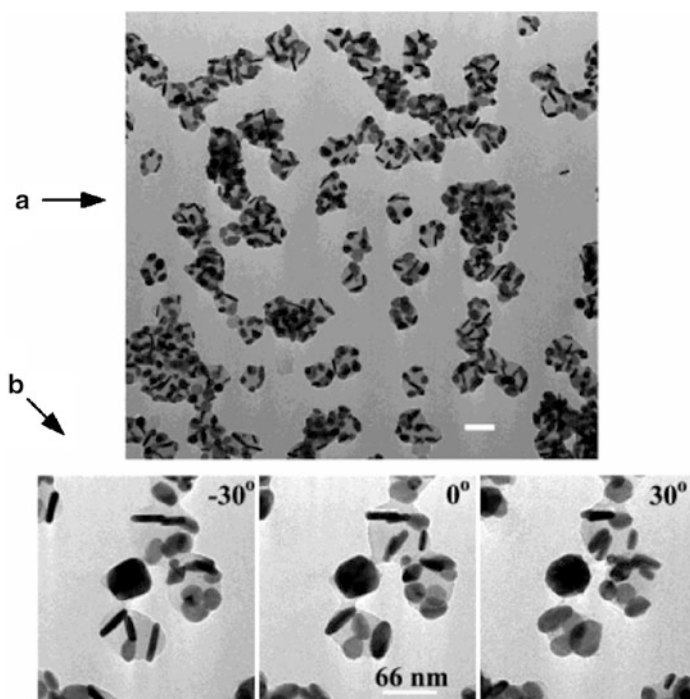


Fig. 39 (a) TEM image of a fresh Ag/PS sample. Scale bar: 100 nm. (b) TEM images of Ag/PS, tilting the sample plane from -30° through 0° to $+30^\circ$. Reproduced from [332] with permission of the American Chemical Society

carboxylated particles, different in situ chemical reduction methods were studied by Mayer et al. to form silver-latex composites using commercial PS latexes [333]. By adjusting the latex surface properties, the reduction method and conditions, or the silver precursor type, various composite materials could be prepared.

In other works, palladium [334–337] and rhodium [335–337] nanoparticles were formed onto the surface of PS-based polymer particles functionalized through the copolymerization of styrene with AA, MAA, and acrylonitrile. The resulting composite colloids were evaluated as catalysts for the hydrogenation of alkenes, the Rh-based composite showing activities close to commercially available products [336]. Using the obtained Pd-functionalized polymer particles, nickel [338], nickel/cobalt [339], or cobalt [340] nanoparticles were anchored onto the surface through chemical metal deposition (electroless plating) [341].

Sulfate-functionalized PS particles (of 710 and 580 nm) obtained by emulsion polymerization were coated with silver or gold nanoparticles through the adsorption of their corresponding metal salts in an ethanol/acetone mixture. This was followed by chemical reduction and a seeding growth step (both performed in ethanol) [342]. The obtained core–shell colloids were able to crystallize into long-range ordered structures with photonic bandgaps (Fig. 40). As well as potential applications as photonic crystals, the ordered structures may find applications as substrates for SERS (surface enhanced Raman spectroscopy) studies.

More recently, noble metals such as gold, silver, platinum, and palladium were deposited onto sulfate-functionalized PS particles through the addition of their respective metal salts in the absence of extra reducing agent [343]. The sulfate groups were supposed to be involved in a redox reaction with the metal salts, eventually leading to the formation of the metal nanoparticles (Fig. 41).

A last example of particular interest that also relies on the adsorption of metal salts was recently proposed for the synthesis of silver nanoparticles inside the

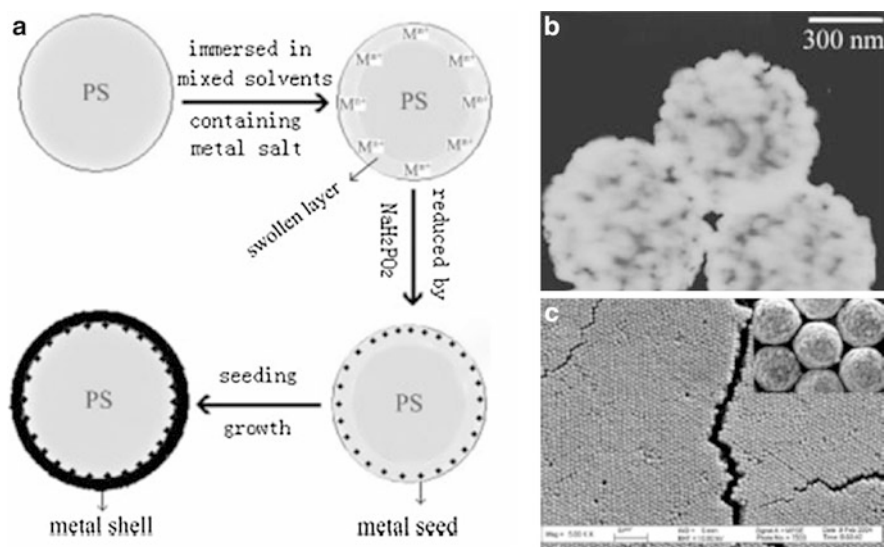
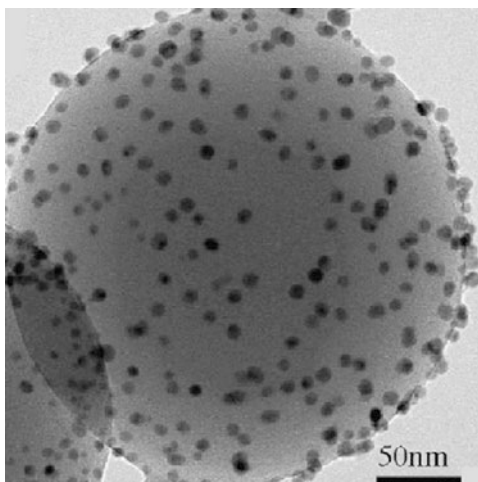


Fig. 40 (a) Procedure for coating PS colloids with gold or silver. (b) TEM image of 580 nm PS colloids coated with gold. (c) SEM image of opals made of gold-coated PS composite colloids. Reproduced from [342] with permission of Wiley-VCH

Fig. 41 TEM image of nanosize-dot-arrayed Ag-PS composite fabricated by means of the redox reaction method. Reprinted from [343] with permission of Elsevier



outer layer of “nano-tree”-type core-shell particles, i.e., particles with a PS core surrounded by regularly branched chains of PEG [344]. Similarly, Mei et al. showed that palladium nanoparticles could be synthesized inside the hairy layer of PS-PNIPAM core-shell particles [345]. In both cases, the composite particles were subsequently used as catalyst in the reduction reaction of 4-nitrophenol in the presence of sodium borohydride.

Instead of precursor metal salts, metal oxides could also be used. Silver-PS core-shell particles were thus recently synthesized using a two-step procedure [346]. First, hydrogen reduction of a saturated silver(I) oxide solution at elevated temperature was carried out in the presence of commercial sulfate-functionalized PS particles (200 nm) used as support for the reduction of Ag salt into silver. The formed Ag nanoparticles were attached to the PS particles (Fig. 42a). Subsequent acetone treatment led to the encapsulation of the silver nanoparticles inside the PS spheres (Fig. 42b), accompanied by a red-shift of the characteristic plasmon resonance frequency of the particles (Fig. 42c).

In alternative procedures, the coating can also be produced by the controlled hydrolysis of metal salts into metal oxides, followed by reduction of the oxide into the corresponding metal. Submicrometer-sized composite spheres of yttrium and zirconium compounds and hollow metallic spheres have been prepared this way by coating cationic PS latex particles with basic yttrium carbonate and basic zirconium sulfate, respectively, followed by calcination of the coated latexes at elevated temperatures [347, 348]. Uniform coatings of copper compounds have been formed in a similar procedure by aging (at high temperature) the aqueous solutions of the metal salt in the presence of urea, PVP, and anionic PS latexes [349]. The coating was shown to proceed by *in situ* heterocoagulation of the precipitating metal colloids on the organic seed surface. Voids were produced in a subsequent step by complete thermal oxidative decomposition of the polymer core.

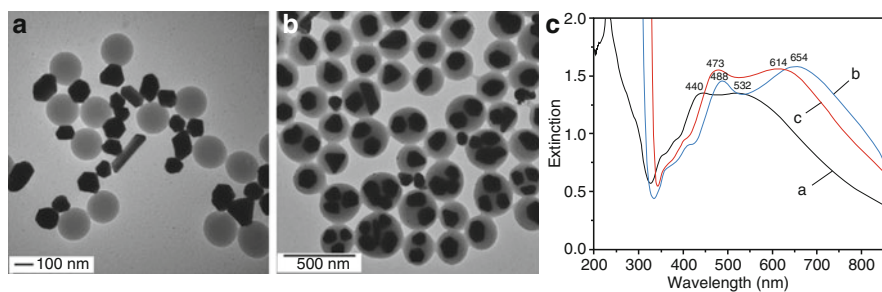


Fig. 42 TEM images of (a) Ag nanoparticles adsorbed onto PS particles, and (b) Ag-PS core-shell particles. (c) Extinction spectra of as-prepared Ag-PS particles (*curve a*), Ag-PS particles dispersed in acetone (*curve b*), and redispersed back in water (*curve c*). Adapted from [346] with permission of the American Chemical Society

Finally, similarly to magnetic nanoparticles or QDs, microgel particles have been used as template for the synthesis of metallic nanoparticles such as silver [182, 321].

8 Summary and Outlook

This review article highlights the synthesis and properties of O/I particles elaborated through emulsion polymerization, which is a well-established technology. The relatively recent advances in the synthesis of these particles have paved the way to a huge range of new materials with outstanding properties. In this article, we have reported selected examples of O/I colloids prepared from either preformed minerals or preformed latex particles. When minerals are used as seeds, suitable interactions of the growing polymer with their surface are provided by the previous adsorption and/or reaction of molecules that can be either inactive or active in the subsequent polymerization process. Such molecules include conventional surfactants, organosilanes and titanates, macromonomers and surfmers, ionic initiators, and ionic monomers. The overall strategy provides an accurate control over the composite particle nanostructure, leading to a multitude of morphologies (core-shell, multinuclear, multipod-like, snowman-like, armored-like, etc.). Furthermore, the strategy affords the opportunity to precisely design the surface properties of the polymer-coated mineral particles by selecting appropriate functional monomers.

In another approach, metallic particles, semiconductors, or metal oxides are generated at the surface or inside polymer colloids used as templates. Again, the seed particle surface must carry suitable functionalities to promote interaction (and thus deposition) of the inorganic precursor. Inorganic nanoparticles are obtained in a subsequent step by thermal decomposition, hydrolysis, chemical reduction or other soft-chemistry processes. These strategies allow selective nucleation and growth of the inorganic particles at the surface or inside the latex particles, which eventually protect them from agglomeration.

Although a general chemical approach to the fabrication of these polymer/inorganic composite particles in a precisely controlled manner is not yet available, impressive progress has been made towards the designed synthesis of colloidal particles made of organic and inorganic domains assembled into unique and well-defined structures. These simple methods will most probably open the way to the fabrication of large amounts of original assemblies.

In practice, an infinite variety of polymer/inorganic particle combinations can be envisaged. This article has attempted to summarize the most important issues to be considered for successful formation of such nanocomposite colloids. The ability to tailor the affinity between the organic and inorganic parts is the key to a happy marriage between these two naturally incompatible compounds. However, despite the considerable advances, excitement, and promise of O/I composite latexes, substantial fundamental research is still necessary to provide a deeper understanding of current synthetic methods, develop new processes, and enable further exploitation of these materials.

We hope that the general concepts and principles reviewed in this article will provide the reader with the necessary background to develop deeper expertise and to create novel O/I hybrid particles and nanocomposites with outstanding characteristics and properties.

References

1. Moriarty P (2001) *Rep Prog Phys* 64:297
2. Cao G (2004) *Nanostructures and nanomaterials – synthesis, properties and applications*. Imperial College Press, London
3. Hofman-Caris CHM (1994) *New J Chem* 18:1087
4. van Herk AM (1997) In: Asua JM (ed) *Polymeric dispersions: principles and applications*, NATO ASI series E: applied sciences, vol 335. Kluwer Academic, Dordrecht, p 435
5. van Herk AM, German AL (1999) In: Arshady R (ed) *Microspheres microcapsules & liposomes*, vol 1. Preparation and chemical applications. Citus Books, London, chap 17, p 457
6. Pomogalio AD (2000) *Russ Chem Rev* 69:53
7. Bourgeat-Lami E (2002) In: R. Arshady, A. Guyot (eds) *Dendrimers, assemblies and nanocomposites*, MML series 5. Citus Books, London, chap 5, p 149
8. Bourgeat-Lami E (2002) *J Nanosci Nanotechnol* 2:1
9. Bourgeat-Lami E (2004) In: Nalwa HS (ed) *Encyclopedia of nanoscience and nanotechnology*, vol 8. American Scientific, Los Angeles, p 305
10. Bourgeat-Lami E, Duguet E (2006) In: Ghosh (ed) *Functional coatings by polymer microencapsulation*. Wiley-VCH, Weinheim, chap 4, p 85
11. Bourgeat-Lami E (2007) In: Kickelbick G (ed) *Hybrid materials, synthesis, characterization and applications*. Wiley-VCH, Weinheim, p 87
12. Castelvetro V, De Vita C (2004) *Adv Colloid Interface Sci* 108/109:167
13. Hussain F, Hojjati M, Okamoto M, Gorga RE (2006) *J Comp Mater* 40:1511
14. Balmer JA, Schmid A, Armes SP (2008) *J Mater Chem* 18:5722
15. Wang T, Keddie JL (2009) *Adv Colloid Interface Sci* 147/148:319
16. Zou H, Wu S, Shen J (2008) *Chem Rev* 108:3893
17. Stöber W, Fink A, Bohn E (1968) *J Colloid Interface Sci* 26:62
18. Kang S, Hong SI, Choe CR, Park M, Rim S, Kim J (2001) *Polymer* 42:879
19. Bourgeat-Lami E, Espiard P, Guyot A (1995) *Polymer* 36:4385

20. Espiard P, Guyot A (1995) *Polymer* 36:4391
21. Espiard P, Guyot A, Perez J, Vigier G, David L (1995) *Polymer* 36:4397
22. Bourgeat-Lami E, Lang J (1998) *J Colloid Interface Sci* 197:293
23. Bourgeat-Lami E, Lang J (1999) *J Colloid Interface Sci* 210:281
24. Corcos F, Bourgeat-Lami E, Novat C, Lang J (1999) *Colloid Polym Sci* 277:1142
25. Zhang K, Chen H, Chen X, Chen Z, Cui Z, Yang B (2003) *Macromol Mater Eng* 288:380
26. Nagao D, Ueno T, Oda D, Konno M (2009) *Colloid Polym Sci* 287:1051
27. Reculusa S, Mingotaud C, Bourgeat-Lami E, Duguet E, Ravaine S (2004) *Nano Lett* 4:1677
28. Nagao D, Hashimoto M, Hayasaka K, Konno M (2008) *Macromol Rapid Commun* 29:1484
29. Zhang K, Zheng L, Zhang X, Chen X, Yang B (2006) *Colloids Surf A Physicochem Eng Asp* 277:145
30. Zeng Z, Yu J, Guo Z (2004) *Macromol Chem Phys* 205:2197
31. Zeng Z, Yu J, Guo Z (2005) *J Polym Sci Part A Polym Chem* 43:2826
32. Qu A, Wen X, Pi P, Cheng J, Yang Z (2008) *J Colloid Interface Sci* 317:62
33. Bourgeat-Lami E, Insulaire M, Reculusa S, Perro A, Ravaine S, Duguet E (2006) *J Nanosci Nanotechnol* 6:432
34. Perro A, Duguet E, Lambert O, Taveau J-C, Bourgeat-Lami E, Ravaine S (2009) *Angew Chem Int Ed Engl* 48:361
35. Van Blaaderen A (2003) *Science* 301:470
36. Reculusa S, Poncet-Legrand C, Perro A, Duguet E, Bourgeat-Lami E, Mingotaud C, Ravaine S (2005) *Chem Mater* 17:3338
37. Reculusa S, Poncet-Legrand C, Ravaine S, Duguet E, Bourgeat-Lami E, Mingotaud C (2004) Nanometric or mesoscopic dissymmetric particles, and method for preparing same. French Patent FR2846572, WO 2004/044061
38. Perro A, Reculusa S, Pereira F, Delville MH, Mingotaud C, Duguet E, Bourgeat-Lami E, Ravaine S (2005) *Chem Commun* 5542
39. Perro A, Reculusa S, Ravaine Bourgeat-Lami E, Duguet E (2005) *J Mater Chem* 15:3745
40. Reculusa S, Poncet-Legrand C, Ravaine S, Mingotaud C, Duguet E, Bourgeat-Lami E (2002) *Chem Mater* 14:2354
41. Perro A, Reculusa S, Bourgeat-Lami E, Duguet E, Ravaine S (2006) *Colloids Surf A Physicochem Eng Asp* 284/285:78
42. Perro A, Nguyen D, Ravaine S, Bourgeat-Lami E, Lambert O, Taveau J-C, Duguet E (2009) *J Mater Chem* 19:4225
43. Nagai K, Ohishi Y, Ishiyama K, Kuramoto N (1989) *J Appl Polym Sci* 38:2183
44. Nagai K (1994) *Macromol Symp* 84:29
45. Ding XF, Zhao JZ, Liu YH, Zhang HB, Wang ZC (2004) *Mater Lett* 58:3126
46. Mahdavian AR, Ashjari M, Makoo AB (2007) *Eur Polym J* 43:336
47. Barthet C, Hickey AJ, Cairns DB, Armes SP (1999) *Adv Mater* 11:408
48. Percy MJ, Barthet C, Lobb JC, Khan MA, Lascelles SF, Vamvakaki M, Armes SP (2000) *Langmuir* 16:6913
49. Amalvy JI, Percy MJ, Armes SP (2001) *Langmuir* 17:4770
50. Fujii S, Read ES, Binks BP, Armes SP (2005) *Adv Mater* 17:1014
51. Fujii S, Armes SP, Binks BP, Murakami R (2006) *Langmuir* 22:6818
52. Chen M, Wu L, Zhou S, You B (2004) *Macromolecules* 37:9613
53. Chen M, Zhou S, You B, Wu L (2005) *Macromolecules* 38:6411
54. Kammona O, Kotti K, Kiparissides C, Celis J-P, Fransær J (2009) *Electrochim Acta* 54:2450
55. Cheng X, Chen M, Zhou S, Wu L (2006) *J Polym Sci Part A Polym Chem* 44:3807
56. Luna-Xavier JL, Bourgeat-Lami E, Guyot A (2001) *Colloid Polym Sci* 279:947
57. Luna-Xavier JL, Guyot A, Bourgeat-Lami E (2002) *J Colloid Interface Sci* 250:82
58. Luna-Xavier JL, Guyot A, Bourgeat-Lami E (2004) *Polym Int* 53:609
59. Qi D-M, Bao Y-Z, Huang Z-M, Weng Z-X (2006) *J Appl Polym Sci* 99:3425
60. Dupin D, Schmid A, Balmer JA, Armes SP (2007) *Langmuir* 27:11812
61. Schmid A, Tonnar J, Armes SP (2008) *Adv Mater* 20:3331
62. Schmid A, Armes SP, Leite CAP, Galembeck F (2009) *Langmuir* 25:2486
63. Schmid A, Scherl P, Armes SP, Leite CAP, Galembeck F (2009) *Macromolecules* 42:3721

64. Lee J, Hong CK, Choe S, Shima SE (2007) *J Colloid Interface Sci* 310:112
65. Zhang F-A, Yu C-L (2007) *Eur Polym J* 43:1105
66. Colver PJ, Colard CA L, Bon SAF (2008) *J Am Chem Soc* 130:16850
67. Hu J, Ma J, Deng W (2008) *Mater Lett* 62:2931
68. Sheibat-Othman N, Bourgeat-Lami E (2009) *Langmuir* 25:10121
69. Binks BP, Horozov TS (eds) (2006) *Colloidal particles at liquid interfaces*. Cambridge University Press, Cambridge
70. Teixeira RFA, Bon SAF (2010) Physical methods for the preparation of hybrid nanocomposite polymer latex particles. *Adv Polym Sci* doi:10.1007/12_2010_65
71. Xue Z, Wiese H (2006) US patent US7094830B2
72. Tiarks F, Leuninger J, Wagner O, Jahns E, Wiese H (2007) *Surf Coat Intern* 90:221
73. Kalele S, Gosavi SW, Urban J, Kulkarni SK (2006) *Curr Sci* 91:1038
74. Kickelbick G, Liz-Marzan LM (2004) In: Nalwa HS (ed) *Encyclopedia of nanoscience and nanotechnology*, vol 2 American Scientific, Los Angeles, p 199
75. Tissot I, Novat C, Lefebvre F, Bourgeat-Lami E (2001) *Macromolecules* 34:5737
76. Bourgeat-Lami E, Tissot I, Lefebvre F (2002) *Macromolecules* 35:6185
77. Tissot I, Reymond JP, Lefebvre F, Bourgeat-Lami E (2002) *Chem Mater* 14:1325
78. Castelvetro V, Manariti A, De Vita C, Ciardelli F (2002) *Macromol Symp* 187:165
79. Hotta Y, Alberius PCA, Bergstro L (2003) *J Mater Chem* 13:496
80. Cornelissen JJLM, Connor EF, Kim H-C, Lee VY, Magibitang T, Rice PM, Volasen W, Sundberg LK, Millar RD (2003) *Chem Commun* 1010
81. Lu Y, McLellan J, Xia Y (2004) *Langmuir* 20:3464
82. Yang J, Lind JU, Trogler WC (2008) *Chem Mater* 20:2875
83. Graf C, Vossen D, Imhof A, Van Blaaderen A (2003) *Langmuir* 19:6693
84. Kobayashi Y, Misawa K, Kobayashi M, Takeda M, Konno M, Satake M, Kawazoe Y, Ohuchi N, Kasuya A (2004) *Colloids Surf A Physicochem Eng Asp* 242:47
85. Rosensweig RE (1985) *Ferrohydrodynamics*. Cambridge University Press, Cambridge
86. Lu A-H, Salabas EL, Schüth F (2007) *Angew Chem Int Ed Engl* 46:1222
87. Pyle BH, Broadway SC, McFeters GA (1999) *Appl Environ Microbiol* 65:1966
88. Cumbal L, Greenleaf J, Leun D, SenGupta AK (2003) *React Funct Polym* 54:167
89. Mornet S, Vasseur S, Grasset F, Veverka P, Goglio G, Demourgues A, Portier J, Pollert E, Duguet E (2006) *Prog Solid State Chem* 34:237
90. Pankhurst QA, Connolly J, Jones SK, Dobson J (2003) *J Phys D Appl Phys* 36:R167
91. Elaissari A, Sauzedde F, Montagne F, Pichot C (2003) In: Elaissari A (ed) *Colloidal polymers: synthesis and characterization*. Marcel Dekker, New York, p 285
92. Arshady R, Pouliquen D, Halbreich A, Roger J, Pons J-N, Bacri J-C, Da Silva MdF, Häfeli U (2002) In: Arshady R, Guyot A (eds) *Dendrimers, assemblies, nanocomposites*, MML series 5. Citus Books, London, p 283
93. Vatta LL, Sanderson RD, Koch KR (2006) *Pure Appl Chem* 78:1793
94. Charmot D (1989) *Prog Colloid Polym Sci* 79:94
95. Lin C-R, Wang C-C, Chen IH (2006) *J Magn Magn Mater* 304:e34
96. Wang Y, Feng L, Pan C (1998) *J Appl Polym Sci* 70:2307
97. Wang PH, Pan CY (2000) *Colloid Polym Sci* 278:245
98. Wang PH, Pan CY (2002) *Colloid Polym Sci* 280:152
99. Jiang J (2007) *Eur Polym J* 43:1724
100. Liu W-J, He W-D, Wang Y-M, Wang D, Zhang Z-C (2005) *Polymer* 46:8366
101. Molday RS, Yen SPS, Rembaum A (1977) *Nature* 268:437
102. Kwon O, Solc J (1986) *J Magn Magn Mater* 54–57:1699
103. Solc J (1983) Colloidal size hydrophobic polymers particulate having discrete particles of an inorganic material dispersed therein. US Patent 4,421,660
104. Wooding A, Kilner M, Lambrick DB (1991) *J Colloid Interface Sci* 144:236
105. Wooding A, Kilner M, Lambrick DB (1992) *J Colloid Interface Sci* 149:98
106. Shen L, Laibinis PE, Hatton TA (1999) *Langmuir* 15:447
107. Meguro K, Yabe T, Ishioka S, Kato K, Esumi K (1986) *Bull Chem Soc Jpn* 59:3019
108. Yanase N, Noguchi H, Asakura H, Suzuta T (1993) *J Appl Polym Sci* 50:765

109. Noguchi H, Yanase N, Uchida Y, Suzuta T (1993) *J Appl Polym Sci* 48:1539
110. Xu X, Friedman G, Humfeldt KD, Majetich SA, Asher SA (2002) *Chem Mater* 14:1249
111. Xu X, Friedman G, Humfeldt KD, Majetich SA, Asher SA (2001) *Adv Mater* 13:1681
112. Wang P-C, Chiu W-Y, Lee C-F, Young T-H (2004) *J Polym Sci A Polym Chem* 42:5695
113. Wang P-C, Chiu W-Y, Young T-H (2006) *J Appl Polym Sci* 100:4925
114. Brijmohan SB, Shaw MT (2007) *J Membrane Sci* 303:64
115. Xie G, Zhang Q, Luo Z, Wu M, Li T (2003) *J Appl Polym Sci* 87:1733
116. Kondo A, Fukuda H (1997) *J Ferment Bioeng* 84:337
117. Kondo A, Kamura H, Higashitani K (1994) *Appl Microbiol Biotechnol* 41:99
118. Khan A (2008) *Mater Lett* 62:898
119. Lee CF, Chou YH, Chiu WY (2007) *J Polym Sci A Polym Chem* 45:3062
120. Lee CF, Chou YH, Chiu WY (2007) *J Polym Sci A Polym Chem* 45:3912
121. Guan N, Liu C, Sun D, Xu J (2009) *Colloids Surf A Physicochem Eng Asp* 335:174
122. Jung S, Park S (2009) *Biotechnol Lett* 31:107
123. Pich A, Bhattacharya S, Ghosh A, Adler H-JP (2005) *Polymer* 46:4596
124. Stevens PD, Fan J, Gardimalla HMR, Yen M, Gao Y (2005) *Org Lett* 7:2085
125. Huang J, Pen H, Xu Z, Yi C (2008) *React Funct Polym* 68:332
126. Liu H, Guo J, Jin L, Yang W, Wang C (2008) *J Phys Chem B* 112:3315
127. Xu Z, Xia A, Wang C, Yang W, Fu S (2007) *Mater Chem Phys* 103:494
128. Li P, Zhu AM, Liu QL, Zhang QG (2008) *Ind Eng Chem Res* 47:7700
129. Pollert E, Knížek K, Marysko M, Záveta K, Lancok A, Boháček J, Horák D, Babić M (2006) *J Magn Magn Mater* 306:241
130. Horák D, Chekina N (2006) *J Appl Polym Sci* 102:4348
131. Horák D, Petrovský E, Kapicka A, Frederichs T (2007) *J Magn Magn Mater* 311:500
132. Qiu G-M, Xu Y-Y, Zhu B-K, Qiu G-L (2005) *Biomacromolecules* 6:1041
133. Guo N, Wu D, Pan X, Lu M (2009) *J Appl Polym Sci* 112:2383
134. Galperin A, Margel S (2007) *J Biomed Mater Res B Appl Biomater* 83B:490
135. Skaat H, Belfort G, Margel S (2009) *Nanotechnology* 22:5106
136. Boguslavsky Y, Margel S (2008) *J Colloid Interface Sci* 317:101
137. Yang Y, Tu C, Gao M (2007) *J Mater Chem* 17:2930
138. Tu C, Yang Y, Gao M (2008) *Nanotechnology* 19:105601/1
139. Montagne F, Mondain-Monval O, Pichot C, Elaïssari A (2006) *J Polym Sci A Polym Chem* 44:2642
140. Xu H, Cui L, Tong N, Gu H (2006) *J Am Chem Soc* 128:15582
141. Cui L, Xu H, He P, Sumitomo K, Yamaguchi Y, Gu H (2007) *J Polym Sci A Polym Chem* 45:5285
142. Ding Y, Hu Y, Jiang X, Zhang L, Yang C (2004) *Angew Chem Int Ed Engl* 43:6369
143. Ding Y, Hu Y, Zhang L, Chen Y, Jiang X (2006) *Biomacromolecules* 7:1766
144. Wu Y, Guo J, Yang W, Wang C, Fu S (2006) *Polymer* 47:5287
145. Guo J, Wang C, Mao W, Yang W, Liu C, Chen J (2008) *Nanotechnology* 19:315605
146. Sacanna S, Philipse AP (2006) *Langmuir* 22:10209
147. Sacanna S, Philipse AP (2007) *Adv Mater* 19:3824
148. Sacanna S, Kegel WK, Philipse AP (2007) *Phys Rev Lett* 98:158301
149. Ge J, Hu Y, Zhang T, Yin Y (2007) *J Am Chem Soc* 129:8974
150. Nagao D, Yokoyama M, Saeki S, Kobayashi Y, Konno M (2008) *Colloid Polym Sci* 286:959
151. Deng YH, Yang WL, Wang CC, Fu SK (2003) *Adv Mater* 15:1729
152. Cai J, Guo J, Ji M, Yang W, Wang C, Fu S (2007) *Colloid Polym Sci* 285:1607
153. Ge J, Huynh T, Hu Y, Yin Y (2008) *Nano Lett* 8:931
154. Furusawa K, Nagashima K, Anzai C (1994) *Colloid Polym Sci* 272:1104
155. Du H, Zhang P, Liu F, Kan S, Wang D, Li T, Tang X (1997) *Polym Int* 43:274
156. Du H, Cao Y, Bai Y, Zhang P, Qian X, Wang D, Li T, Tang X (1998) *J Phys Chem B* 102:2329
157. Sauzedde F, Elaïssari A, Pichot C (1999) *Colloid Polym Sci* 277:846
158. Sauzedde F, Elaïssari A, Pichot C (1999) *Colloid Polym Sci* 277:1041
159. Sauzedde F, Elaïssari A, Pichot C (2000) *Macromol Symp* 151:617
160. Gu S, Shiratori T, Konno M (2003) *Colloid Polym Sci* 281:1076

161. Gu S, Onishi J, Kobayashi Y, Nagao D, Konno M (2005) *J Colloid Interface Sci* 289:419
162. Lee J, Senna M (1995) *Colloid Polym Sci* 273:76
163. Sayar F, Güven G, Piskin E (2006) *Colloid Polym Sci* 284:965
164. Sun H, Yu J, Gong P, Xu D, Zhang C, Yao S (2005) *J Magn Magn Mater* 294:273
165. Candau F (1997) In: Lovell PA, El-Aasser MS (eds) *Emulsion polymerization and emulsion polymers*. Wiley, Chichester, p 723
166. Pichot C (2006) In: Pichot C, Daniel JC (eds) *Les latex synthétiques élaboration, propriétés, applications*. Lavoisier, Paris, p 207
167. Li X, Zhang L, Jin R (1999) *Polym Adv Technol* 10:90
168. Macková H, Králová D, Horák D (2007) *J Polym Sci A Polym Chem* 45:5884
169. Ménager C, Sandre O, Mangili J, Cabuil V (2004) *Polymer* 45:2475
170. Yang S, Liu H, Zhang Z (2008) *Langmuir* 24:10395
171. Hong RY, Feng B, Liu G, Wang S, Li HZ, Ding JM, Zheng Y, Wei DG (2009) *J Alloy Compd* 476:612
172. Liu H, Wang C, Gao Q, Chen J, Liu X, Tong Z (2009) *Mater Lett* 63:884
173. Ugelstad J, Berge A, Ellingsen T, Schmid R, Nilsen TN, Mørk PC, Stenstad P, Hornes E, Olsvik (1992) *Prog Polym Sci* 17:87
174. Ugelstad J, Ellingsen T, Berge A, Helgée B (1983) *Magnetic polymer particles and process for the preparation thereof*. WO 83/03920
175. Lindlar B, Boldt M, Eiden-Assmann S, Maret G (2002) *Adv Mater* 14:1656
176. Pich A, Bhattacharya S, Adler HJP (2005) *Polymer* 46:1077
177. Pich A, Bhattacharya S, Lu Y, Boyko V, Adler H-JP (2004) *Langmuir* 20:10706
178. Omer-Mizrahi M, Margel S (2009) *J Colloid Interface Sci* 329:228
179. Tapeinos C, Kartsonakis I, Liatsi P, Daniilidis I, Kordas G (2008) *J Am Ceram Soc* 91:1052
180. Suzuki D, Kawaguchi H (2006) *Colloid Polym Sci* 284:1443
181. Rubio-Retama J, Zafeiropoulos NE, Serafinelli C, Rojas-Reyna R, Voit B, Cabarcos EL, Stamm M (2007) *Langmuir* 23:10280
182. Zhang J, Xu S, Kumacheva E (2004) *J Am Chem Soc* 126:7908
183. Lee C-F, Lin C-C, Chien C-A, Chiu W-Y (2008) *Eur Polym J* 44:2768
184. Brugger B, Richtering W (2007) *Adv Mater* 19:2973
185. Conley RF (1996) In: *Practical dispersion – a guide to understanding and formulating slurries*. VCH, New York
186. Schofield JD (2002) *Prog Org Coat* 45:249
187. Hou WH, Lloyd TB, Fowkes FM (1992) In: Daniels ES, Sudol T, El-Aasser M (eds) *Polymer latexes: preparation, characterization and applications*, ACS symposium series 492. ACS, Washington DC, chap 25, pp 405–421
188. Sperry PR, Wiersema RJ, Nyi K (1978) *Dispersing paint pigments*. US Patent 4,102,843
189. Schofield JD (1982) *Dispersible inorganic pigment*. US Patent 4,349,389
190. Solc J (1983) *Colloidal size hydrophobic polymers particulate having discrete particles of an inorganic material dispersed therein*. US Patent 4,421,660
191. Martin RW (1984) *Polymer-encapsulated dispersed solids and methods*. Eur Patent Appl 0104498
192. Martin RW (1986) *Method of encapsulating finely divided solid particles*. US Patent 4,608,401
193. Solc J (1987) *Method for preparing colloidal size particulate*. US Patent 4,680,200
194. Hoy KL, Glancy CW, Lewis JMO (1990) *Micro-composite systems and processes for making same*. Eur Patent Appl 0392065
195. Martin RW (1992) *Encapsulating finely divided solid particles in stable suspensions*. US Patent 4,771,086
196. Hees U, Kluge M, Raulfs FW, Schoepke H, Siemensmeyer K, Van Gelder R, Weiser J, Heissler H, Adams S, Renz G, Simpson PA (2004) *Method for treating particulate pigments*. WO 2004113454
197. Templeton-Knight RL (1990) *J Oil Colour Chem Assoc* 73:459
198. Templeton-Knight RL (1990) *Chem Ind* 512

199. Lorimer JP, Mason TJ, Kershaw D, Livsey I, Templeton-Knight RL (1991) *Colloid Polym Sci* 269, 392
200. Hasegawa M, Arai K, Saito S (1987) *J Polym Sci Part A Polym Chem* 25:3117
201. Hasegawa M, Arai K, Saito S (1987) *J Appl Polym Sci* 33:411
202. Hoy KL, Smith OW (1991) *ACS Polym Mater Sci Eng Preprint* 65:78
203. Caris CHM, van Elven LPM, van Herk AM, German A (1998) 19th FATIPEC Conference Proceeding 3:341
204. Caris CHM, van Elven LPM, van Herk AM, German A (1989) *Brit Polym J* 21:133
205. Caris CHM, van Herk AM, German AL (1990) 20th FATIPEC Conference Proceedings 325
206. Caris CHM, Kuijpers RPM, van Herk AM, German AL (1990) *Makromol Chem Macromol Symp* 35/36, 535
207. Janssen EAWG, van Herk AM, German AL (1993) *ACS Div Polym Chem Polym Preprint* 34:532
208. Janssen RQF, van Herk AM, German AL (1993) *J Oil Colour Chem Assoc* 11:455
209. Janssen RQF, van Herk AM, German AL (1994) 22th FATIPEC Conference Proceedings 1:104
210. Caris CHM (1990) Polymer encapsulation of inorganic submicron particles in aqueous dispersion. Ph.D. Thesis, Eindhoven University of Technology, The Netherlands
211. Janssen RQF (1995) Polymer encapsulation of titanium dioxide. Efficiency, stability and compatibility. Ph.D. Thesis, Eindhoven University of Technology, The Netherlands
212. Yang M, Dan Y (2006) *J Appl Polym Sci* 101:4056
213. Haga Y, Watanabe T, Yosomiya R (1991) *Angew Makromol Chem* 189:23
214. Nguyen D, Zondanos HS, Farrugia JM, Serelis AK, Such CH, Hawkett BS (2008) *Langmuir* 24:2140
215. Daigle JC, Claverie JP (2008) *J Nanomater* 609184
216. Charleux B, D'Agosto F, Delaittre G (2010) Preparation of hybrid latex particles and core-shell particles through the use of controlled radical polymerization techniques in aqueous media. *Adv Polym Sci* doi:10.1007/12_2010_64
217. Yu D-G, An JO, Bae JY, Lee YE, Ahn SD, Kang S-Y, Suh KS (2004) *J Appl Polym Sci* 92:2970
218. Yu D-G, An J-H, Bae JY, Ahn SD, Kang S-Y, Suh KS (2005) *J Appl Polym Sci* 97:72
219. Badila M, Brochon C, Hebraud A, Hadziioannou G (2008) *Polymer* 49:4529
220. Zhang P, Zhang HP, Li ZH, Wu YP, van Ree T (2009) *Polym Adv Technol* 20:571
221. Liu Y, Chen X, Wang R, Xin JH (2006) *Mater Lett* 60:3731
222. Chen T, Colver PJ, Bon SAF (2007) *Adv Mater* 19:2286
223. Ai Z, Sun G, Zhou Q, Xie C (2006) *J Appl Polym Sci* 102:1466
224. Kondo Y, Yoshikawa H, Awaga K, Murayama M, Mori T, Sunada K, Bandow S, Iijima S (2008) *Langmuir* 24:547
225. Yang Su-C, Yang D-J, Kim J, Hong J-M, Kim H-G, Kim I-D, Lee H (2008) *Adv Mater* 20:1059
226. Chigane M, Watanabe M, Izaki M, Yamaguchi I, Shinagawa T (2009) *Electrochem SolidState Lett* 12:E5
227. Shiho H, Kawahashi N (2000) *Colloid Polym Sci* 278:270
228. Li GK, Zhang ZC (2004) *Mater Lett* 58:2768
229. Syoufian A, Inoue Y, Yada M, Nakashima K (2007) *Mater Lett* 61:1572
230. Wang P, Chen D, Tang F-Q (2006) *Langmuir* 22:4832
231. Imhof A (2001) *Langmuir* 17:3579
232. Caruso F, Shi X, Caruso RA, Susa A (2001) *Adv Mater* 13:740
233. Eiden S, Maret G (2002) *J Colloid Interface Sci* 250:281
234. Liu H, Ye H, Zhang Y (2007) *Appl Surf Sci* 253:7219
235. Liu H, Ye H, Zhang Y (2008) *Colloids Surfaces A Physicochem Eng Asp* 315:1
236. Karlsson PM, Esbjörnsson NB, Holmberg K (2009) *J Colloid Interface Sci* 337:364
237. Agrawal M, Pich A, Zafeiropoulos NE, Gupta S, Pionteck J, Simon F, Stamm M (2007) *Chem Mater* 19:1845
238. Chen JH, Cheng C-Y, Chiu W-Y, Lee C-F, Liang N-Y (2008) *Eur Polym J* 44:3271

239. Yang Y, Kong XZ, Kan CY, Sun CG (1999) *Polym Adv Technol* 10:54
240. Yu J, Yu J, Guo Z-X, Gao Y-F (2001) *Macromol Rapid Commun* 22:1261
241. Wu W, He T, Chen J-F, Zhang X, Chen Y (2006) *Mater Lett* 60:2410
242. Batzilla Th, Tulke A (1998) *J Coat Technol* 70:77
243. Alexandre M, Dubois P (2000) *Mater Sci Eng* 28:1
244. Ray SS, Okamoto M (2003) *Prog Polym Sci* 28:1539
245. Okada A, Usuki A (2006) *Macromol Mater Eng* 291:1449
246. Chen B, Evans JRG, Greewell HC, Boulet P, Coveney PV, Bowden AA, Whiting A (2008) *Chem Soc Rev* 37:568
247. Paulis M, Leiza JR (2009) In: Mittal V (ed) *Advances in polymer nanocomposites technology* Nova, New York, chap 5
248. Solomon DH, Rosser MJ (1965) *J Appl Polym Sci* 12:1261
249. Solomon DH, Loft BC (1968) *J Appl Polym Sci* 12:1253
250. Talapatra S, Guhaniyogi SC, Chakravarti SK (1985) *J Macromol Sci Chem* A22:1611
251. Bhattacharya J, Chakravarti SK, Talapatra S, Saha SK (1989) *J Polym Sci A Polym Chem* 27:3977
252. Lee DC, Jang LW (1996) *J Appl Polym Sci* 61:1117
253. Noh MW, Lee DC (1999) *Polym Bull* 42:619
254. Noh MW, Jang LW, Lee DC (1999) *J Appl Polym Sci* 74:179
255. Noh MW, Lee DC (1999) *J Appl Polym Sci* 74:2811
256. Tong X, Zhao H, Tang T, Feng Z, Huang B (2002) *J Polym Sci A Polym Chem* 40:1706
257. Pan M, Shi X, Li X, Hu H, Zhang L (2004) *J Appl Polym Sci* 94:277
258. Kim TH, Jang LW, Lee DC, Choi HJ, Jhon MS (2002) *Macromol Rapid Commun* 23:191
259. Bandyopadhyay S, Giannelis E, Hsieh, A (2000) *Polym Mater Sci Eng* 82:208
260. Diaconu G, Asua JM, Paulis M, Leiza JR (2007) *Macromol Symp* 259:305
261. Diaconu G, Paulis M, Leiza JR (2008) *Polymer* 49:2444
262. Laus M, Camerani M, Lelli M, Sparnacci K, Sandrolini F (1998) *J Mater Sci* 33:2883
263. Wang D, Zhu J, Yao Q, Wilkie CA (2002) *Chem Mater* 14:3837
264. Liu G, Zhang L, Li Z, Qu X (2005) *J Appl Polym Sci* 98:1010
265. Feng X, Zhong A, Chen D (2006) *J Appl Polym Sci* 101:3963
266. Yang W-T, Ko T-H, Wang S-C, Shih P-I, Chang M-J, Jiang GJ (2008) *Polym Comp* 29:409
267. Min H, Wang J, Hui H, Jie W (2006) *J Macromol Sci B Phys* 45:623
268. Qutubuddin S, Fu X, Tajuddin Y (2002) *Polym Bull* 48:143
269. Sedlakova Z, Plestil J, Baldrian J, Slouf M, Holub P (2009) *Polym Bull* 63:365
270. Choi YS, Wang KH, Xu M, Chung IJ (2002) *Chem Mater* 14:2936
271. Kim YK, Choi YS, Wang KH, Chung IJ (2002) *Chem Mater* 14:4990
272. Xu M, Choi YS, Kim YK, Wang KH, Chung IJ (2003) *Polymer* 44:6387
273. Choi YS, Xu M, Chung IJ (2005) *Polymer* 46:531
274. Li H, Yang Y, Yu Y (2004) *J Adhes Sci Technol* 18:1759
275. Greesh N, Hartmann PC, Cloete V, Sanderson RD (2008) *J Polym Sci A Polym Chem* 46:3619
276. Chen G, Ma Y, Qi Z (2001) *Scr Mater* 44:125
277. Chou CS, Laffleur EE, Lorah DP, Slone RV, Neglia KD (2005) *Aqueous nanocomposite dispersions: processes, compositions and uses thereof*. US Patent 6,838,507
278. Meneghetti P, Qutubuddin S (2004) *Langmuir* 20:3424
279. Li H, Yu Y, Yang Y (2005) *Eur Polym J* 41:2016
280. Negrete-Herrera N, Letoffe JM, Putaux JL, David L, Bourgeat-Lami E (2004) *Langmuir* 20:1564
281. Negrete-Herrera N, Persoz S, Putaux JL, David L, Bourgeat-Lami E (2006) *J Nanosci Nanotechnol* 6:421
282. Negrete-Herrera N, Putaux JL, Bourgeat-Lami E (2006) *Prog Solid State Chem* 34:121
283. Negrete-Herrera N, Putaux J-L, David L, De Haas F, Bourgeat-Lami E (2007) *Macromol Rapid Commun* 28:1567
284. Ruggerone R, Plummer CJG, Negrete-Herrera N, Bourgeat-Lami E, Manson J-AE (2009) *Eur Polym J* 45:621

285. Voorn DJ, Ming W, van Herk AM (2006) *Macromolecules* 39:4654
286. Voorn DJ, Ming W, van Herk AM (2006) *Macromol Symp* 245:584
287. Choi YS, Choi MH, Wang KH, Kim SO, Kim YK, Chung IJ (2001) *Macromolecules* 34:8978
288. Yeom EH, Kim WN, Kim JK, Lee S-S, Park M (2004) *Mol Cryst Liq Cryst* 425:85
289. Lin KF, Lin SC, Chien AT, Hsieh CC, Yen MH, Lee CH, Lin CS, Chiu WY, Lee YH (2006) *J Polym Sci A Polym Chem* 44:5572
290. Zhang J, Chen K, Zhao H (2008) *J Polym Sci A Polym Chem* 46:2632
291. Guillot S, Bergaya F, de Azevedo C, Warmont F, Tranchant J-F (2009) *J Colloid Interface Sci* 333:563
292. Voorn DJ, Ming W, Van Herk AM (2006) *Macromolecules* 39:2137
293. Alivisatos AP (1996) *Science* 271:933
294. Murphy CJ (2002) *Anal Chem* 520A
295. Tomczak N, Janczewski D, Han M, Vancso GJ (2009) *Prog Polym Sci* 34:393
296. Trindade T, O'Brien P, Pickett NL (2001) *Chem Mater* 13:3843
297. Murray CB, Norris DJ, Bawendi MG (1993) *J Am Chem Soc* 115:8706
298. Peng X, Wickham J, Alivisatos AP (1998) *J Am Chem Soc* 120:5343
299. Peng X, Manna L, Yang W, Wickham J, Scher E, Kadavanich A, Alivisatos AP (2000) *Nature* 404:59
300. Peng ZA, Peng X (2001) *J Am Chem Soc* 123:183
301. Peng X (2002) *Chem Eur J* 8:334
302. Spanhel L, Haase M, Weller H, Henglein A (1987) *J Am Chem Soc* 109:5649
303. Huang J, Sooklal K, Murphy CJ, Ploehn HJ (1999) *Chem Mater* 11:3595
304. Sherman RL Jr, Chen Y, Ford WT (2004) *J Nanosci Nanotech* 4:1032
305. Hines MA, Guyot-Sionnest P (1996) *J Phys Chem* 100:468
306. Dabbousi BO, Rodriguez-Viejo J, Mikulec FV, Heine JR, Mattoussi H, Ober R, Jensen KF, Bawendi MG (1997) *J Phys Chem B* 101:9463
307. Yang X, Zhang Y (2004) *Langmuir* 20:6071
308. Sherman RL Jr, Ford WT (2005) *Langmuir* 21:5218
309. Lee BH, Kwon K-W, Shim M (2007) *J Mater Chem* 17:1284
310. Yang Y, Wen Z, Dong Y, Gao M (2006) *Small* 2:898
311. Janczewski D, Tomczak N, Han M-Y, Vancso GJ (2009) *Macromolecules* 42:1801
312. Kuang M, Wang D, Bao H, Gao M, Möhwald H, Jiang M (2005) *Adv Mater* 17:267
313. Gong Y, Gao M, Wang D, Möhwald H (2005) *Chem Mater* 17:2648
314. Li J, Liu B, Li J (2006) *Langmuir* 22:528
315. Zhang J, Coombs N, Kumacheva E (2002) *J Am Chem Soc* 124:14512
316. Zhang J, Coombs N, Kumacheva E, Lin Y, Sargent EH (2002) *Adv Mater* 14:1756
317. Chu YC, Wang CC, Huang YH, Chen CY (2005) *Nanotechnology* 16:376
318. Wang C-C, Chen A-L, Chen IH (2006) *J Inorg Organomet Polym Mater* 16:31
319. Wang C-C, Chen A-L, Chen I-H (2006) *Polym Adv Technol* 17:598
320. Cheng X, Zhao Q, Yang Y, Tjong SC, Li RKY (2008) *J Colloid Interface Sci* 326:121
321. Xu S, Zhang J, Paquet C, Lin Y, Kumacheva E (2003) *Adv Funct Mater* 13:468
322. Wu W, Zhou T, Shen J, Zhou S (2009) *Chem Commun*:4390
323. Quaroni L, Chumanov G (1999) *J Am Chem Soc* 121:10642
324. Bao H, Chumanov G, Czerw R, Carroll DL, Foulger SH (2005) *Colloid Polym Sci* 283:653
325. Obare SO, Jana NR, Murphy CJ (2001) *Nano Lett* 1:601
326. Gu S, Onishi J, Mine E, Kobayashi Y, Konno M (2004) *J Colloid Interface Sci* 279:284
327. Ohnuma A, Cho EC, Camargo PHC, Au L, Ohtani B, Xia Y (2009) *J Am Chem Soc* 131:1352
328. Ohnuma A, Cho EC, Jiang M, Ohtani B, Xia Y. (2009) *Langmuir* 25:13880
329. Kim JH, Lee TR (2004) *Chem Mater* 16:3647
330. Kim JH, Lee TR (2004) *Polym Mater Sci Eng* 90:637
331. Wen F, Zhang W, Wei G, Wang Y, Zhang J, Zhang M, Shi L (2008) *Chem Mater* 20:2144
332. Hao E, Kelly KL, Hupp JT, Schatz GC (2002) *J Am Chem Soc* 124:15182
333. Mayer ABR, Grebner W, Wannemacher R (2000) *J Phys Chem B* 104:7278
334. Wang PH, Pan C-Y (2001) *Colloid Polym Sci* 279:171
335. Tamai H, Sakurai S, Hirota Y, Nishiyama F, Yasuda H (1995) *J Appl Polym Sci* 56:441

336. Tamai H, Hamamoto S, Nishiyama F, Yasuda H (1995) *J Colloid Interface Sci* 171:250
337. Tamai H, Sumi T, Nishiyama F, Yasuda H (1996) *J Appl Polym Sci* 60:1727
338. Wang PH, Pan CY (2000) *Colloid Polym Sci* 278:245
339. Wang PH, Pan C-Y (2000) *Colloid Polym Sci* 278:581
340. Wang PH, Pan CY (2002) *Colloid Polym Sci* 280:152
341. Warshawsky A, Upson DA (1989) *J Polym Sci A Polym Chem* 27:2963
342. Zhang J, Liu J, Wang S, Shan P, Wang Z, Ming N (2004) *Adv Funct Mater* 14:1089
343. Ou JL, Chang CP, Sung Y, Ou KL, Tseng CC, Ling HW, Ger MD (2007) *Colloids Surfaces A Physicochem Eng Asp* 305:36
344. Lu Y, Mei Y, Walker R, Ballauff M, Drechsler M (2006) *Polymer* 47:4985
345. Mei Y, Lu Y, Polzer F, Ballauff M (2007) *Chem Mater* 19:1062
346. Kumbhar A S, Chumanov G (2009) *Chem Mater* 21:2835
347. Kawahashi N, Persson C, Matijevic E (1991) *J Mater Chem* 1:577
348. Kawahashi H, Matijevic E (1991) *J Colloid Interface Sci* 143:103
349. Kawahashi N, Shiho H (2000) *J Mater Chem* 10:2294